보건학박사 학위논문

Study on the source apportionment and toxicological effects of $PM_{2.5}$ measured in Seoul, South Korea and Beijing, China

한국 서울과 중국 베이징의 대기 중 $PM_{2.5}$의 오염원 기여도 및 독성 평가

2021 년 8 월

서울대학교 대학원

보건학과 환경보건학 전공

박 지 은

한국 서울과 중국 베이징의 대기 중 $PM_{2.5}$의 오염원 기여도 및 독성 평가

지도교수 이 승 묵

이 논문을 보건학박사 학위논문으로 제출함
2021년 8월

서울대학교 대학원
환경보건학과 환경보건학 전공
박 지 은

박지은의 박사학위논문을 인준함
2021년 8월

위 원 장	**김 호**
부위원장	**최 경 호**
위 원	**조 경 덕**
위 원	**허 종 배**
위 원	**이 승 묵**

Study on the source apportionment and toxicological effects of $PM_{2.5}$ measured in Seoul, South Korea and Beijing, China

A dissertation submitted in partial fulfillment of

the requirements for the degree of

Doctor of Philosophy in Public Health

To the Faculty of the Graduate School of Public Health at

Seoul National University

by

Jieun Park

Supervised by Professor Seung-Muk Yi

August, 2021

Data approved by:

Chair	**Ho Kim**
Vice Chair	**Kyungho Choi**
Examiner	**Kyung-Duk Zoh**
Examiner	**Jongbae Heo**
Examiner	**Seung-Muk Yi**

ABSTRACT

Jieun Park

Department of Environmental Health Sciences

Graduate School of Public Health

Seoul National University

Substantial economic growth due to the rapid development has caused severe air pollution in East Asian countries. One of the most concerned air pollutants is fine particulate matter ($PM_{2.5}$) due to its ability to penetrate deeply into the lung through inhalation and elicit adverse health effects such as local and systemic inflammation. Among East Asian countries, South Korea and China are one of the most polluted countries which have been actively pursuing on reducing $PM_{2.5}$ concentrations by implementing air quality policies. In spite of the efforts toward $PM_{2.5}$ reduction, South Korea and China are still suffering from high $PM_{2.5}$ concentrations. Since long-range transboundary air pollution affects neighboring countries, it is important to perform a comprehensive investigation in the major cities of both countries.

This study focused on assessing the impact of organic extracts of $PM_{2.5}$ collected in Seoul, South Korea on primary human lung epithelial cells and identifying the relevant components and sources which induced lung epithelial cell injury. Twelve selected $PM_{2.5}$ samples from May 2016 to January 2017 were used to

evaluate the effects of organic compounds of $PM_{2.5}$ on inflammation, cellular aging, and macroautophagy in human lung epithelial cells isolated from healthy donors. Organic extracts of $PM_{2.5}$ specifically induced neutrophilic chemokine, interleukin-8, via extracellular signal-regulated kinase activation. While average $PM_{2.5}$ mass concentrations, OC and EC had no significant correlations, the polycyclic aromatic hydrocarbons and n-alkanes were the most relevant components of $PM_{2.5}$ with neutrophilic inflammation. Vegetative detritus and residential bituminous coal combustion sources were strongly correlated with neutrophilic inflammation, aging, and macroautophagy activation.

Though numerous studies are available on the characterization and source apportionment of $PM_{2.5}$ in South Korea and China, studies on simultaneous ground-based $PM_{2.5}$ monitoring and source apportionment in two countries are not available. In this study, simultaneous daily ground-based monitoring of $PM_{2.5}$ in Seoul and Beijing was conducted and the positive matrix factorization (PMF) model was utilized for the source apportionment of ambient $PM_{2.5}$ in the two sites. While nine contributing factors were identified, secondary nitrate, secondary sulfate, mobile, biomass burning, incineration, soil and aged sea salt sources were commonly found in both sites. Additionally, industry combined with coal combustion and oil combustion sources were identified in Seoul site and industry and coal combustion sources were identified for Beijing site. Ionic species (SO_4^{2-}, NO_3^-, and NH_4^+) accounted for more than 50% of the total mass concentration of $PM_{2.5}$, and secondary nitrate and secondary sulfate were the most dominant sources in both sites. Since secondary aerosols are largely affected by precursors from primary emissions and

meteorological conditions, the variations in the heating (November 15th to March 15th) and non-heating (March 16th to November 14th) seasons were analyzed. Potential source contribution function (PSCF) maps showed that the potential source areas of secondary nitrate and secondary sulfate for Seoul and Beijing were in mostly located in north and east china, thus both sites are affected by regional and long-range transport. During the heating season, industrial complex areas in northern China were shown as potential source areas for Beijing and coal-fired power plants near the Yangtze River and Henan province were identified as potential source areas for Seoul. During the non-heating season, coastal areas in eastern China to west part of South Korea were found to be potential source areas of secondary nitrate and secondary sulfate in both sites.

This study focused on investigating the characteristics of organic compounds and sources of the $PM_{2.5}$ organic extracts collected in Seoul, South Korea and Beijing, China and evaluated the production of $PM_{2.5}$ organic extract induced IL-8 on human lung epithelial cells. The expression levels of IL-8 in Beijing were significantly higher than that of Seoul. Moreover, organic compounds within $PM_{2.5}$ were found to be more important in inducing neutrophilic inflammation than $PM_{2.5}$ mass concentrations itself. For Seoul, PAHs and biomass burning source showed strong correlations with IL-8 expression levels. However, organic compounds such as aliphatic diacaids, alkylcyclohexanes and alkanoic acids showed positive correlations with expression levels of IL-8 at Beijing. In addition, biogenic SOC and anthropogenic SOC showed strong correlations with IL-8 expression levels. The

results indicated that organic compounds and sources which play important role in inflammation at Seoul and Beijing are different.

Keywords: $PM_{2.5}$, source apportionment, long-range transport, lung epithelial cells, cytokine

Student Number: 2018-39295

Table of Contents

List of Tables

List of Figures

Abbreviations

CMB	Chemical Mass Balance
COPD	Chronic Obstructive Pulmonary Disease
EC	Elemental Carbon
ERK	Extracellular Signal-Regulated Kinase
GC/MS	Gas Chromatography/Mass Spectrometry
GDAS	Global Data Assimilation System
HAECs	Primary Human Airway Epithelial Cells
HCEs	High Concentration Events
HYSPLIT	Hybrid Single-Particle Lagrangian Integrated Trajectory
IARC	International Agency for Research on Cancer
IL-8	Interleukin-8
j-PSCF	joint-PSCF
LDH	Lactate Dehydrogenase
NAAQS	National Ambient Air Quality Standars
OC	Organic Carbon
OECD	Organisation for Economic Cooperation and Development
PAHs	Polycyclic Aromatic Hydrocarbons
PMF	Positive Matrix Factorization
PSCF	Potential Source Contribution Function
SOC	Secondary Organic Carbon
SRM	Standard Reference Materials

Chapter 1.
Backgrounds

1. Introduction

Due to substantial economic activities, rapid development and urbanization have caused severe air pollution in East Asian countries. While PM_{10} with larger particles tend to be removed by filtration, fine particulate matter ($PM_{2.5}$) with an aerodynamic diameter of 2.5 μm is capable to penetrate into the end of the respiratory tract through inhalation and cause adverse health effects (Dockery et al., 1993; Pinkerton et al., 2000; Kocbach, 2008; Araujo et al., 2009). In 2013, the International Agency for Research on Cancer (IARC) classified ambient $PM_{2.5}$ as a Group 1 carcinogen (Loomis et al., 2013). According to World Health Organization (WHO), exposure to ambient air pollution causes around 3 million deaths which is 5.4% of all deaths in the world. With a capability of inducing adverse health effects, $PM_{2.5}$ became a critical pollutant which has been regulated worldwide.

As the airway is the first line of defense against inhaled $PM_{2.5}$, studies have discovered that particulate matter elicits oxidative stress and inflammation, which induce inflammatory lung diseases such as chronic obstructive pulmonary disease and lung cancer (Anenberg et al., 2010; Kloog et al., 2013). $PM_{2.5}$ not only cause local inflammation but also cause systemic inflammation which may even lead to mortality due to cardiovascular diseases (Kocbach, 2008; Wang et al., 2013). Numerous studies have found the strong correlations of $PM_{2.5}$ with pulmonary and cardiovascular diseases as well as mortality (Pope and Dockery 1999; Donaldson et al., 2003; Davel et al., 2012; Bell et al., 2014; Tsai et al., 2013; Shah et al., 2015; Feng et al., 2016).

China has been suffering from air pollution due to high $PM_{2.5}$ concentrations. As a second largest economy in the world, energy consumption in China has peaked to 3,123 million tonnes oil equivalent (Mtoe) and became the world's largest energy consumer as of 2016 (Caulcrick, 2018). Most of the energy consumed are being used for power generation and are known as a large contributing factor for anthropogenic air pollutants (Xu et al., 2015). Furthermore, growths of population density and vehicles intensified air pollution. In China, air pollution causes around 1,032,833 premature deaths and shortens Chinese life expectancy by 25 months. In addition, ambient $PM_{2.5}$ is the fourth leading risk factor that causes death by cancer, chronic respiratory diseases, cardiovascular and circulatory diseases in China (Yang et al., 2013). With the fact that the severe haze affected approximately 800 million people in 1.3 million km^2 of area (Huang et al., 2014) and continuous occurrences of high concentration events (HCEs), China's State Council has implemented *Action Plan on Prevention and Control of Air Pollution* (hereinafter Action Plan) on 10^{th} September of 2013 (Zhang et al., 2016). The Action Plan was designed to control and reduce air pollution in period of 2013 to 2017. China has achieved a major goal of reducing the annual average $PM_{2.5}$ concentration in Beijing to less than 60 $\mu g/m^3$ in 2017 (Zhang et al., 2016).

In spite of these efforts toward $PM_{2.5}$ reduction, in 2019, China ranked second in East Asia in terms of the highest annual average $PM_{2.5}$ concentration (Air, 2019). Forty-seven cities in China are in the top 100 polluted cities in the world. As China is among the largest countries in the world, the deterioration in its air quality has regional and international impacts because of the long-range transport of

pollutants to other Asian countries that are downwind and even to North America (Wuebbles et al., 2007). Transboundary air pollution affects neighboring countries because of the conducive meteorological and geographical characteristics.

As South Korea is located in downwind of China, high $PM_{2.5}$ concentration events are unavoidable (Kim et al., 2009; Park et al., 2016). South Korea has been actively pursuing the reduction of $PM_{2.5}$ concentrations in air by implementing stringent air quality policies. In Korea, the *Comprehensive Action Plan on Fine Dust* was implemented in 2017, which aimed to reduce $PM_{2.5}$ emissions by 30% by 2022 in comparison to the level in 2014 and to reduce the annual average $PM_{2.5}$ concentrations in Seoul to 17–18 μg/m^3 (Lee, 2018). Though, the $PM_{2.5}$ level in South Korea was the highest among the Organisation for Economic Cooperation and Development (OECD) countries in 2019 (Air, 2019).

Air quality worsens during cold seasons when the centralized heating system begins in China and westerly winds actively transport air masses to South Korea. However, $PM_{2.5}$ is a mixture of complex chemicals elucidated from various sources under different meteorological conditions, fraction of its constituents varies greatly depending on the location. Moreover, the mechanism of $PM_{2.5}$ toxicities may be different depending on chemical characteristics, sources, and regions (Valavanidis et al., 2008). To investigate the effects of $PM_{2.5}$, number of toxicological studies used various commercial cell lines such as mouse macrophage cell line (RAW264.7), A549, and 16HBE (Zhou et al., 2015; Leclercq et al., 2016; MohseniBandpi et al., 2017; Xu et al., 2020). In addition, particles generated in smog chamber or standard reference materials (SRM) were used for the exposure (Künzi et al., 2015; Leclercq

et al., 2016; Xu et al., 2020). Yet, the effects of collected ambient $PM_{2.5}$ on primary human airway epithelial cells (HAECs) isolated directly from healthy donors are not studied.

Numerous studies are available on the characterization and source apportionment of $PM_{2.5}$ in South Korea (Lee et al., 2008; Choi et al., 2013; Heo et al., 2014; Park et al., 2020) and China (Zheng et al., 2005; Huang et al., 2014; Li et al., 2016; Tan et al., 2017; Gao et al., 2018). However, studies on simultaneous ground-based $PM_{2.5}$ monitoring and source apportionment in both South Korea and China are not available. In order to implement an effective $PM_{2.5}$ reduction and control policy in South Korea and China, it is important to perform a comprehensive investigation in the major cities of both countries. This study may increase efficiency by focusing on controlling sources those are most harmful with high toxicities.

2. Objectives of the study

The overall aim of the study was to investigate the chemical characteristics and source apportionment of $PM_{2.5}$ in Seoul, South Korea and Beijing, China and to assess toxicological effects of $PM_{2.5}$ organic extracts from two sites in human lung epithelial cells.

The following detailed objectives were set for each study:

Chapter 2: The objective of this chapter was to assess the impact of $PM_{2.5}$ organic extracts collected during the high concentration events in Seoul, South Korea on primary human lung epithelial cells. The relevant organic compounds and sources to neutrophilic inflammation, aging and macroautophagy activation were identified to provide evidence to regulate the harmful components of $PM_{2.5}$ in Seoul.

Chapter 3: Simultaneous ground-based monitoring and chemical analyses of $PM_{2.5}$ in Seoul, South Korea and Beijing, China were conducted for a period of one year. The objective of this chapter was to identify sources and estimate source contributions using PMF model and to determine potential source areas using the potential source contribution function (PSCF) in two sites.

Chapter 4: The previous study found the high induction of IL-8 by $PM_{2.5}$ organic extracts from Seoul. This chapter was expanded by increasing number of samples and analysis of polar organic compounds for detailed source apportionment using PMF. This chapter focused on investigating the characteristics of organic compounds

and sources of the $PM_{2.5}$ organic extracts collected in Seoul, South Korea and Beijing, China and evaluated the production of $PM_{2.5}$ organic extract induced IL-8 on human lung epithelial cells.

References

Air, I.Q., 2019. World Air Quality Report Region & City PM2.5 Ranking. *Index Quality Air*.

Anenberg, S.C., Horowitz, L.W., Tong, D.Q. and West, J.J., 2010. An estimate of the global burden of anthropogenic ozone and fine particulate matter on premature human mortality using atmospheric modeling. *Environmental health perspectives*, *118*(9), pp.1189-1195.

Araujo, J.A. and Nel, A.E., 2009. Particulate matter and atherosclerosis: role of particle size, composition and oxidative stress. *Particle and fibre toxicology*, *6*(1), pp.1-19.

Bell, M.L., Ebisu, K., Leaderer, B.P., Gent, J.F., Lee, H.J., Koutrakis, P., Wang, Y., Dominici, F. and Peng, R.D., 2014. Associations of PM2. 5 constituents and sources with hospital admissions: analysis of four counties in Connecticut and Massachusetts (USA) for persons≥ 65 years of age. *Environmental health perspectives*, *122*(2), pp.138-144.

Caulcrick, O.O., 2018. The Electricity Model for China–Insights and Implications of Energy Policies.

Choi, J.K., Heo, J.B., Ban, S.J., Yi, S.M. and Zoh, K.D., 2013. Source apportionment of PM2. 5 at the coastal area in Korea. *Science of the Total Environment*, *447*, pp.370-380.

Davel, A.P., Lemos, M., Pastro, L.M., Pedro, S.C., de André, P.A., Hebeda, C., Farsky, S.H., Saldiva, P.H. and Rossoni, L.V., 2012. Endothelial dysfunction in the pulmonary artery induced by concentrated fine particulate matter exposure is associated with local but not systemic inflammation. *Toxicology*, *295*(1-3), pp.39-46.

Dockery, D.W., Pope, C.A., Xu, X., Spengler, J.D., Ware, J.H., Fay, M.E., Ferris Jr, B.G. and Speizer, F.E., 1993. An association between air pollution and

mortality in six US cities. *New England journal of medicine*, *329*(24), pp.1753-1759.

Donaldson, K., Stone, V., Borm, P.J., Jimenez, L.A., Gilmour, P.S., Schins, R.P., Knaapen, A.M., Rahman, I., Faux, S.P., Brown, D.M. and MacNee, W., 2003. Oxidative stress and calcium signaling in the adverse effects of environmental particles (PM10). *Free Radical Biology and Medicine*, *34*(11), pp.1369-1382.

Feng, S., Gao, D., Liao, F., Zhou, F. and Wang, X., 2016. The health effects of ambient PM2.5 and potential mechanisms. *Ecotoxicology and environmental safety*, *128*, pp.67-74.

Gao, J., Wang, K., Wang, Y., Liu, S., Zhu, C., Hao, J., Liu, H., Hua, S. and Tian, H., 2018. Temporal-spatial characteristics and source apportionment of PM2. 5 as well as its associated chemical species in the Beijing-Tianjin-Hebei region of China. *Environmental Pollution*, *233*, pp.714-724.

Heo, J.B., Hopke, P.K. and Yi, S.M., 2009. Source apportionment of PM 2.5 in Seoul, Korea. *Atmospheric Chemistry and Physics*, *9*(14), pp.4957-4971.

Huang, R.J., Zhang, Y., Bozzetti, C., Ho, K.F., Cao, J.J., Han, Y., Daellenbach, K.R., Slowik, J.G., Platt, S.M., Canonaco, F. and Zotter, P., 2014. High secondary aerosol contribution to particulate pollution during haze events in China. *Nature*, *514*(7521), pp.218-222.

Kim, Y.J., Woo, J.H., Ma, Y.I., Kim, S., Nam, J.S., Sung, H., Choi, K.C., Seo, J., Kim, J.S., Kang, C.H. and Lee, G., 2009. Chemical characteristics of long-range transport aerosol at background sites in Korea. *Atmospheric Environment*, *43*(34), pp.5556-5566.

Kloog, I., Ridgway, B., Koutrakis, P., Coull, B.A. and Schwartz, J.D., 2013. Long-and short-term exposure to PM2. 5 and mortality: using novel exposure models. *Epidemiology (Cambridge, Mass.)*, *24*(4), p.555.

Kocbach, A., 2008. Pro-inflammatory potential of particles from residential wood smoke and traffic: Importance of physicochemical characteristics.

Künzi, L., Krapf, M., Daher, N., Dommen, J., Jeannet, N., Schneider, S., Platt, S., Slowik, J.G., Baumlin, N., Salathe, M. and Prévôt, A.S., 2015. Toxicity of aged gasoline exhaust particles to normal and diseased airway epithelia. *Scientific reports*, *5*(1), pp.1-10.

Leclercq, B., Happillon, M., Antherieu, S., Hardy, E.M., Alleman, L.Y., Grova, N., Perdrix, E., Appenzeller, B.M., Guidice, J.M.L., Coddeville, P. and Garçon, G., 2016. Differential responses of healthy and chronic obstructive pulmonary diseased human bronchial epithelial cells repeatedly exposed to air pollution-derived PM4. *Environmental Pollution*, *218*, pp.1074-1088.

Lee, H., Park, S.S., Kim, K.W. and Kim, Y.J., 2008. Source identification of PM2.5 particles measured in Gwangju, Korea. *Atmospheric Research*, *88*(3-4), pp.199-211.

Lee, S., 2018. Korea's New Comprehensive Plan on Fine Dust and Its Implications for Policy and Research. *Research in Brief*, (29), pp.1-7.

Li, H., Wang, Q.G., Yang, M., Li, F., Wang, J., Sun, Y., Wang, C., Wu, H. and Qian, X., 2016. Chemical characterization and source apportionment of PM2. 5 aerosols in a megacity of Southeast China. *Atmospheric Research*, *181*, pp.288-299.

Loomis, D., Grosse, Y. and Lauby-Secretan, B., International Agency for Research on Cancer Monograph Working Group IARC. The carcinogenicity of outdoor air pollution. *Lancet Oncol2013141262–1263*.

MohseniBandpi, A., Eslami, A., Shahsavani, A., Khodagholi, F. and Alinejad, A., 2017. Physicochemical characterization of ambient PM2. 5 in Tehran air and its potential cytotoxicity in human lung epithelial cells (A549). *Science of the Total Environment*, *593*, pp.182-190.

Park, E.H., Heo, J., Kim, H. and Yi, S.M., 2020. Long term trends of chemical constituents and source contributions of PM2.5 in Seoul. *Chemosphere*, *251*, p.126371.

Park, S.S., Cho, S.Y., Jung, C.H. and Lee, K.H., 2016. Characteristics of water-soluble inorganic species in PM10 and PM2.5 at two coastal sites during spring in Korea. *Atmospheric Pollution Research*, *7*(2), pp.370-383.

Pinkerton, K.E., Green, F.H., Saiki, C., Vallyathan, V., Plopper, C.G., Gopal, V., Hung, D., Bahne, E.B., Lin, S.S., Ménache, M.G. and Schenker, M.B., 2000. Distribution of particulate matter and tissue remodeling in the human lung. *Environmental Health Perspectives*, *108*(11), pp.1063-1069.

Pope III, C.A. and Dockery, D.W., 1999. Epidemiology of particle effects. In *Air pollution and health* (pp. 673-705). Academic Press.

Shah, A.S., Lee, K.K., McAllister, D.A., Hunter, A., Nair, H., Whiteley, W., Langrish, J.P., Newby, D.E. and Mills, N.L., 2015. Short term exposure to air pollution and stroke: systematic review and meta-analysis. *bmj*, *350*.

Tan, J., Zhang, L., Zhou, X., Duan, J., Li, Y., Hu, J. and He, K., 2017. Chemical characteristics and source apportionment of PM2.5 in Lanzhou, China. *Science of the Total Environment*, *601*, pp.1743-1752.

Tsai, S.S., Chang, C.C. and Yang, C.Y., 2013. Fine particulate air pollution and hospital admissions for chronic obstructive pulmonary disease: a case-crossover study in Taipei. *International journal of environmental research and public health*, *10*(11), pp.6015-6026.

Valavanidis, A., Fiotakis, K. and Vlachogianni, T., 2008. Airborne particulate matter and human health: toxicological assessment and importance of size and composition of particles for oxidative damage and carcinogenic mechanisms. *Journal of Environmental Science and Health, Part C*, *26*(4), pp.339-362.

Wang, G., Zhen, L., Lü, P., Jiang, R. and Song, W., 2013. Effects of ozone and fine particulate matter (PM2.5) on rat cardiac autonomic nervous system and systemic inflammation. *Wei sheng yan jiu= Journal of hygiene research*, *42*(4), pp.554-560.

Wuebbles, D.J., Lei, H. and Lin, J., 2007. Intercontinental transport of aerosols and photochemical oxidants from Asia and its consequences. *Environmental pollution*, *150*(1), pp.65-84.

Xu, C., Hong, J., Ren, Y., Wang, Q. and Yuan, X., 2015. Approaches for controlling air pollutants and their environmental impacts generated from coal-based electricity generation in China. *Environmental Science and Pollution Research*, *22*(16), pp.12384-12395.

Xu, F., Shi, X., Qiu, X., Jiang, X., Fang, Y., Wang, J., Hu, D. and Zhu, T., 2020. Investigation of the chemical components of ambient fine particulate matter (PM2. 5) associated with in vitro cellular responses to oxidative stress and inflammation. *Environment international*, *136*, p.105475.

Yang, G., Wang, Y., Zeng, Y., Gao, G.F., Liang, X., Zhou, M., Wan, X., Yu, S., Jiang, Y., Naghavi, M. and Vos, T., 2013. Rapid health transition in China, 1990–2010: findings from the Global Burden of Disease Study 2010. *The lancet*, *381*(9882), pp.1987-2015.

Zhang, H., Wang, S., Hao, J., Wang, X., Wang, S., Chai, F. and Li, M., 2016. Air pollution and control action in Beijing. *Journal of Cleaner Production*, *112*, pp.1519-1527.

Zheng, M., Salmon, L.G., Schauer, J.J., Zeng, L., Kiang, C.S., Zhang, Y. and Cass, G.R., 2005. Seasonal trends in PM2.5 source contributions in Beijing, China. *Atmospheric Environment*, *39*(22), pp.3967-3976.

Zhou, Z., Liu, Y., Duan, F., Qin, M., Wu, F., Sheng, W., Yang, L., Liu, J. and He, K., 2015. Transcriptomic analyses of the biological effects of airborne PM2.

5 exposure on human bronchial epithelial cells. *PloS one*, *10*(9), p.e0138267.

Chapter 2.

The impact of organic extracts of seasonal $PM_{2.5}$ on primary human lung epithelial cells and their chemical characterization

ABSTRACT

Lung epithelial cells serve as the first line of defense against various inhaled pollutant particles. To investigate the adverse health effects of organic extracts of $PM_{2.5}$ collected in Seoul, South Korea, we collected twelve selected $PM_{2.5}$ samples from May 2016 to January 2017 and evaluated the effects of organic compounds of $PM_{2.5}$ on inflammation, cellular aging, and macroautophagy in human lung epithelial cells isolated directly from healthy donors. Organic extracts of $PM_{2.5}$ specifically induced neutrophilic chemokine, interleukin-8, via extracellular signal-regulated kinase activation. Moreover, $PM_{2.5}$ significantly increased the expression of aging markers (p16, p21, and p27) and activated macroautophagy. Average mass concentrations, OC and EC, had no significant correlations with $PM_{2.5}$ effects. However, polycyclic aromatic hydrocarbons and n-alkanes were the most relevant components of $PM_{2.5}$ correlated with neutrophilic inflammation. Vegetative detritus and residential bituminous coal combustion sources were strongly correlated with neutrophilic inflammation, aging, and macroautophagy activation. These data suggest that the chemical composition of $PM_{2.5}$ is crucially important to determine the adverse health effects of $PM_{2.5}$. Our study provides encouraging evidence to regulate the harmful components of $PM_{2.5}$ in Seoul.

Keywords: $PM_{2.5}$, organic compounds, lung epithelial cells, cytokine, senescence, macroautophagy

1. Introduction

The persistent occurrence of ambient air pollution has attracted a large amount of attention as a global environmental issue. The International Agency for Research on Cancer (IARC) classified particulate matter from outdoor air pollution as a Group 1 carcinogen in 2013 (Loomis et al., 2013). In particular, ambient fine particulate matter ($PM_{2.5}$) which has an aerodynamic diameter of 2.5 μm or less is well known to be correlated with an increase in mortality and morbidity caused by cardiovascular and pulmonary impairments (Davel et al., 2012; Bell et al., 2014; Tsai et al., 2013; Shah et al., 2015; Feng et al., 2016). As the airway is the first line of defense against inhaled $PM_{2.5}$, studies have discovered that particulate matter elicits oxidative stress and inflammation, which induce inflammatory lung diseases such as chronic obstructive pulmonary disease (COPD) and lung cancer (Pope and Dockery, 1999; Donaldson et al., 2003; Anenberg et al., 2010; Kloog et al., 2013). Potential mechanisms of $PM_{2.5}$-induced adverse health effects on the human respiratory system have been consistently found in toxicological, experimental-based studies and in epidemiological studies (Bell et al., 2014; Gualtieri et al., 2011; Lu et al., 2015; Xing et al., 2016). To investigate the effects of $PM_{2.5}$, number of toxicological studies used commercial lung epithelial cells (Rumelhard et al., 2007; Alessandria et al., 2014; Cachon et al., 2014; Song et al., 2017) and Standard Reference Materials (SRM) urban particulate matter. However, the effects of collected ambient particulate matter, especially in Seoul, South Korea, on primary human airway epithelial cells (HAECs) isolated directly from healthy donors are not studied.

Due to the complexity of $PM_{2.5}$ itself, the adverse health effects of $PM_{2.5}$ may be different depending on chemical characteristics, sources, and regions. While $PM_{2.5}$ is composed of various chemical constituents, organic material is chemical constituents that comprise about 20-40% of $PM_{2.5}$ mass in urban area (He et al., 2001; Dan et al., 2004; Putaud et al., 2010) and organic carbon (OC) and elemental carbon (EC) are highly related to adverse health effects such as emergency room visits and cardiopulmonary diseases (Lanki et al., 2006; Vedal et al., 2013; Qiao et al., 2014). In addition, organic compounds such as polycyclic aromatic hydrocarbons (PAHs) are prominent carcinogens (Baird et al., 2005; Gilli et al., 2007; Dilger et al., 2016). Thus, finding the sources of $PM_{2.5}$ based on local chemical characteristics and linking to toxicological effects is needed. With the supposition that the $PM_{2.5}$ in Seoul will have distinct organic compounds and contributing sources, we analyzed organic compounds in $PM_{2.5}$ and identified potential contributing sources by using a receptor model. Recently, the frequency of high concentration events (HCEs) has been increasing in Seoul. According to *The 2016 Environmental Performance Index Report*, more than 50% of Korean people are exposed to dangerous levels of $PM_{2.5}$ (Hsu et al., 2016). In the present study, we investigated the impact of organic extracts of $PM_{2.5}$ collected in Seoul, South Korea on primary human lung epithelial cells and identified the relevant components and sources in $PM_{2.5}$.

2. Materials and methods

2.1 Sampling site and collection procedure

$PM_{2.5}$ samples were collected on the rooftop of the Graduate School of Public Health building (37.581°N, 127.001°E) at Seoul National University in Seoul, Korea. Samples were collected for twenty-four-hour by using a high-volume air sampler and a low-volume air sampler equipped with filter pack (URG-2000-30FG, URG, USA) and cyclone (URG-2000-30EH, URG, USA). A high-volume air sampler loaded with quartz microfiber filters (Whatman™, UK) collected $PM_{2.5}$ with a flow rate of 40 cfm, and the collected filters were used for organic extraction. A low-volume air sampler was loaded with Teflon filters (PTFE membrane, Pall Corporation, USA) to measure mass concentrations and with quartz filters (Quartz microfiber filter, Pall Corporation, USA) to quantify the concentrations of OC and EC. The $PM_{2.5}$ mass concentration was measured with a semi-micro balance (accuracy of 0.01 mg) (CP225D, Sartorius), and twelve samples that were collected during HCEs between May 2016 and January 2017 were selected. Three HCE samples from each season were selected by the Korean national air quality standards of $PM_{2.5}$ which is 24 h average concentration of 35 $\mu g/m^3$. Thus, a total of twelve HCE samples were used for this study.

2.2 Organic extraction of the collected $PM_{2.5}$ samples

Quartz filters were baked in a furnace at 450℃ for 24 h, and the collected filters were stored at -20℃ before use. Samples were punched by a stainless cutter, and two of the punched filters (4 cm x 4 cm) were used for extraction. Solvent

mixture of dichloromethane:methanol (3:1, v/v) was used for sample extractions with ultrasonic bath. The extracted samples were concentrated to 10 mL by a Turbovap II (Zymark Co., USA) with N_2 gas and 0.2 μm Acrodisc Syringe Filters (Pall Corporation, USA) were used for filtration. The filtered samples were then concentrated to 1 mL with a Turbovap II and Reacti-Therm (Thermo Fisher Scientific, USA) under a gentle stream of N_2 gas and were stored at -20°C. The concentrated samples were used for organic compound analysis and *in vitro* experiments.

2.3 Cells

Normal human bronchial epithelial cells (BEAS-2B from ATCC, Manassas, VA, USA) were maintained in defined keratinocyte-SFM (Gibco by Thermo Fisher Scientific, Waltham, MA, USA) at 37°C under 5% CO_2. Normal primary HAECs were obtained after review and approval by the Seoul National University Hospital Institutional Review Board (SNUH IRB number: H-1602-108-742). Primary HAECs were isolated and grown as previously described and is detailed in Lee et al., 2017.

2.4 Cell viability

Cell viability was measured by MTT and lactate dehydrogenase (LDH) release assays. LDH release assays were performed using a CytoTox-ONE™ homogeneous membrane integrity assay kit (Promega, Madison, WI, USA). Detailed method is stated in Lee et al., 2015.

2.5 Protein extraction and western blot analysis

Equal amounts of protein were resolved by gradient SDS-polyacrylamide gel electrophoresis (Thermo Fisher Scientific, Waltham, MA, USA) and transferred to nitrocellulose membranes (Thermo Fisher Scientific). The membranes were blocked with 5% skim milk blocking buffer for 1 h to block non-specific binding and incubated overnight at 4°C with primary antibodies. Then the membranes were washed with washing buffer three times and incubated with horseradish peroxidase-conjugated secondary antibodies in blocking buffer for 1 h. After successive washes, the membranes were developed using a SuperSignal West Pico Chemiluminescent Kit (Thermo Fisher Scientific).

2.6 Multiplex Bead Assay

The levels of cytokines in cell culture media were determined using a Bio-Plex Pro™ Cytokine Assay Kit (Bio-Rad, Hercules, CA) according to the manufacturer's instructions.

2.7 GC/MS analysis and OC/EC analysis

Gas chromatography-mass spectrometry (7080B/5977B, Agilent Technologies, Inc., USA) was employed to quantify 52 organic compounds in each extract. The analyzed species included 23 species of PAHs, 17 species of n-alkanes, 7 species of hopanes and 5 species of alkylcyclohexanes and isoprenoids.

The samples collected in the low-volume sampler were punched (1.5 cm x 1.0 cm) to analyze major components of carbon species which are OC and EC. OC

and EC were analyzed with a carbon aerosol analyzer (Sunset Laboratory Inc., USA). Thermal/optical transmittance (TOT) method was used for the data quantification.

2.8 Source apportionment of organic compounds in $PM_{2.5}$ using CMB model

Source apportionment of the OC fraction of $PM_{2.5}$ was performed by using a chemical mass balance (CMB v8.2) provided by the U.S. Environmental Protection Agency (EPA). The CMB air quality model is one of the receptor models that has been widely used to identify sources and quantify source contributions (Coulter, 2004). The concentrations of organic compounds, OC, and EC in twelve samples were used as ambient data in addition to the speciated source profile data. The optimal set of source profiles contained four sources which are vegetative detritus (Rogge et al., 1993), residential bituminous coal combustion soot (Zhang et al., 2008), diesel engines (Lough et al., 2007), and gasoline motor vehicles (Lough et al., 2007).

3. Results

3.1 The effect of $PM_{2.5}$ organic compounds on cell viability in lung epithelial cells (BEAS-2B)

As $PM_{2.5}$ organic compounds have been shown to be cytotoxic, we first evaluated the dose dependent effect of $PM_{2.5}$ organic compounds on the viability of lung epithelial cells. BEAS-2B cells were treated with vehicle control (V.C., dichloromethane) and $PM_{2.5}$ organic extracts (0.1, 0.5, 1, 2%) of single sample (sample collected on November 8th, 2016) for 24 h, and cell viability assays (MTT and LDH release assays) were performed. $PM_{2.5}$ organic extracts (1%) or less did not affect cell viability (Figure 2-1). Based on this result, we used $PM_{2.5}$ (1%) in all experiments. Data were analysed with a two-tailed unpaired *t-test* to assess statistical differences between groups. All statistical analyses were performed using GraphPad Prism software (San Diego, CA, USA). A p-value < 0.05 was considered to be statistically significant.

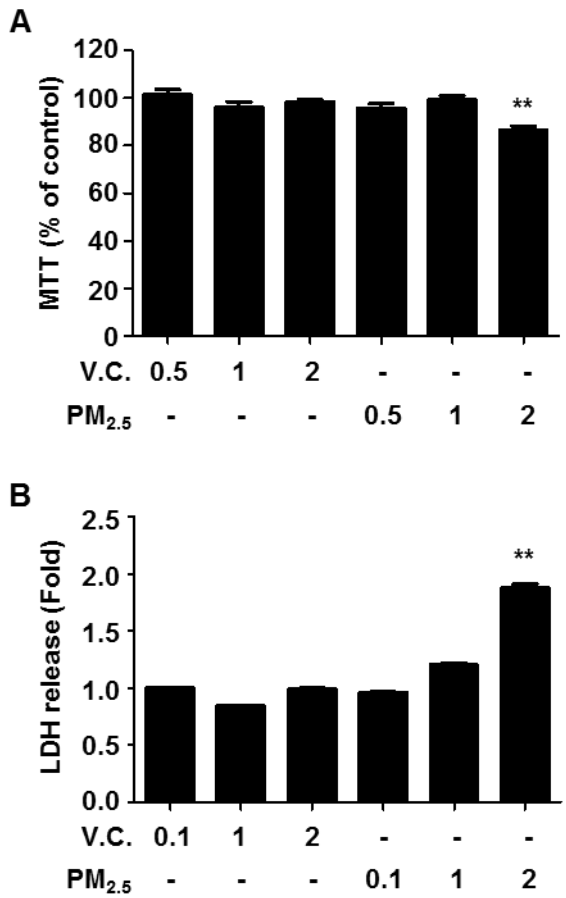

Figure 2-1 The effects of $PM_{2.5}$ on cell viability in lung epithelial cells: (A) MTT, (B) LDH release assay, **$p<0.05$.

3.2 The effect of $PM_{2.5}$ organic compounds on cytokine production and the expression of aging and macroautophagy markers in BEAS-2B cells

To test whether $PM_{2.5}$ organic compounds (collected on November 8th 2016) induce the production of pro-inflammatory or anti-inflammatory cytokines in lung epithelial cells, BEAS-2B cells were incubated with V.C. and $PM_{2.5}$ (1%) for 24 h. The levels of interleukin-1β (IL-1β), IL-6, IL-8, tumor necrosis factor-α (TNF-α), IL-17, basic fibroblast growth factor (bFGF), and vascular endothelial growth factor (VEGF) in cell culture media were determined by a multiplex bead assay. $PM_{2.5}$ organic compounds exclusively induced the production of IL-8 but not IL-1β, IL-6, TNF-α, IL-17, bFGF, or VEGF (Figure 2-2A and B). IL-8 is the primary cytokine involved in the recruitment of neutrophils to the site of infection or damage (Richman-Eisenstat et al., 1993; Pease and Sabroe, 2002). IL-8 released from lung epithelial cells is well known to recruit neutrophils to the lung, thus further amplifying inflammation. Many studies have reported that IL-8 and neutrophils have been detected in COPD patients. It has been suggested that mitogen-activated protein (MAP) kinases, especially extracellular signal-regulated kinase (ERK), play a role in $PM_{2.5}$-induced pro-inflammatory signaling (Wang et al., 2010). Therefore, we investigated the role of the ERK pathway in $PM_{2.5}$-induced IL-8 production. $PM_{2.5}$ activated ERK (Figure 2-2C), and blocking ERK activation by a chemical inhibitor (U0126) decreased the $PM_{2.5}$-mediated production of IL-8 (Figure 2-2D). These data suggest that the ERK pathway is responsible for IL-8 release in response to $PM_{2.5}$ stimulation in lung epithelial cells.

Senescence and macroautophagy activation in lung epithelial cells were reported to be involved in the pathogenesis of inflammatory lung diseases such as COPD (Kuwano et al., 2016). To investigate the effect of $PM_{2.5}$ on senescence and macroautophagy activation in lung epithelial cells, BEAS-2B cells were treated with $PM_{2.5}$ organic extracts for 24 h, and the expression levels of senescence markers (p16, p21, and p27) and a macroautophagy marker (light chain 3B, LC3B) were evaluated by Western blot analysis. Significant increase in the expression levels of p16, p21, p27, and LC3B were shown (Figure 2-3).

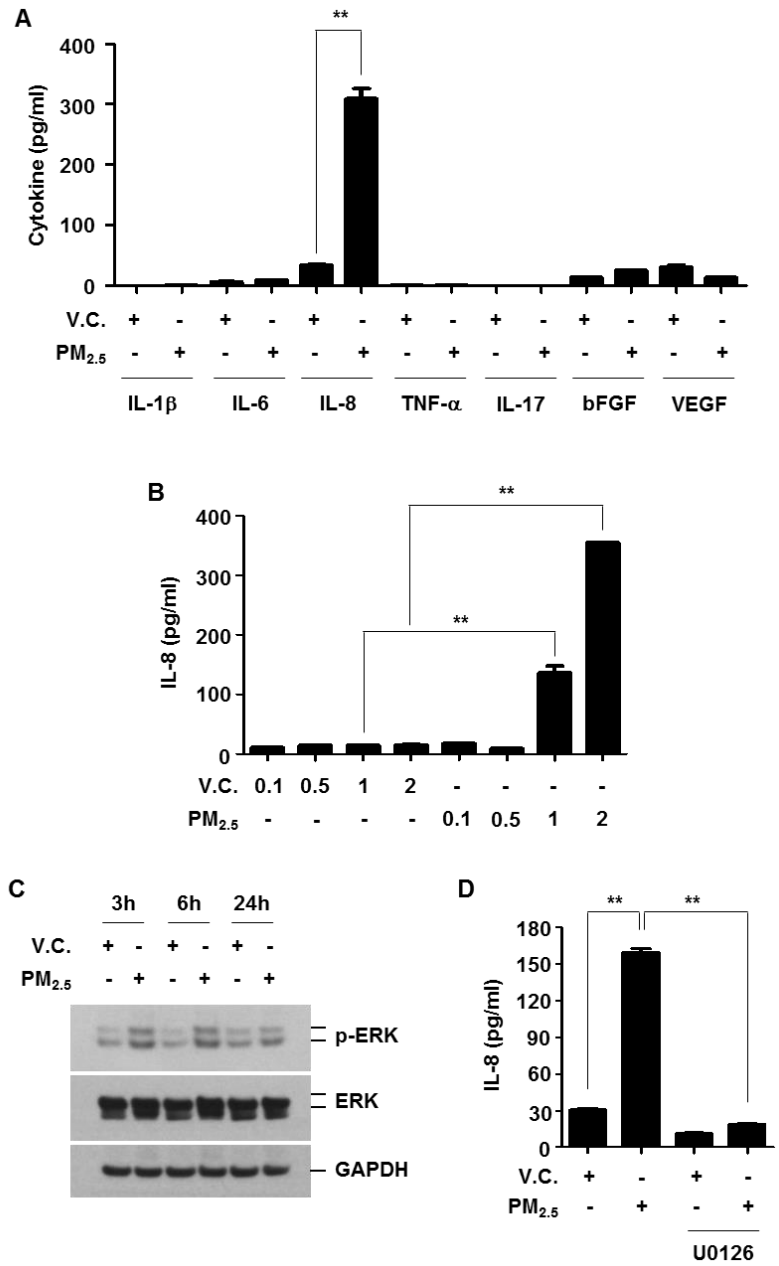

Figure 2-2 The effects of $PM_{2.5}$ on cytokine production in BEAS-2B cells: (A) BEAS-2B cells treated with V.C. or $PM_{2.5}$ organic compounds (1%) for 24 h, (B) Cells incubated with various concentrations (%) for 24 h, (C) Western blot analysis for p-ERK, ERK, and GAPDH, (D) Treatment of U0126 and measurement of IL-8 with a multiplex bead assay

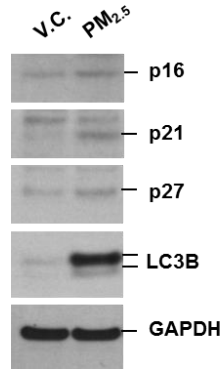

Figure 2-3 The effects of $PM_{2.5}$ on the expression of aging and macroautophagy markers in BEAS-2B cells

3.3 The effect of $PM_{2.5}$ organic compounds on inflammation, aging, and macroautophagy activation in primary HAECs

To confirm the activation of ERK and increased levels of IL-8 in primary cells, primary HAECs from six healthy control patients with no symptoms of COPD or respiratory diseases were collected using a bronchial brush. The epithelial lineage was verified by immunohistochemical staining. Cultured primary HAECs stained intensely and exclusively for epithelial-specific markers (cytokeratin and E-cadherin). No expression was observed for macrophages and endothelial lineage markers (CD11b and CD31) (data not shown). Verified HAECs from six donors were exposed to twelve $PM_{2.5}$ organic extracts (1%) for 24 h. $PM_{2.5}$ (1%) did not affect cell viability of primary HAECs as well as BEAS-2B cells (data not shown). $PM_{2.5}$ activated ERK and induced IL-8 production (Figure 2-4A and C). The expression levels of active ERK and IL-8 were significantly higher when the cells were exposed to fall and winter samples than when cells were exposed to spring and summer samples (Figure 2-4B and C). Moreover, we observed that $PM_{2.5}$ significantly increased the expression levels of senescence markers (p16, p21, and p27) and activated macroautophagy (Figure 2-5A and B). No significant seasonal differences were found in the expression levels of senescence and macroautophagy markers (Figure 2-5B).

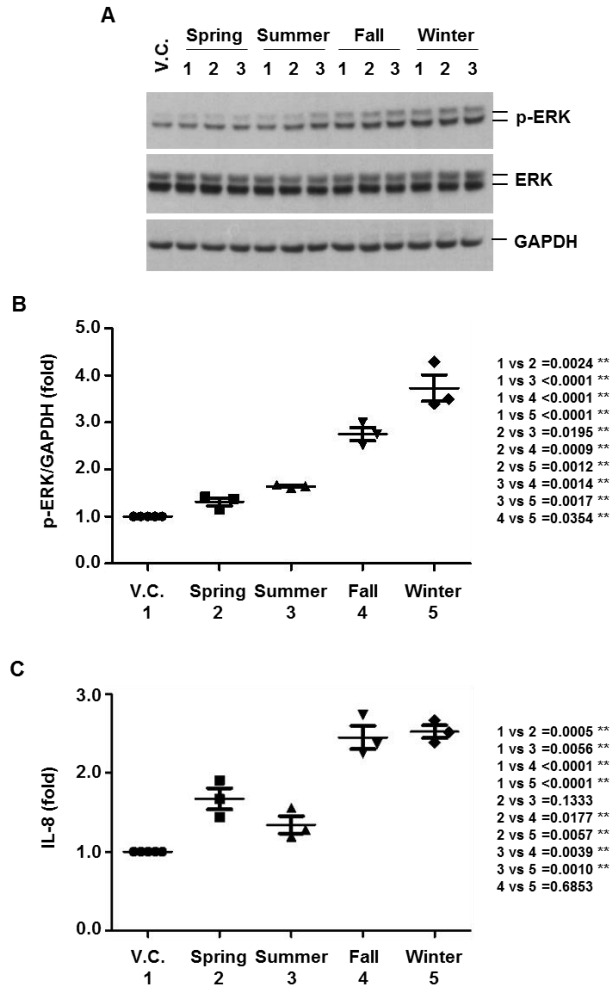

Figure 2-4 The effects of $PM_{2.5}$ on ERK activation and IL-8 production in primary HAECs: (A) Western blot analysis for p-ERK, ERK, and GADPH, (B) p-ERK expression normalized to GAPDH in each season, (C) IL-8 concentrations in each season

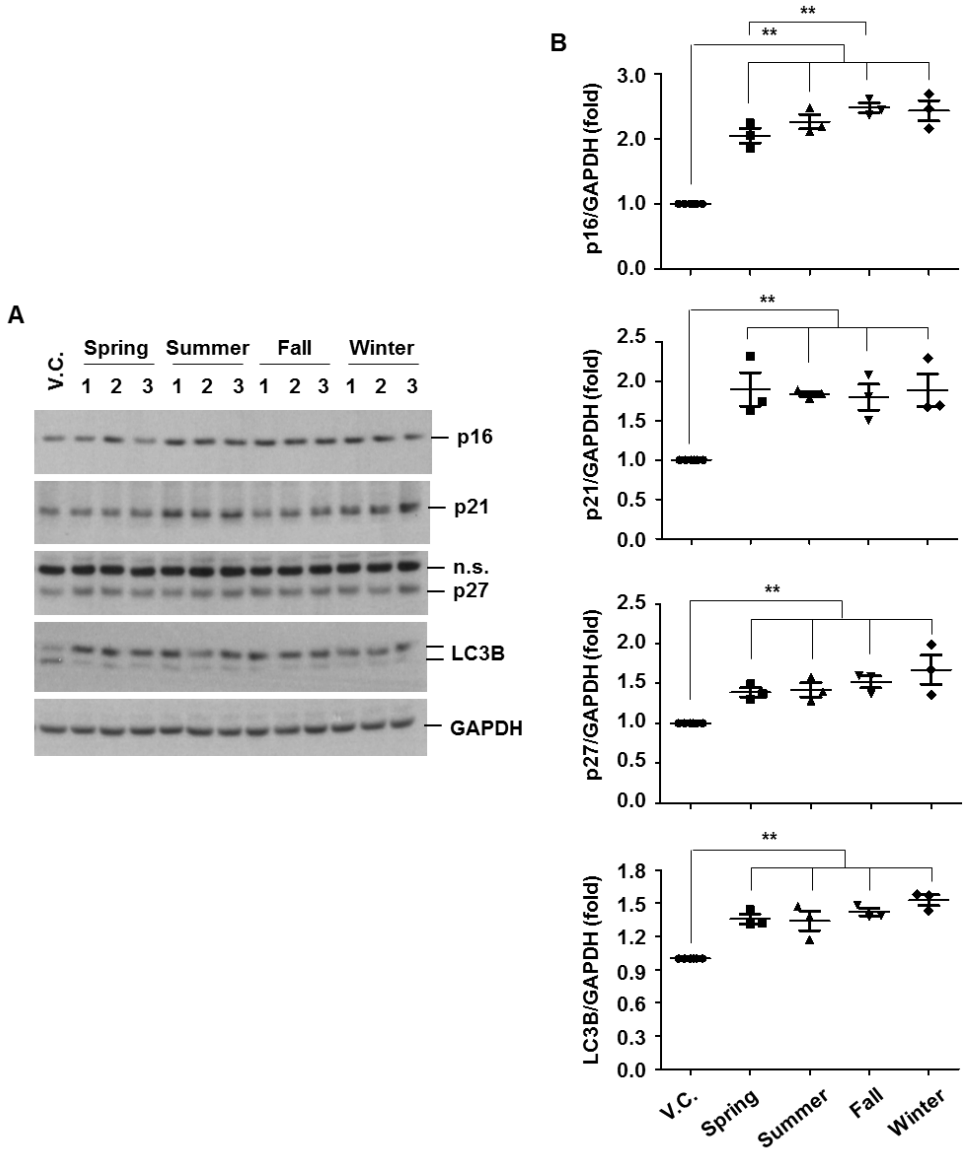

Figure 2-5 The effects of $PM_{2.5}$ on the expression of aging and autophagy markers in primary HAECs: (A) Western blot analysis for p16, p21, p27, LC3B, and GAPDH, (B) Seasonal variation for the expression levels of senescence and macroautophagy markers

3.4 Analysis of $PM_{2.5}$ constituents correlated with inflammation, aging, and macroautophagy activation

As Figure 2-6A shows, the average mass concentration of the twelve $PM_{2.5}$ samples was 83.2±3.85 μg/m^3. Divided seasonally, the highest average $PM_{2.5}$ mass concentration was observed in spring (149±11.2 μg/m^3), followed by winter (76.4±3.41 μg/m^3), summer (59.0±10.1 μg/m^3), and fall (48.4±5.97 μg/m^3). The average concentrations of OC and EC in the twelve samples were 11.5±0.34 μg/m^3 and 1.32±0.05 μg/m^3, respectively. The seasonal averages of OC and EC concentrations showed similar trend as the seasonal average $PM_{2.5}$ mass concentrations; thus, the average concentrations were the highest in the spring (OC: 15.3±0.43 μg/m^3, EC: 2.06±0.05 μg/m^3), followed by winter (OC: 13.2±0.41 μg/m^3, EC: 1.38±0.14 μg/m^3), fall (OC: 9.53±1.25 μg/m^3, EC: 1.00±0.06 μg/m^3) and summer (OC: 7.92±1.51 μg/m^3, EC: 0.84±0.20 μg/m^3).

The overall average and seasonal average concentrations of the sum of PAHs, n-alkanes, hopanes and alkylcyclohexanes and isoprenoids were calculated and are presented in Figure 2-6B (Table 2-1). While n-alkanes had the highest average concentrations among organic compounds, the highest average concentration was observed in winter (96.9±9.05 ng/m^3), followed by fall (80.1±2.15 ng/m^3), summer (79.5±7.18 ng/m^3) and spring (74.4±1.75 ng/m^3). The average concentrations of alkylcyclohexanes and isoprenoids were the highest in winter (92.1±15.4 ng/m^3) and the lowest in spring (23.8±6.97 ng/m^3). For PAHs, the average concentration in winter (34.0±2.00 ng/m^3) was the highest, followed by fall (22.3±2.65 ng/m^3), spring (9.88±0.44 ng/m^3), and summer (7.13±0.37 ng/m^3).

Unlike other organic compounds, hopanes had the highest average concentration in summer (1.57±0.13 ng/m^3), followed by fall (1.25±0.09 ng/m^3), spring (1.04±0.03 ng/m^3), and winter (0.69±0.12 ng/m^3). The seasonal trends of organic compounds did not follow those of $PM_{2.5}$ and OC.

The association between $PM_{2.5}$ organic compounds and IL-8 production was measured by using the Pearson correlation coefficient (r). R values greater than 0.70 with a p-value less than 0.05 were considered highly correlated compounds. $PM_{2.5}$ mass concentrations, OC and EC had negative or no significant correlations with inflammation, aging, and macroautophagy activation, while several organic compounds showed significant correlations.

The results showed that increases in PAHs and several n-alkanes were highly associated with increases in both ERK activation and IL-8 production (Table 2-2, Table 2-3). PAHs such as phenanthrene, anthracene, fluoranthene, pyrene, cyclopenta[cd]pyrene, benzo[a]anthracene, benzo[b]fluoranthene, benzo[k]fluoranthene, benzo[a]pyrene, benzo[e]pyrene, indeno[1,2,3-cd]pyrene, dibenzo[a,h]anthracene, picene, benzo[ghi]perylene, and coronene showed a high correlation with the expression levels of active ERK and IL-8. The n-alkanes that had high correlations with active ERK and IL-8 were C27, C30, C31, C32, C33, and C34. Among alkylcyclohexanes and isoprenoids, only dibenzofuran was highly correlated with active ERK and IL-8 (Table 2-4).

PAHs and n-alkanes also showed high correlations with the expression of aging and macroautophagy markers (Table 2-5 and Table 2-6). The PAHs highly correlated with p27 were pyrene, cyclopenta[cd]pyrene, benzo[a]anthracene,

benzo[b]fluoranthene, benzo[e]pyrene, indeno[1,2,3-cd]pyrene, and benzo[ghi]perylene. The macroautophagy marker, LC3B, was highly correlated with fluoranthene, pyrene, benzo[a]anthracene, benzo[b]fluoranthene, indeno[1,2,3-cd]pyrene, benzo[ghi]perylene, and coronene.

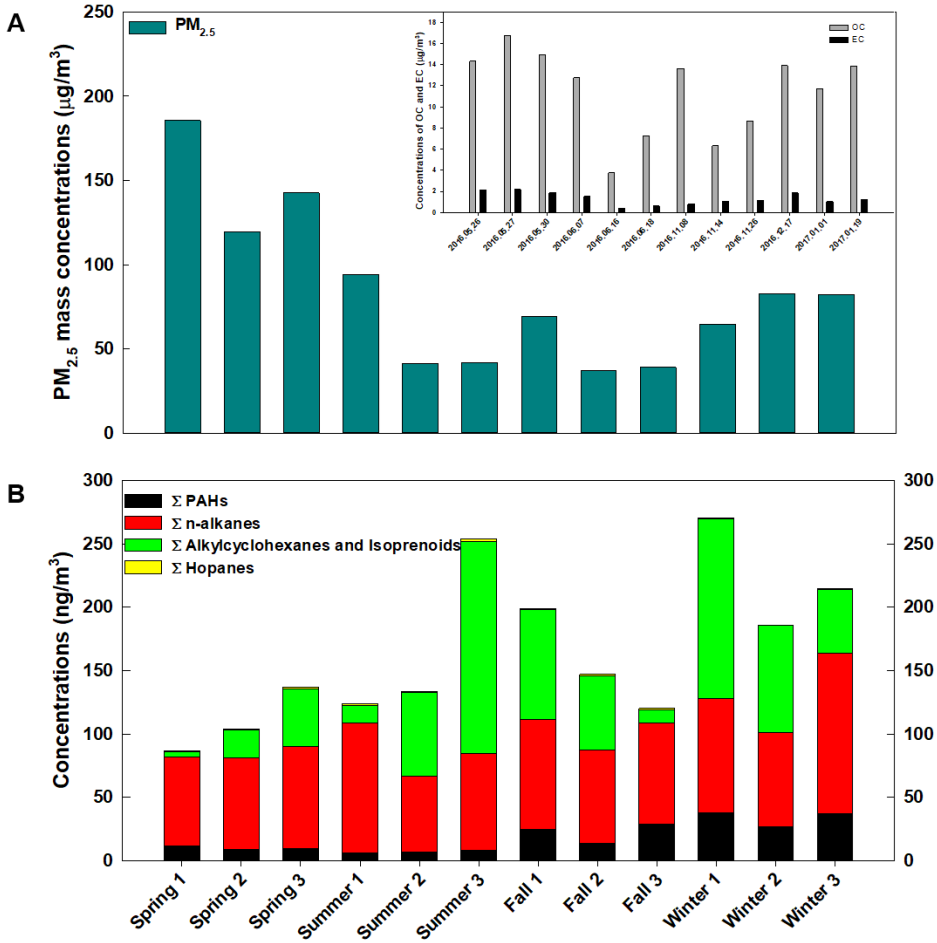

Figure 2-6 $PM_{2.5}$ mass concentrations and concentrations of organic compounds: (A) $PM_{2.5}$ mass concentrations and OC and EC concentrations in twelve samples (B) Concentrations of organic compounds, including PAHs, n-alkanes, alkylcyclohexanes and isoprenoids, and hopanes

Table 2-1 Average concentrations for chemical species

Chemical Species	Total (N=12)		Spring (N=3)		Summer (N=3)		Fall (N=3)		Winter (N=3)	
	mean	SEM	mean	SEM	mean	SEM	mean	SEM	mean	SEM
$PM_{2.5}$	83.23	3.85	149.10	11.19	59.03	10.10	48.36	5.97	76.42	3.41
OC	11.49	0.34	15.34	0.43	7.92	1.51	9.53	1.25	13.16	0.41
EC	1.32	0.05	2.06	0.05	0.84	0.20	1.00	0.06	1.38	0.14
ΣPAHs	18.34	1.00	9.88	0.44	7.13	0.37	22.34	2.65	34.00	2.00
Σn-alkanes	82.72	1.47	74.41	1.75	79.53	7.18	80.07	2.15	96.86	9.05
ΣHopanes	1.14	0.04	1.04	0.03	1.57	0.13	1.25	0.09	0.69	0.12
ΣAlkylcyclohexanes &Isoprenoids	62.47	4.28	0.30	0.02	0.31	0.02	0.34	0.02	0.72	0.04

Table 2-2 Correlation between IL-8/active ERK and PAHs

PAHs	IL-8		p-ERK	
	r	p value	r	p value
PAHs sum	**0.89**	**<0.001**	**0.92**	**<0.001**
1-Methylnaphthalene	0.06	0.845	-0.01	0.967
2-Methylnaphthalene	0.40	0.248	0.27	0.449
2,6-Dimethylnaphthalene	0.15	0.642	0.38	0.219
Fluorene	0.54	0.068	0.50	0.102
Phenanthrene	**0.82**	**0.001**	**0.89**	**<0.001**
Anthracene	**0.70**	**0.012**	**0.71**	**0.009**
Fluoranthene	**0.80**	**0.003**	**0.90**	**<0.001**
Pyrene	**0.85**	**<0.001**	**0.91**	**<0.001**
Benzo[ghi]flouranthene	0.81	0.100	0.34	0.578
Cyclopenta[cd]pyrene	**0.75**	**0.005**	**0.60**	**0.040**
Benzo[a]anthracene	**0.85**	**<0.001**	**0.83**	**<0.001**
Chrysene	0.79	0.064	0.75	0.083
Benzo[b]fluoranthene	**0.86**	**<0.001**	**0.90**	**<0.001**
Benzo[k]fluoranthene	**0.93**	**<0.001**	**0.87**	**0.002**
Benzo[a]pyrene	**0.90**	**<0.001**	**0.93**	**<0.001**
Benzo[e]pyrene	**0.89**	**<0.001**	**0.88**	**<0.001**
Perylene	0.23	0.466	0.04	0.908
Indeno[1,2,3-cd]pyrene	**0.88**	**<0.001**	**0.88**	**<0.001**
Dibenzo[a,h]anthracene	**0.86**	**<0.001**	**0.89**	**<0.001**
Picene	**0.86**	**<0.001**	**0.88**	**<0.001**
Benzo[ghi]perylene	**0.86**	**<0.001**	**0.87**	**0.001**
Coronene	**0.90**	**<0.001**	**0.90**	**<0.001**
Dibenz[a,e]pyrene	0.22	0.487	0.34	0.277

r>0.7 with p value<0.05 are shown in bold

Table 2-3 Correlation between IL-8/active ERK and n-alkanes

n-alkanes	IL-8		p-ERK	
	r	p value	r	p value
n-alkanes sum	0.36	0.248	0.59	0.044
n-C21	-0.12	0.880	0.95	0.054
n-C22	0.12	0.848	0.79	0.115
n-C23	0.10	0.871	0.81	0.100
n-C24	0.15	0.806	0.87	0.053
n-C25	0.41	0.420	**0.92**	**0.010**
n-C26	-0.49	0.181	-0.22	0.575
n-C27	**0.87**	**<0.001**	**0.92**	**<0.001**
n-C28	0.27	0.512	0.49	0.219
n-C29	0.36	0.252	0.22	0.498
n-C30	**0.80**	**0.002**	**0.76**	**0.004**
n-C31	**0.93**	**<0.001**	**0.83**	**<0.001**
n-C32	**0.91**	**<0.001**	**0.84**	**<0.001**
n-C33	**0.93**	**<0.001**	**0.89**	**<0.001**
n-C34	**0.83**	**<0.001**	**0.80**	**0.002**
n-C35	-0.38	0.225	-0.19	0.549
n-C36	-0.71	0.009	-0.80	0.002
n-C37	-0.10	0.760	-0.03	0.915

r>0.7 with p value<0.05 are shown in bold

Table 2-4 Correlation between IL-8/active ERK and alkylcyclohexanes & Isoprenoids

Alkylcyclohexanes & Isoprenoids	IL-8		p-ERK	
	r	p value	r	p value
Alkylcyclohexanes and Isoprenoids sum	-0.31	0.328	-0.31	0.324
Dibenzofuran	**0.61**	**0.036**	**0.76**	**0.004**
9-Methyl-fluorene	0.34	0.278	0.49	0.108
2-Methylnonadecane	0.17	0.595	0.26	0.423
3-Methylnonadecane	0.20	0.529	0.30	0.340
Nonadecylcyclohexane	-0.46	0.129	-0.76	0.005

r>0.6 with p value<0.05 are shown in bold

Table 2-5 Correlation between p16, p21, p27, LC3B levels and PAHs

PAHs	p16		p21		p27		LC3B	
	r	p value	r	p value	r	p value	r	p value
PAHs sum	0.50	0.100	0.17	0.606	**0.75**	**0.005**	**0.71**	**0.009**
1-Methylnaphthalene	0.19	0.557	-0.43	0.162	-0.21	0.512	-0.12	0.700
2-Methylnaphthalene	0.37	0.297	0.07	0.842	0.04	0.908	0.32	0.363
2,6-Dimethylnaphthalene	0.06	0.854	0.00	0.997	0.51	0.088	0.20	0.539
Fluorene	**0.69**	**0.012**	0.05	0.871	0.46	0.129	0.46	0.138
Phenanthrene	0.50	0.095	0.22	0.486	**0.69**	**0.014**	**0.69**	**0.013**
Anthracene	**0.58**	**0.047**	0.36	0.250	**0.65**	**0.022**	0.54	0.069
Fluoranthene	0.35	0.299	0.14	0.677	**0.68**	**0.020**	**0.72**	**0.012**
Pyrene	0.44	0.150	0.20	0.532	**0.74**	**0.006**	**0.72**	**0.008**
Benzo[ghi]flouranthene	-0.20	0.749	0.22	0.728	0.74	0.149	0.52	0.374
Cyclopenta[cd]pyrene	0.44	0.150	0.47	0.127	**0.81**	**0.001**	**0.63**	**0.029**
Benzo[a]anthracene	0.57	0.052	0.37	0.243	**0.77**	**0.003**	**0.71**	**0.010**
Chrysene	-0.21	0.697	0.47	0.350	0.72	0.107	0.74	0.093
Benzo[b]fluoranthene	0.44	0.150	0.17	0.591	**0.70**	**0.011**	**0.71**	**0.009**
Benzo[k]fluoranthene	0.40	0.282	0.01	0.979	0.61	0.081	0.56	0.120
Benzo[a]pyrene	0.51	0.092	0.14	0.666	**0.67**	**0.016**	**0.66**	**0.019**
Benzo[e]pyrene	0.49	0.109	0.16	0.620	**0.71**	**0.010**	**0.65**	**0.022**
Perylene	-0.21	0.520	0.28	0.373	0.34	0.279	0.03	0.926
Indeno[1,2,3-cd]pyrene	**0.63**	**0.049**	0.44	0.200	**0.78**	**0.008**	**0.85**	**0.002**
Dibenzo[a,h]anthracene	0.42	0.176	0.13	0.693	**0.68**	**0.014**	**0.66**	**0.021**
Picene	0.43	0.161	0.14	0.673	**0.69**	**0.014**	**0.65**	**0.022**
Benzo[ghi]perylene	0.56	0.095	0.29	0.416	**0.71**	**0.022**	**0.73**	**0.017**
Coronene	0.50	0.096	0.24	0.445	**0.67**	**0.018**	**0.73**	**0.007**
Dibenz[a,e]pyrene	0.00	0.999	-0.23	0.464	0.40	0.203	0.34	0.287

r>0.5 with p value<0.05 are shown in bold

Table 2-6 Correlation between p16, p21, p27, LC3B levels and n-alkanes

n-alkanes	p16		p21		p27		LC3B	
	r	p value	r	p value	r	p value	r	p value
n-alkanes sum	-0.06	0.851	-0.05	0.883	0.47	0.120	**0.65**	**0.022**
n-C21	-0.80	0.204	-0.62	0.379	-0.01	0.990	0.56	0.443
n-C22	-0.69	0.198	-0.22	0.718	0.33	0.587	0.66	0.227
n-C23	-0.80	0.104	-0.39	0.521	0.19	0.759	0.55	0.340
n-C24	-0.78	0.118	-0.41	0.497	0.21	0.738	0.57	0.315
n-C25	-0.65	0.160	0.02	0.975	0.37	0.470	0.67	0.143
n-C26	-0.16	0.683	-0.21	0.583	0.15	0.699	0.11	0.787
n-C27	0.35	0.271	0.05	0.888	**0.59**	**0.044**	**0.75**	**0.005**
n-C28	-0.44	0.277	-0.09	0.830	0.10	0.806	0.48	0.233
n-C29	0.09	0.772	0.26	0.417	0.39	0.213	0.44	0.155
n-C30	0.39	0.212	0.27	0.401	0.57	0.052	**0.71**	**0.009**
n-C31	**0.72**	**0.009**	0.13	0.689	**0.65**	**0.021**	**0.68**	**0.015**
n-C32	0.51	0.088	0.22	0.484	**0.67**	**0.018**	**0.69**	**0.013**
n-C33	**0.63**	**0.027**	0.12	0.722	**0.67**	**0.017**	**0.67**	**0.017**
n-C34	0.47	0.127	0.11	0.727	**0.60**	**0.039**	**0.60**	**0.038**
n-C35	-0.23	0.482	-0.09	0.781	-0.14	0.661	-0.07	0.830
n-C36	-0.59	0.043	-0.12	0.706	-0.54	0.071	-0.56	0.057
n-C37	-0.08	0.802	-0.31	0.321	0.00	0.993	0.09	0.787

3.5 Analysis of CMB results correlated with inflammation, aging, and macroautophagy activation

The CMB model using molecular marker was performed to calculate source contributions to OC in $PM_{2.5}$. Even though only up to 20% of organic compounds can be quantified, these have been applied for source apportionment through CMB (Schauer et al., 2000; Zheng et al., 2002). Source contribution estimates and percentages obtained from the CMB model are displayed in Figure 2-7 (Table 2-7). The percent contribution was calculated by dividing the source contribution estimates by the OC concentrations. Four sources were identified as major contributors: vegetative detritus, diesel engines, gasoline motor vehicles, and residential bituminous coal combustion soot.

The source with the highest percent contribution was gasoline motor vehicles (7.8%). The contribution of gasoline motor vehicles in summer (13.5%) was 11.6% higher than that in spring (1.9%). Vegetative detritus, a biogenic source from leaf abrasions (Rogge et al., 1993), had an overall average contribution of 6.0%. The contributions of vegetative detritus in fall (8.6%) and winter (8.4%) were higher than those in spring (3.6%) and summer (2.4%). Residential bituminous coal combustion soot sources had an average contribution to OC of 2.9%. The significantly higher contributions of residential bituminous coal combustion soot in fall (4.1%) and winter (5.9%) than in spring (1.1%) and summer (0.2%) may be due to the higher usage of residential heating during cold seasons. The contribution of diesel engines to the total samples was 2.8%. Although the contributions of diesel engines in spring (4.9%) and summer (3.1%) were higher than those in fall (1.9%) and winter (1.8%), the overall contributions were relatively consistent throughout the seasons. Although

the four identified primary sources explained approximately 18% of the total $PM_{2.5}$ source contributions, marked seasonal variations were observed.

Correlations between four major primary contributing sources and ERK activation, IL-8 production, and the expression levels of aging and macroautophagy markers were examined (Figure 2-8), and p-ERK, IL-8, p27, and LC3B showed a high correlation with vegetative detritus and residential bituminous coal combustion. Diesel engines and gasoline motor vehicle sources did not show any association. IL-8 release had high correlations with vegetative detritus (r=0.84) and residential bituminous coal combustion soot (r=0.85). Similarly, ERK activation had a high correlation with vegetative detritus (r=0.82) and residential bituminous coal combustion soot (r=0.91). The expression levels of p27 and LC3B had moderately high correlations with vegetative detritus (r=0.58, r=0.72) and residential bituminous coal combustion soot (r=0.54, r=0.63).

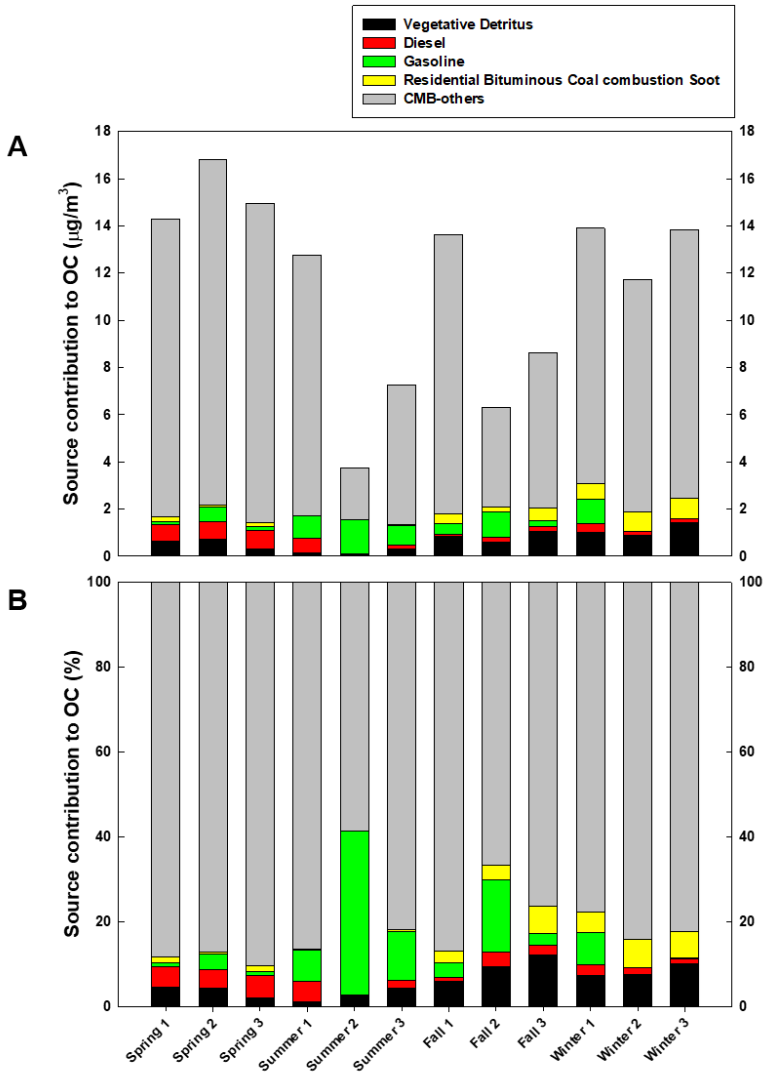

Figure 2-7 Results of the molecular marker of CMB source apportionments for the twelve samples. (A) Source contribution estimates of the four sources. (B) Percent contributions to OC of the four sources.

Table 2-7 Source apportionment of OC estimated by the CMB model (Unit: μg/m^3)

	VegDet		Diesel		GasMV		RSBT	
	SCE	std	SCE	std	SCE	std	SCE	std
Spring 1	0.65	0.07	0.71	0.19	0.11	0.19	0.21	0.03
Spring 2	0.73	0.08	0.73	0.18	0.63	0.17	0.10	0.03
Spring 3	0.31	0.04	0.79	0.18	0.15	0.15	0.19	0.03
Summer 1	0.15	0.03	0.62	0.18	0.94	0.17	0.01	0.02
Summer 2	0.11	0.02	0.00	0.06	1.44	0.26	-0.02	0.02
Summer 3	0.32	0.04	0.13	0.07	0.84	0.20	0.04	0.03
Fall 1	0.83	0.09	0.11	0.07	0.46	0.24	0.40	0.05
Fall 2	0.59	0.07	0.23	0.08	1.07	0.24	0.21	0.04
Fall 3	1.05	0.11	0.20	0.08	0.25	0.27	0.54	0.07
Winter 1	1.02	0.11	0.37	0.10	1.05	0.37	0.66	0.08
Winter 2	0.91	0.10	0.16	0.07	-0.51	0.34	0.80	0.09
Winter 3	1.41	0.15	0.16	0.08	0.02	0.36	0.86	0.10

VegDet: vegetative detritus; GasMV: gasoline vehicle emission; RSBT: residential bituminous coal combustion; SCE: source contribution estimate

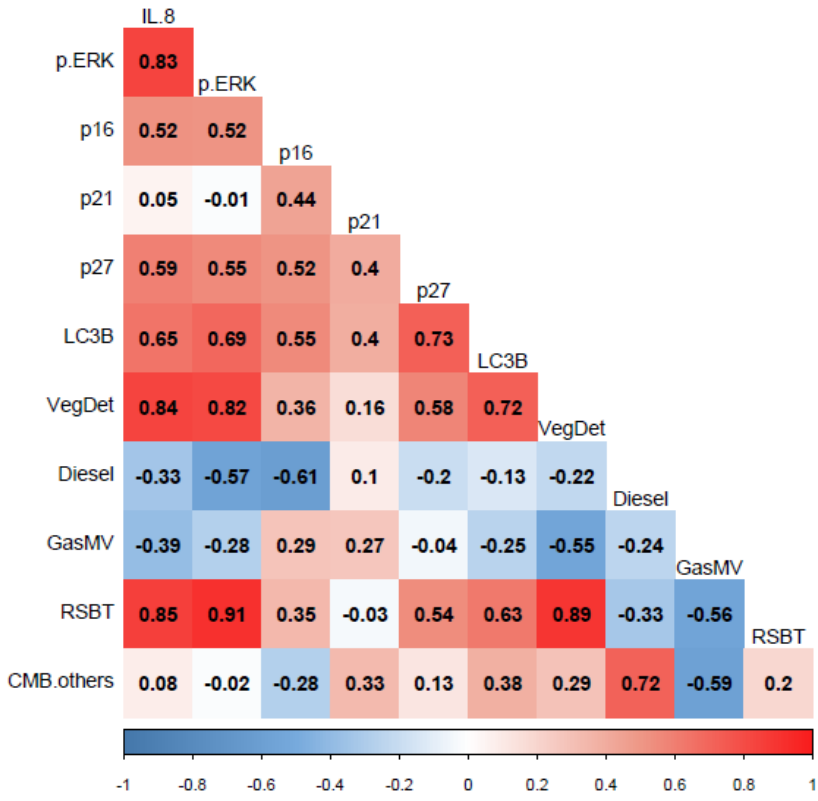

Figure 2-8 Correlation matrix between four sources and ERK activation, IL-8 production, and the expression levels of aging/macroautophagy markers (VegDet: vegetative detritus, GasMV: gasoline motor vehicles, RSBT: residential bituminous coal combustion).

4. Discussion

The constituents and sources of ambient $PM_{2.5}$ organic aerosols inducing adverse health effects are not yet well understood. In the present study, we show that organic extracts of $PM_{2.5}$ collected in Seoul during HCEs induce neutrophilic inflammation, cellular aging, and macroautophagy activation in primary lung epithelial cells. In particular, several organic constituents (i.e., PAHs and n-alkanes), as well as specific sources, including the biomass related source (i.e., vegetative detritus) and residential bituminous coal combustion soot, were found to be highly correlated with increases in inflammation and cell senescence, and macroautophagy activation.

PAHs and n-alkanes were most relevant components to mediate ERK activation-dependent IL-8 production. The PAHs compounds including benzo[a]pyrene, cyclopenta[cd]pyrene, dibenzo[a,h]anthracene, benzo[a]anthracene, benzo[b]fluoranthene, benzo[k]fluoranthene, and indeno[1,2,3-cd]pyrene were significantly involved in causing IL-8 production. Similar to our results, previous studies have demonstrated that the exposure to PAHs in $PM_{2.5}$, major components of carbonaceous species significantly induces pro-inflammatory cytokine production (Den Hartigh et al., 2010; Chen et al., 2019). The IL-8 release and ROS generation are known to be mainly related to OC, especially PAHs which are primary organic compounds from heating sources.

The average concentrations of PAHs were higher during cold seasons than that of warm seasons in Seoul and found that $PM_{2.5}$ samples from cold seasons were highly correlated with inflammation. The study which was conducted in Nanjing, China, shows similar seasonal trend. Cold seasons have higher levels of PAHs which

mediate lung epithelial cell death and inflammation (Chen et al., 2019). While many studies have reported that $PM_{2.5}$ induces the release of several inflammatory cytokines such as IL-1β, IL-6, TNF-α, organic extracts of $PM_{2.5}$ collected in Seoul specifically induced IL-8 production, which might be due to the difference in chemical composition of $PM_{2.5}$ from different locations and difference in cell-type.

PAHs may be emitted both from natural and anthropogenic sources. However, anthropogenically produced PAHs are predominant (Maliszewska-Kordybach, 1999). Due to the relationship between temperature and vapor pressure, airborne PAHs are more likely to bound to particulate matter in winter; on the contrary, larger fraction are in gas phase in summer (Gualtieri et al., 2010; Holme et al., 2019). As PAHs are also produced in the process of incomplete combustion of organic materials (Kim et al., 2013), high concentrations of PAHs during fall and winter may have affected high contributions of residential bituminous coal combustion soot.

In this study, n-alkanes with high molecular weight such as C27 to C34 were significantly correlated with inflammation. N-alkanes are usually used as marker for sources such as coal combustion, motor vehicle exhaust, and vegetative detritus and are well-known to be related to IL-8 release and ROS generation (Perrone et al., 2013; Chen et al., 2019). In this study, vegetative detritus which is a biogenic source was identified by n-alkanes. Though the average carbon preference index (CPI) (Tissot and Welte, 1984) of the analyzed samples was 0.8 which indicates the anthropogenic influence of the source.

Many epidemiologic studies have discovered the association between $PM_{2.5}$ sources and mortality (Laden et al., 2000; Ostro et al., 2011; Heo et al., 2014). In

Korea, biomass burning, gasoline, and diesel emission sources were found to be substantially associated with cardiovascular and respiratory mortality (Heo et al., 2014). Toxicological studies have found the cytotoxicity and adverse health effects of sources such as combustion and vehicle emission (Lippmann and Chen, 2009; Diaz et al., 2012; Künzi et al., 2015; Wang et al., 2016; Velali et al., 2018; Xu et al., 2020). In this study, vegetative detritus and residential bituminous coal combustion sources were found to be highly correlated with inflammation, aging and macroautophagy activation. No significant correlation between vehicle emission sources and inflammation, aging and macroautophagy markers may be resulted from usage of different $PM_{2.5}$ collection method such as particles generated in smog chamber or SRM, cell types and receptor model such as positive matrix factorization from EPA (Künzi et al., 2015; Xu et al., 2020; Leclercq et al., 2016).

5. Conclusions

Organic extracts of $PM_{2.5}$ collected in Seoul, South Korea, during HCEs induced inflammation, cellular aging, and macroautophagy activation in primary lung epithelial cells. The average mass concentrations, OC and EC had no significant correlations with $PM_{2.5}$ effects. Both PAHs and n-alkanes were the most relevant components of $PM_{2.5}$ for inflammation, aging and macroautophagy activation. The findings support the idea that the chemical constituents of $PM_{2.5}$ are more important than the level of $PM_{2.5}$ mass concentrations and even low concentration of $PM_{2.5}$ may have adverse impacts on the public health (Feng et al., 2016; Elliott and Copes, 2011; Park et al., 2018).

To our knowledge, this is the first study to assess the effects of organic compounds of seasonal ambient $PM_{2.5}$ collected in Seoul on inflammation, cellular aging, and macroautophagy in primary lung epithelial cells. Though the cells were not cultured at the air-liquid interface which provide similar environment as human lungs, $PM_{2.5}$ organic extracts exposure to the cells from various donors have led to similar results. Our results may be used as a reference for the implementation of $PM_{2.5}$ reduction policy based on chemical constituents and sources which cause adverse health effects. The limitation of this study was that we did not consider other chemical constituents which may have affected lung epithelial cells. Therefore, further studies which analyze other chemical constituents of $PM_{2.5}$ with larger number of samples for detailed source apportionment are needed.

References

Alessandria, L., Schilirò, T., Degan, R., Traversi, D. and Gilli, G., 2014. Cytotoxic response in human lung epithelial cells and ion characteristics of urban-air particles from Torino, a northern Italian city. *Environmental Science and Pollution Research*, *21*(8), pp.5554-5564.

Anenberg, S.C., Horowitz, L.W., Tong, D.Q. and West, J.J., 2010. An estimate of the global burden of anthropogenic ozone and fine particulate matter on premature human mortality using atmospheric modeling. *Environmental health perspectives*, *118*(9), pp.1189-1195.

Baird, W.M. and Hooven, L.A., 2005. a Mahadevan, Brinda. *Carcinogenic polycyclic aromatic hydrocarbon-DNA adducts and mechanism of action. Environmental and Molecular Mutagenesis*, *45*, pp.106-114.

Bell, M.L., Ebisu, K., Leaderer, B.P., Gent, J.F., Lee, H.J., Koutrakis, P., Wang, Y., Dominici, F. and Peng, R.D., 2014. Associations of PM2. 5 constituents and sources with hospital admissions: analysis of four counties in Connecticut and Massachusetts (USA) for persons≥ 65 years of age. *Environmental health perspectives*, *122*(2), pp.138-144.

Cachon, B.F., Firmin, S., Verdin, A., Ayi-Fanou, L., Billet, S., Cazier, F., Martin, P.J., Aissi, F., Courcot, D., Sanni, A. and Shirali, P., 2014. Proinflammatory effects and oxidative stress within human bronchial epithelial cells exposed to atmospheric particulate matter (PM2. 5 and PM> 2.5) collected from Cotonou, Benin. *Environmental pollution*, *185*, pp.340-351.

Chen, Q., Luo, X.S., Chen, Y., Zhao, Z., Hong, Y., Pang, Y., Huang, W., Wang, Y. and Jin, L., 2019. Seasonally varied cytotoxicity of organic components in PM2.5 from urban and industrial areas of a Chinese megacity. *Chemosphere*, *230*, pp.424-431.

Coulter, C.T., 2004. EPA-CMB8.2 users manual. *http://www. epa. gov/scram001/ models/receptor/EPA-CMB82Manual. pdf*.

Dan, M.O., Zhuang, G., Li, X., Tao, H. and Zhuang, Y., 2004. The characteristics of carbonaceous species and their sources in PM2.5 in Beijing. *Atmospheric Environment*, *38*(21), pp.3443-3452.

Davel, A.P., Lemos, M., Pastro, L.M., Pedro, S.C., de André, P.A., Hebeda, C., Farsky, S.H., Saldiva, P.H. and Rossoni, L.V., 2012. Endothelial dysfunction in the pulmonary artery induced by concentrated fine particulate matter exposure is associated with local but not systemic inflammation. *Toxicology*, *295*(1-3), pp.39-46.

Den Hartigh, L.J., Lame, M.W., Ham, W., Kleeman, M.J., Tablin, F. and Wilson, D.W., 2010. Endotoxin and polycyclic aromatic hydrocarbons in ambient fine particulate matter from Fresno, California initiate human monocyte inflammatory responses mediated by reactive oxygen species. *Toxicology in Vitro*, *24*(7), pp.1993-2002.

Diaz, E.A., Chung, Y., Papapostolou, V., Lawrence, J., Long, M.S., Hatakeyama, V., Gomes, B., Calil, Y., Sato, R., Koutrakis, P. and Godleski, J.J., 2012. Effects of fresh and aged vehicular exhaust emissions on breathing pattern and cellular responses–pilot single vehicle study. *Inhalation toxicology*, *24*(5), pp.288-295.

Dilger, M., Orasche, J., Zimmermann, R., Paur, H.R., Diabaté, S. and Weiss, C., 2016. Toxicity of wood smoke particles in human A549 lung epithelial cells: the role of PAHs, soot and zinc. *Archives of toxicology*, *90*(12), pp.3029-3044.

Donaldson K, Stone V, Borm P, Jimenez L, Gilmour P, Schins R, Knaapen A, Rahman I, Faux S, Brown D, MacNee W (2003) Oxidative stress and calcium signaling in the adverse effects of environmental particles (PM_{10}). *Free Radic.ell Biol. Med. 34* (11), 1369-1382. DOI 10.1016/S0891-5849(03)00150-3.

Elliott, C.T. and Copes, R., 2011. Burden of mortality due to ambient fine particulate air pollution (PM 2.5) in interior and Northern BC. *Canadian journal of public health*, *102*(5), pp.390-393.

Feng, S., Gao, D., Liao, F., Zhou, F. and Wang, X., 2016. The health effects of ambient PM2.5 and potential mechanisms. *Ecotoxicology and environmental safety*, *128*, pp.67-74.

Gilli, G., Pignata, C., Schilirò, T., Bono, R., La Rosa, A. and Traversi, D., 2007. The mutagenic hazards of environmental PM2.5 in Turin. *Environmental research*, *103*(2), pp.168-175.

Gualtieri, M., Øvrevik, J., Holme, J.A., Perrone, M.G., Bolzacchini, E., Schwarze, P.E. and Camatini, M., 2010. Differences in cytotoxicity versus pro-inflammatory potency of different PM fractions in human epithelial lung cells. *Toxicology in vitro*, *24*(1), pp.29-39.

Gualtieri, M., Øvrevik, J., Mollerup, S., Asare, N., Longhin, E., Dahlman, H.J., Camatini, M. and Holme, J.A., 2011. Airborne urban particles (Milan winter-PM2.5) cause mitotic arrest and cell death: Effects on DNA, mitochondria, AhR binding and spindle organization. *Mutation Research/Fundamental and Molecular Mechanisms of Mutagenesis*, *713*(1-2), pp.18-31.

Kebin, H., Fumo, Y. and Yongliang, M., 2001. The characteristics of PM2.5 in Beijing. *China*, *35*(29), pp.4959-4970.

Heo, J., Schauer, J.J., Yi, O., Paek, D., Kim, H. and Yi, S.M., 2014. Fine particle air pollution and mortality: importance of specific sources and chemical species. *Epidemiology*, pp.379-388.

Holme, J.A., Brinchmann, B.C., Refsnes, M., Låg, M. and Øvrevik, J., 2019. Potential role of polycyclic aromatic hydrocarbons as mediators of cardiovascular effects from combustion particles. *Environmental Health*, *18*(1), pp.1-18.

Hsu A, Esty D, Levy M, de Sherbinin A (2016) *The 2016 Environmental Performance Index Report, Technical Report*; Yale Center for Environmental Law and Policy: New Haven, CT.

Kloog, I., Ridgway, B., Koutrakis, P., Coull, B.A. and Schwartz, J.D., 2013. Long-and short-term exposure to PM2. 5 and mortality: using novel exposure models. *Epidemiology (Cambridge, Mass.)*, *24*(4), p.555.

Künzi, L., Krapf, M., Daher, N., Dommen, J., Jeannet, N., Schneider, S., Platt, S., Slowik, J.G., Baumlin, N., Salathe, M. and Prévôt, A.S., 2015. Toxicity of aged gasoline exhaust particles to normal and diseased airway epithelia. *Scientific reports*, *5*(1), pp.1-10.

Kuwano, K., Araya, J., Hara, H., Minagawa, S., Takasaka, N., Ito, S., Kobayashi, K. and Nakayama, K., 2016. Cellular senescence and autophagy in the pathogenesis of chronic obstructive pulmonary disease (COPD) and idiopathic pulmonary fibrosis (IPF). *Respiratory investigation*, *54*(6), pp.397-406.

Laden, F., Neas, L.M., Dockery, D.W. and Schwartz, J., 2000. Association of fine particulate matter from different sources with daily mortality in six US cities. *Environmental health perspectives*, *108*(10), pp.941-947.

Lanki, T., de Hartog, J.J., Heinrich, J., Hoek, G., Janssen, N.A., Peters, A., Stölzel, M., Timonen, K.L., Vallius, M., Vanninen, E. and Pekkanen, J., 2006. Can we identify sources of fine particles responsible for exercise-induced ischemia on days with elevated air pollution? The ULTRA study. *Environmental health perspectives*, *114*(5), pp.655-660.

Leclercq, B., Happillon, M., Antherieu, S., Hardy, E.M., Alleman, L.Y., Grova, N., Perdrix, E., Appenzeller, B.M., Guidice, J.M.L., Coddeville, P. and Garçon, G., 2016. Differential responses of healthy and chronic obstructive pulmonary diseased human bronchial epithelial cells repeatedly exposed to air pollution-derived PM4. *Environmental Pollution*, *218*, pp.1074-1088.

Lee, K.H., Jang, A.H. and Yoo, C.G., 2015. 17-Allylamino-17-Demethoxygeldanamycin and the Enhancement of PS-341–Induced Lung Cancer Cell Death by Blocking the NF-κB and PI3K/Akt Pathways. *American journal of respiratory cell and molecular biology*, *53*(3), pp.412-421.

Lee, K.H., Jeong, J., Koo, Y.J., Jang, A.H., Lee, C.H. and Yoo, C.G., 2017. Exogenous neutrophil elastase enters bronchial epithelial cells and suppresses cigarette smoke extract–induced heme oxygenase-1 by

cleaving sirtuin 1. *Journal of Biological Chemistry*, *292*(28), pp.11970-11979.

Lee, K.H., Lee, C.H., Woo, J., Jeong, J., Jang, A.H. and Yoo, C.G., 2018. Cigarette smoke extract enhances IL-17A-induced IL-8 production via up-regulation of IL-17R in human bronchial epithelial cells. *Molecules and cells*, *41*(4), p.282.

Lippmann, M. and Chen, L.C., 2009. Health effects of concentrated ambient air particulate matter (CAPs) and its components. *Critical reviews in toxicology*, *39*(10), pp.865-913.

Loomis, D., Grosse, Y. and Lauby-Secretan, B., International Agency for Research on Cancer Monograph Working Group IARC. The carcinogenicity of outdoor air pollution. *Lancet Oncol2013141262–1263*.

Lough, G.C., Christensen, C.G., Schauer, J.J., Tortorelli, J., Mani, E., Lawson, D.R., Clark, N.N. and Gabele, P.A., 2007. Development of molecular marker source profiles for emissions from on-road gasoline and diesel vehicle fleets. *Journal of the Air & Waste Management Association*, *57*(10), pp.1190-1199.

Lu, F., Xu, D., Cheng, Y., Dong, S., Guo, C., Jiang, X. and Zheng, X., 2015. Systematic review and meta-analysis of the adverse health effects of ambient PM2.5 and PM10 pollution in the Chinese population. *Environmental research*, *136*, pp.196-204.

Maliszewska-Kordybach, B., 1999. Sources, concentrations, fate and effects of polycyclic aromatic hydrocarbons (PAHs) in the environment. Part A: PAHs in air. *Polish journal of environmental studies*, *8*, pp.131-136.

Ostro, B., Tobias, A., Querol, X., Alastuey, A., Amato, F., Pey, J., Pérez, N. and Sunyer, J., 2011. The effects of particulate matter sources on daily mortality: a case-crossover study of Barcelona, Spain. *Environmental health perspectives*, *119*(12), pp.1781-1787.

Park, J., Park, E.H., Schauer, J.J., Yi, S.M. and Heo, J., 2018. Reactive oxygen species (ROS) activity of ambient fine particles (PM2.5) measured in Seoul, Korea. *Environment international*, *117*, pp.276-283.

Pease, J.E. and Sabroe, I., 2002. The role of interleukin-8 and its receptors in inflammatory lung disease. *American Journal of Respiratory Medicine*, *1*(1), pp.19-25.

Perrone, M.G., Gualtieri, M., Consonni, V., Ferrero, L., Sangiorgi, G., Longhin, E., Ballabio, D., Bolzacchini, E. and Camatini, M., 2013. Particle size, chemical composition, seasons of the year and urban, rural or remote site origins as determinants of biological effects of particulate matter on pulmonary cells. *Environmental pollution*, *176*, pp.215-227.

Pope III, C.A. and Dockery, D.W., 1999. Epidemiology of particle effects. In *Air pollution and health* (pp. 673-705). Academic Press.

Putaud, J.P., Van Dingenen, R., Alastuey, A., Bauer, H., Birmili, W., Cyrys, J., Flentje, H., Fuzzi, S., Gehrig, R., Hansson, H.C. and Harrison, R.M., 2010. A European aerosol phenomenology–3: Physical and chemical characteristics of particulate matter from 60 rural, urban, and kerbside sites across Europe. *Atmospheric Environment*, *44*(10), pp.1308-1320.

Qiao, L., Cai, J., Wang, H., Wang, W., Zhou, M., Lou, S., Chen, R., Dai, H., Chen, C. and Kan, H., 2014. PM2.5 constituents and hospital emergency-room visits in Shanghai, China. *Environmental science & technology*, *48*(17), pp.10406-10414.

Richman-Eisenstat, J.B., Jorens, P.G., Hebert, C.A., Ueki, I. and Nadel, J.A., 1993. Interleukin-8: an important chemoattractant in sputum of patients with chronic inflammatory airway diseases. *American Journal of Physiology-Lung Cellular and Molecular Physiology*, *264*(4), pp.L413-L418.

Rogge, W.F., Hildemann, L.M., Mazurek, M.A., Cass, G.R. and Simoneit, B.R., 1993. Sources of fine organic aerosol. 5. Natural gas home appliances. *Environmental science & technology*, *27*(13), pp.2736-2744.

Rumelhard, M., Ramgolam, K., Auger, F., Dazy, A.C., Blanchet, S., Marano, F. and Baeza-Squiban, A., 2007. Effects of PM2.5 components in the release

of amphiregulin by human airway epithelial cells. *Toxicology letters*, *168*(2), pp.155-164.

Schauer, J.J. and Cass, G.R., 2000. Source apportionment of wintertime gas-phase and particle-phase air pollutants using organic compounds as tracers. *Environmental science & technology*, *34*(9), pp.1821-1832.

Shah, A.S., Lee, K.K., McAllister, D.A., Hunter, A., Nair, H., Whiteley, W., Langrish, J.P., Newby, D.E. and Mills, N.L., 2015. Short term exposure to air pollution and stroke: systematic review and meta-analysis. *bmj*, *350*.

Song, L., Li, D., Li, X., Ma, L., Bai, X., Wen, Z., Zhang, X., Chen, D. and Peng, L., 2017. Exposure to PM2.5 induces aberrant activation of NF-κB in human airway epithelial cells by downregulating miR-331 expression. *Environmental toxicology and pharmacology*, *50*, pp.192-199.

Tissot, B.P. and Welte, D.H., 2013. *Petroleum formation and occurrence*. Springer Science & Business Media.

Tsai, S.S., Chang, C.C. and Yang, C.Y., 2013. Fine particulate air pollution and hospital admissions for chronic obstructive pulmonary disease: a case-crossover study in Taipei. *International journal of environmental research and public health*, *10*(11), pp.6015-6026.

Vedal, S., Campen, M.J., McDonald, J.D., Larson, T.V., Sampson, P.D., Sheppard, L., Simpson, C.D. and Szpiro, A.A., 2013. National Particle Component Toxicity (NPACT) initiative report on cardiovascular effects. *Research Report (Health Effects Institute)*, (178), pp.5-8.

Velali, E., Papachristou, E., Pantazaki, A., Besis, A., Samara, C., Labrianidis, C. and Lialiaris, T., 2018. In vitro cellular toxicity induced by extractable organic fractions of particles exhausted from urban combustion sources-Role of PAHs. *Environmental Pollution*, *243*, pp.1166-1176.

Wang, F.F., Geng, C.M., Hao, W.D., Zhao, Y.D., Qin, L.I., Wang, H.M. and Yan, Q.I.A.N., 2016. The cellular toxicity of PM2.5 emitted from coal combustion in human umbilical vein endothelial cells. *Biomedical and Environmental Sciences*, *29*(2), pp.107-116.

Wang, S., Prophete, C., Soukup, J.M., Chen, L.C., Costa, M., Ghio, A., Qu, Q., Cohen, M.D. and Chen, H., 2010. Roles of MAPK pathway activation during cytokine induction in BEAS-2B cells exposed to fine World Trade Center (WTC) dust. *Journal of immunotoxicology*, *7*(4), pp.298-307.

Xing, Y.F., Xu, Y.H., Shi, M.H. and Lian, Y.X., 2016. The impact of PM2.5 on the human respiratory system. *Journal of thoracic disease*, *8*(1), p.E69.

Xu, F., Shi, X., Qiu, X., Jiang, X., Fang, Y., Wang, J., Hu, D. and Zhu, T., 2020. Investigation of the chemical components of ambient fine particulate matter (PM2. 5) associated with in vitro cellular responses to oxidative stress and inflammation. *Environment international*, *136*, p.105475.

Zhang, Y., Schauer, J.J., Zhang, Y., Zeng, L., Wei, Y., Liu, Y. and Shao, M., 2008. Characteristics of particulate carbon emissions from real-world Chinese coal combustion. *Environmental science & technology*, *42*(14), pp.5068-5073.

Zheng, M., Cass, G.R., Schauer, J.J. and Edgerton, E.S., 2002. Source apportionment of PM2.5 in the southeastern United States using solvent-extractable organic compounds as tracers. *Environmental science & technology*, *36*(11), pp.2361-2371.

Lee, K.H., Lee, C.H., Woo, J., Jeong, J., Jang, A.H. and Yoo, C.G., 2018. Cigarette smoke extract enhances IL-17A-induced IL-8 production via up-regulation of IL-17R in human bronchial epithelial cells. *Molecules and cells*, *41*(4), p.282.

Chapter 3.

Source apportionment of $PM_{2.5}$ in Seoul, South Korea and Beijing, China

ABSTRACT

East Asian countries experience severe air pollution owing to their rapid development and urbanization induced by substantial economic activities. South Korea and China are among the most polluted East Asian countries with high mass concentrations of $PM_{2.5}$. Even though the occurrence of transboundary air pollution among neighboring countries has been recognized, studies involving simultaneous ground-based $PM_{2.5}$ monitoring and source apportionment in South Korea and China have not been conducted so far. This study was designed to conduct simultaneous daily ground-based continuous monitoring of $PM_{2.5}$ in Seoul and Beijing for one year. The mass concentrations of $PM_{2.5}$ and its major chemical components were analyzed simultaneously at Seoul and Beijing during 2019. The positive matrix factorization model was utilized for the source apportionment of ambient $PM_{2.5}$ in the two sites. Secondary nitrate, secondary sulfate, mobile, biomass burning, incineration, soil and aged sea salt sources were identified as contributing factors at both sites. Additionally, for Seoul site, industry combined with coal combustion and oil combustion sources were identified while industry and coal combustion sources were identified for Beijing site. Ionic species accounted for more than 50% of the total mass concentration of $PM_{2.5}$, and secondary nitrate and secondary sulfate were the most dominant sources in both sites. Since secondary aerosols are largely affected by precursors from primary emissions and meteorological conditions, the variations in the heating and non-heating seasons were analyzed. Potential source contribution function maps showed that the potential source areas of secondary nitrate and secondary sulfate in Seoul and Beijing were mostly from long-range transport. During the heating season, industrial complex areas in northern China were shown

as potential source areas for Beijing and coal-fired power plants near the Yangtze River and Henan province were identified as potential source areas for Seoul. During the non-heating season, coastal areas in eastern China to west part of South Korea were found to be potential source areas of secondary nitrate and secondary sulfate in both sites.

Keywords: $PM_{2.5}$, source apportionment, positive matrix factorization (PMF), potential source contribution function (PSCF)

1. Introduction

East Asian countries experience severe air pollution because of their rapid development and urbanization induced by substantial economic activities. Fine particulate matter ($PM_{2.5}$) in air is a critical pollutant because of its ability to penetrate the lungs through inhalation, which can cause adverse health effects such as local and systemic inflammation (Dockery et al., 1993; Pinkerton et al., 2000; Kocbach, 2008; Feng et al., 2016).

Among all East Asian countries, South Korea and China are among the most polluted. Both countries are actively pursuing the reduction of $PM_{2.5}$ concentrations in air by implementing stringent air quality policies. In Korea, the Comprehensive Action Plan on Fine Dust was implemented in 2017, which aimed to reduce $PM_{2.5}$ emissions by 30% by 2022 in comparison to the level in 2014 and to reduce the annual average $PM_{2.5}$ concentration in Seoul to 17–18 $\mu g/m^3$ (Lee, 2018). China has achieved a major goal of reducing the annual average $PM_{2.5}$ concentration in Beijing to less than 60 $\mu g/m^3$ in 2017 that was set in the Action Plan on Prevention and Control of Air Pollution (hereinafter Action Plan) (Zhang et al., 2016).

In spite of these efforts toward $PM_{2.5}$ reduction, China and South Korea are ranked second and third in East Asia, respectively, in terms of the highest annual average $PM_{2.5}$ concentration (Air, 2019). Forty-seven cities in China are in the top 100 polluted cities in the world. The $PM_{2.5}$ level in South Korea was the highest among the Organisation for Economic Cooperation and Development (OECD) countries in 2019 (Air, 2019). Since the commencement of $PM_{2.5}$ monitoring in 2015 in South Korea, high daily average $PM_{2.5}$ concentrations have been observed

between January and March and continuous high concentration events have occurred because of the stagnation of air masses caused by low wind speeds of less than 2 m/s.

As China is among the largest countries in the world, the deterioration in its air quality has regional and international impacts because of the long-range transport of pollutants to other Asian countries that are downwind and even to North America (Wuebbles et al., 2007). Transboundary air pollution affects neighboring countries because of the conducive meteorological and geographical characteristics. Numerous studies are available on the characterization and source apportionment of $PM_{2.5}$ in South Korea and China; however, studies on simultaneous ground-based $PM_{2.5}$ monitoring and source apportionment in both South Korea and China are not available. To implement an effective $PM_{2.5}$ reduction and control policy in South Korea and China, it is important to perform a comprehensive investigation in the major cities of both countries.

In this study, simultaneous ground-based monitoring of $PM_{2.5}$ in Seoul in South Korea and Beijing in China were conducted for a period of one year including the analysis of chemical components of the particulate matter samples. The positive matrix factorization (PMF) model was applied to the results for identifying sources, source-wise apportionment of pollutants, and the estimation of various contributing factors to the observed ambient $PM_{2.5}$ values of both cities. In addition, the potential source contribution function (PSCF) was applied to the backward air trajectories of the two cities to delineate the potential emission source areas.

2. Methods

2.1 Description of sampling sites

Samples of $PM_{2.5}$ were collected simultaneously in Seoul, South Korea and Beijing, China from January 2019 to December 2019. Daily samples were collected for 23 h at both sites. In Seoul, $PM_{2.5}$ samples were collected on the rooftop of the Graduate School of Public Health building (37.465°N, 126.954°E) at Seoul National University (SNU). SNU is located in the southern part of Seoul where heavy transportation, mountains, and residential areas coexist. In China, the samples were collected from the Chinese Research Academy of Environmental Sciences (40.042°N, 116.413°E), which is located in the periphery of the fifth ring road, approximately 15 km north of the center of Beijing.

2.2 Sampling procedure and chemical analyses

Identical sets of sampling equipment consisting of a three-channel low-volume air sampler and a high-volume air sampler (TE-HVPLUS, TISCH, USA) were installed at the two sites. The three-channel low-volume air sampler consisted of a filter pack system (URG-2000-30FG, URG, USA) and a cyclone (URG-2000-30EH, URG, USA) and had a flow rate of 16.7 L min^{-1}. In each channel of the low-volume air sampler, two different Teflon filters (PTFE, MTL, UK; PTFE, Pall Corporation, USA) and a quartz filter (quartz microfiber filter, Pall Corporation, USA) were loaded to collect $PM_{2.5}$. The Teflon filters were used to measure mass concentration using a semi-micro balance (accuracy of 0.01 mg) (CP225D, Sartorius, Germany). The concentrations of the trace elements were analyzed using an energy

dispersive X-ray fluorescence (EDXRF) spectrometer (EDXRF Spectrometer, Thermo Fisher, USA) at the Mokpo University. Seventeen trace elements (Mg, Al, Si, Ca, Ti, V, Cr, Mn, Ba, Fe, Ni, Cu, Zn, As, Se, Br, and Pb) were analyzed. Among the 17 trace elements, crustal elements were calculated using the following equation (Gu et al., 2010; Miller-Schulze et al., 2015) and others were classified as non-crustal elements.

$$[\text{Crustal}] = 1.889[\text{Al}] + 1.400[\text{Ca}] + 1.430[\text{Fe}] + 1.658[\text{Mg}] + 1.582[\text{Mn}] + 2.139[\text{Si}] + 1.668[\text{Ti}]$$

Ionic species (SO_4^{2-}, NO_3^-, NH_4^+, Na^+, K^+, Cl^-) were analyzed using ion chromatography (ICS-1100, Thermo Fisher Scientific, USA). The carbonaceous species (OC: organic carbon and EC: elemental carbon) were analyzed using a carbon aerosol analyzer (Model 3, Sunset Laboratory Inc., USA). The details of the analytical methods were given in a previous study (Park et al., 2018). The high-volume air samplers with a flow rate of 40 cfm were loaded with quartz microfiber filters (Whatman™, UK). The filters were prebaked for 12 h at 450 °C before use and were stored in the freezer at −20 °C. The $PM_{2.5}$ collected using the high-volume air samplers were used for the analysis of carbonaceous species.

2.3 Source apportionment using PMF

Receptor models, especially multivariate factor analysis models such as PMF and UNMIX have been widely used in many previous studies (Heo et al., 2009, 2017; Deng et al., 2018; Jain et al., 2020; Park et al., 2020; Khan et al., 2021). In this study, EPA's PMF 5.0 was employed for the source apportionment of $PM_{2.5}$ in Seoul

and Beijing. Inputs include mass concentrations of chemical components and associated uncertainties. This study used the uncertainty calculation method described by Heo et al. (2009).

A total of 26 parameters, namely $PM_{2.5}$, OC, EC, Na^+, NO_3^-, SO_4^{2-}, NH_4^+, K^+, Cl^-, Mg, Al, Si, Ca, Ti, V, Cr, Mn, Ba, Fe, Ni, Cu, Zn, As, Se, Br, and Pb, were analyzed for the samples from the Seoul and Beijing sites. Species with low signal to noise ratio were selected as 'weak' or excluded for both sites (Paatero and Hopke, 2003). The $PM_{2.5}$ concentration was selected as a total variable and 12% of additional modeling uncertainty was included to avoid unconsidered errors. The PMF model was run multiple times to find the optimal number of factors that can explain the distribution of parameters at the two receptor sites. The PMF model identified nine factors for both sites. In addition, bootstrap, displacement, and bootstrap–displacement analyses were performed for error estimation.

2.4 Conditional probability function (CPF)

To better understand the location of the sources using wind direction and wind speed, the conditional probability function (CPF) were obtained using the R Openair Package (Carslaw and Ropkins, 2012). Wind speed and wind direction data were obtained from the Korea Meteorological Administration's website (http://www.kma.go.kr). Hourly data from the automated synoptic observing system (37.44°N, 126.96°E), which is located 2.3 km from the Seoul sampling site, were used. For Beijing, hourly archived meteorological data from Beijing International

Airport (40.08°N, 116.58°E) which is located at 15.2 km northeast of the sampling site was used.

2.5 Backward trajectory and potential source contribution function (PSCF)

The PSCF is an effective tool that is widely used to locate possible source areas (Begum et al., 2010; Heo et al., 2013; Zong et al., 2018). We combined the generated backward trajectories at each site with daily contribution data from the sources indicated by the PMF results.

Backward trajectories for the two sites were derived by the hybrid single-particle Lagrangian integrated trajectory 4 (HYSPLIT 4) model of the National Oceanic and Atmospheric Administration, USA. Meteorological data with a resolution of 1° from the Global Data Assimilation System (GDAS) were used to calculate the 72 h backward trajectory endpoint dataset for every hour at half of the mixing height at each site. GDAS 1° was selected because of its better performance in retrieving contributions from various directions (Su et al., 2015).

If the air parcel arriving at the *ij*th cell has a high PSCF value, this indicates that it is a potential source location. The equation is PSCFij = mij/nij. The total number of end points that pass the *ij*th cell is nij. The number of end points that pass the *ij*th cell when the source concentrations are higher than a criterion value is mij. In this study, the criterion value was the 75th percentile of each source contribution concentration. To avoid high uncertainties, the weight function was applied to

calculate the PSCF value, and the equation described by Heo et al. (2013) was used. The joint-PSCF (j-PSCF), which can identify the significantly influencing potential areas at both the Seoul and Beijing sites, was used.

3. Results and Discussion

3.1 Seasonal variations of chemical constituents of $PM_{2.5}$

A summary of the annual and seasonal variations of $PM_{2.5}$ and its chemical constituents during 2019 at the two sites are presented in Table 3-1. $PM_{2.5}$ samples were collected for a total of 313 days in Seoul and 227 days in Beijing during 2019. Flow rate, $PM_{2.5}$ mass closures, and ion balance were considered for elimination and for arriving at the final number of samples. Temporal variations of chemical constituents of $PM_{2.5}$ in Seoul and Beijing are shown in Figure 3-1.

Table 3-1 Summary of $PM_{2.5}$ and chemical constituents in Seoul and Beijing

Chemical species	Unit	Seoul										Beijing									
		Total (N=313)		Spring (N=82)		Summer (N=77)		Autumn (N=71)		Winter (N=83)		Total (N=227)		Spring (N=63)		Summer (N=84)		Autumn (N=60)		Winter (N=20)	
		Avg.	Stdev.	Avg.	Stdev.	Avg.	Stdev.	Avg.	Stdev.	Avg.	Stdev.	Avg.	Stdev.	Avg.	Stdev.	Avg.	Stdev.	Avg.	Stdev.	Avg.	Stdev.
$PM_{2.5}$	$\mu g/m^3$	27.1	19	32.6	24	19.4	10.9	18.7	10.6	36.1	19.3	40.9	29.3	47	36.9	31.1	15.6	47.5	30.9	43.6	32.9
OC	$\mu g/m^3$	4.6	2.2	5.6	2.6	3.2	1.2	4	1.7	5.5	2.2	7.1	3.6	9.1	4.3	5.3	1.8	7.3	3	8.4	4.5
EC	$\mu g/m^3$	0.5	0.3	0.6	0.2	0.4	0.1	0.5	0.2	0.6	0.4	0.7	0.3	0.8	0.4	0.5	0.2	0.8	0.3	0.6	0.3
NO_3^-	$\mu g/m^3$	6.4	7.4	7.9	8.8	2.5	3.5	4.2	3.8	10.6	8.2	11.2	13.3	15.3	17.5	6.9	7.2	12.6	13.3	13.1	14.3
SO_4^{2-}	$\mu g/m^3$	4.4	3.3	4.6	3.7	5.3	3.2	3	2.2	4.5	3.6	5.8	4.4	6.3	5.7	6	3.7	5.3	3.8	5.1	4.4
NH_4^+	$\mu g/m^3$	3.2	3.1	3.8	4	2.5	2.1	1.8	1.4	4.3	3.4	4.4	4.3	5.4	5.8	3.6	2.8	4.4	4.1	4.7	4.7
K^+	$\mu g/m^3$	0.6	1.6	0.5	0.2	0.6	0.1	0.4	0.1	0.8	2.5	0.4	0.2	0.2	0.2	0.4	0.2	0.6	0.2	0.5	0.2
ΣTrace metals	$\mu g/m^3$	1.4	1.2	1.7	1.3	0.5	0.3	1.1	0.8	2.3	1.4	4	3.3	4.7	2.7	2.1	1	5.6	4.7	4.8	2.3
Mg	ng/m^3	-	-	-	-	-	-	-	-	-	-	213.6	150.3	246.1	134.4	142.5	66.1	279.1	211.7	213.8	107.5
Al	ng/m^3	236.5	285.9	238.3	280.4	62.3	53.7	173.5	166.8	299.7	337.3	435.2	517.6	558.5	458.3	212.6	163.4	627.9	764.9	294.9	200.4
Si	ng/m^3	479.6	519.2	603.2	589.4	167.2	117.2	426.9	367.1	664.6	629.2	1126.2	1091.5	1396.2	986.5	643.2	371.2	1599.5	1613.9	871.6	454.7
Cl	ng/m^3	308.2	351.6	299.1	336.3	23.5	18.6	167.1	168.8	676.1	314.2	598.3	934.3	696.5	789.4	85.2	83.8	847	1174.9	1756.1	1150.6
Ca	ng/m^3	160.9	150.7	200.5	130.5	78.6	36.2	134.8	96.5	220.2	218.9	716.9	495.6	870.4	448.5	449.9	211.7	940.7	669.9	682.5	340.9
Ti	ng/m^3	17.8	12.8	21.1	15.2	10.9	5.3	15.7	8.8	21.8	14.4	33	26	38.7	24.4	21.7	10.6	44.8	37.2	26.9	12.1
V	ng/m^3	1.3	1.1	1.9	1.2	1.8	1	0.6	0.4	1	0.9	0.7	0.5	0.7	0.4	0.6	0.4	0.9	0.7	0.5	0.3
Cr	ng/m^3	2.1	1.1	2.2	1.2	1.6	0.7	1.9	1.1	2.4	1.1	2.8	1.6	2.9	1.5	2.1	0.9	3.8	1.9	3.1	1.6
Mn	ng/m^3	15	9.2	18	10.4	9.3	5	12.7	7.1	19.2	9.3	34.5	22.6	32.9	16.1	23.7	9.5	50.9	32	36.1	15.9
Fe	ng/m^3	284.9	178.6	341.5	205	182.4	86.2	252.2	134.6	351.7	197.6	712.2	438.6	734.2	371.4	490.2	183.9	1005.7	589.8	693.4	338.5
Ni	ng/m^3	2.1	1.4	2.9	1.7	2.3	1.3	1.2	0.8	1.8	1.1	1.2	0.8	1.1	0.7	1.3	0.8	1.1	0.7	1.1	0.5
Cu	ng/m^3	2.8	1.7	3	1.8	2.4	1.6	2.5	1.4	3.2	2	3.6	3.9	3.8	3	2.3	0.9	4.9	6.4	4.6	2.6
Zn	ng/m^3	56	35.8	62.4	35.4	42.1	28.2	55.3	38.3	63.3	36.9	97.6	76.2	100.3	88.2	74.3	44.2	114.7	89.7	137.4	71.8
As	ng/m^3	5.4	3.6	4.1	2.4	4.4	3.7	6.7	4.5	6.1	3.1	3.6	2.4	3.3	2.5	2.8	1.8	4.7	2.9	3.9	2
Br	ng/m^3	7.8	5.1	9.9	5.4	4.7	2.1	5.9	3.5	10.1	5.7	8.4	7.4	9.9	7.5	5.2	3.6	10	9.5	13	7.2
Pb	ng/m^3	22.5	14.5	19	11.8	14.9	8.3	23.5	15.8	31.1	15.3	23.3	17.7	23.9	18.6	15.4	9.4	28.6	20	39.2	19.6

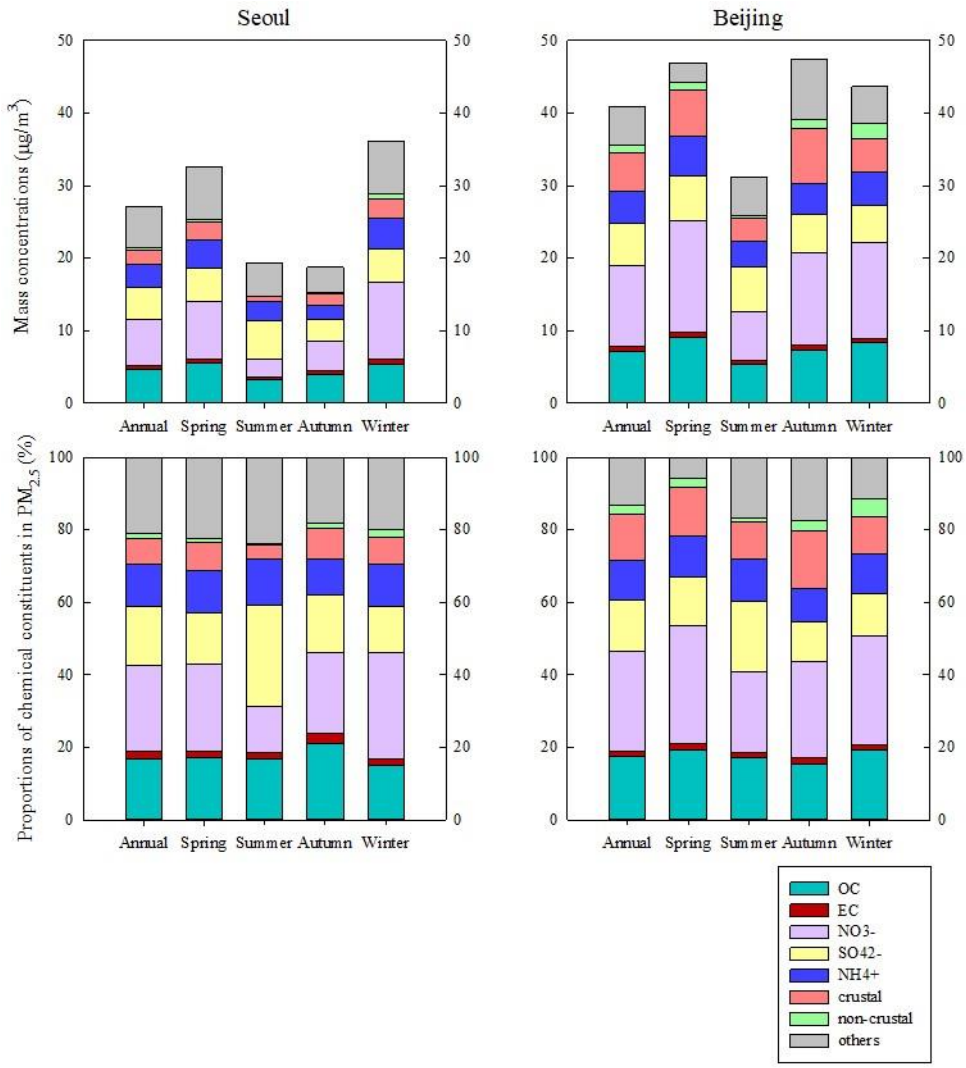

Figure 3-1 Temporal variations of chemical components of $PM_{2.5}$ in Seoul and Beijing

3.1.1 Seoul

The annual average mass concentration of $PM_{2.5}$ in 2019 was 27.1 ± 19.0 μg/m^3 in Seoul. In Seoul, the average mass concentration of $PM_{2.5}$ was the highest in winter (36.1 ± 19.3 μg/m^3) followed by spring (32.6 ± 24.0 μg/m^3), summer (19.4 ± 10.9 μg/m^3), and autumn (18.7 ± 10.6 μg/m^3). Annual and seasonal average mass concentrations of $PM_{2.5}$ did not exceed the ambient air quality standard for $PM_{2.5}$ in South Korea (24 h: 35 μg/m^3 or less), but high concentration episodes (HCEs) occurred on 70 days (approximately 20%). Most of the HCEs occurred in winter and spring. The most abundant chemical components were ionic species. The average mass concentrations of NO_3^-, SO_4^{2-}, and NH_4^+ were 6.4 ± 7.4 μg/m^3, 4.4 ± 3.3 μg/m^3, and 3.2 ± 3.1 μg/m^3, respectively, and they accounted for 23.7%, 16.3%, and 11.6% of the mass concentration of $PM_{2.5}$, respectively, which is 51.6% of the total. Although the mass concentration of $PM_{2.5}$ varied seasonally, the proportion of the ionic species in the $PM_{2.5}$ did not vary. SO_4^{2-}, which is formed at high temperatures, showed a high average concentration in summer. On the other hand, the NO_3^- concentration was four times higher in winter (10.6 ± 8.2 μg/m^3) than in summer (2.5 ± 3.5 μg/m^3) because it is likely to be formed at low temperatures. The average concentrations of OC and EC were 4.6 ± 2.2 μg/m^3 and 0.5 ± 0.3 μg/m^3, respectively. Carbonaceous species (OC: 17.0% and EC: 1.9%) accounted for 18.9% of the total mass concentration of $PM_{2.5}$. The average concentration of the carbonaceous species was the highest in spring followed by winter, autumn, and summer. The average concentrations of OC and EC in 2019 have dramatically decreased compared to those during 2013–2015, at 6.3 and 1.1 μg/m^3, respectively (Park et al., 2018). The average annual concentration of crustal elements was 1.9 ± 2.0 μg/m^3, which is

approximately 7.0% of the total mass concentration of $PM_{2.5}$. The average concentration of non-crustal elements was 0.4 ± 0.4 μg/m^3, contributing 1.5% of the total mass concentration of $PM_{2.5}$. The concentrations of crustal and non-crustal elements were higher in winter (2.7 and 0.8 μg/m^3) and spring (2.5 and 0.4 μg/m^3) compared to those in autumn (1.6 and 0.3 μg/m^3) and summer (0.7 and 0.1 μg/m^3).

3.1.2 Beijing

In Beijing, the annual mass concentration of $PM_{2.5}$ ranged from 5.1 to 165.1 μg/m^3 and the average mass concentration of $PM_{2.5}$ was 40.9 ± 29.3 μg/m^3 (Table 3-1). The average mass concentrations of $PM_{2.5}$ were the highest in autumn (47.5 ± 30.9 μg/m^3), followed by spring (47.0 ± 36.9 μg/m^3), winter (43.6 ± 32.9 μg/m^3), and summer (31.1 ± 15.6 μg/m^3). Annual and seasonal average mass concentrations of $PM_{2.5}$ were less than China's National Ambient Air Quality Standards (NAAQS) specified daily-$PM_{2.5}$ concentration of 75 μg/m^3. During the sampling period, HCEs occurred on 25 days (11%) during winter and spring. The low occurrence of HCEs was probably due to the relatively smaller number of samples collected during winter (N = 20) compared to that in other seasons (spring: N = 63, summer: N = 84, and autumn: N = 60).

The average annual concentrations of NO_3^-, SO_4^{2-}, and NH_4^+ were 11.2 ± 13.3 μg/m^3, 5.8 ± 4.4 μg/m^3, and 4.4 ± 4.3 μg/m^3, respectively, and these major ionic species accounted for 52.4% of the total mass concentration of $PM_{2.5}$. The average concentrations of NO_3^- and SO_4^{2-} were the highest in spring. While the emission of

SO_2 has reduced, the steady increase in the emission of NH_3 has led to an increase in NO_3^- (Geng et al., 2019).

Because of the implementation of the Action Plan from 2013 to 2017, SO_4^{2-} displays a substantial reduction; however, NO_3^- has the least reduction. In 2017, the contribution of SO_4^{2-} and NO_3^- in $PM_{2.5}$ was 14% and 28%, respectively (Geng et al., 2019). These results are similar to the results of our study, which suggest that efforts to reduce $PM_{2.5}$ have continued even after the Action Plan ended.

The annual average concentrations of OC and EC were 7.13 and 0.66 μg/m^3, respectively. The average concentration of OC was the highest in spring, followed by winter, autumn, and summer. The average concentration of OC in spring was 1.7 times higher than that in summer. The major sources of OC are biomass burning, coal combustion, and mobile sources, (Zheng et al., 2005) and it is likely that the contribution of these sources has decreased, resulting in seasonal variations. The average concentration of EC was the highest in autumn, followed by spring, winter, and summer. Local emissions, heating in autumn, and westerly winds might have led to the high average concentration of EC in autumn and other cold seasons (Feng et al., 2009).

The concentrations of trace elements account for 15.3% of the total mass concentration of $PM_{2.5}$. The annual average concentration of crustal elements was 5.3 ± 4.6 μg/m^3, which is about 5 times higher than that of non-crustal elements (1.0 ± 1.1 μg/m^3). The concentration of crustal elements was high in autumn and spring, whereas the concentration of non-crustal elements was high in winter and autumn. Strong winds from desert regions cause dust storms that transport a substantial

quantity of crustal elements, and thus, high concentrations in spring (Wang et al., 2007; Guan et al., 2018). The high concentration of crustal elements in autumn may be due to the high average mass concentration of $PM_{2.5}$ and the frequent occurrence of HCEs.

3.2 Source apportionment

In this study, 294 and 226 samples measured in Seoul and Beijing, respectively, were used for source apportionment. A total of 26 species were used as input data for Seoul and Beijing sites. Nine factors contributed to $PM_{2.5}$ in both cities and sources which were identified in both sites were secondary nitrate, secondary sulfate, mobile, biomass burning, incineration, soil and aged sea salt. For Seoul site, industry combined with coal combustion and oil combustion sources were identified while industry and coal combustion sources were identified for Beijing site. The source profiles of two sites are presented in Figure 3-2 and Figure 3-4, daily source contributions for the nine sources are displayed in Figure 3-3 and Figure 3-5 and a summary of the source contributions is presented in Table 3-2. The CPF plots for the biomass burning, oil combustion, mobile, incineration, industry and coal combustion sources for Seoul and Beijing were presented in Figure 3-6 and Figure 3-8, respectively, and were used as supporting evidence for evaluating regional and local transport. In addition, the CPF plots for heating and non-heating season were displayed in Figure 3-7 and Figure 3-9. Heating season represents Beijing's official central heating period which is from November 15th to March 15th. Results of the j-PSCF model using the upper 25% of two most contributing sources, secondary

nitrate and secondary sulfate are presented in Figure 3-10. The j-PSCF model enabled us to identify the significantly influential potential areas for both Seoul and Beijing sites. Moreover, PSCF maps for nine sources for each site are displayed in Figure 3-11 to Figure 3-16.

The first factor, secondary nitrate, was characterized by high loadings of NO_3^- and NH_4^+ and a medium loading of OC (Viana et al., 2008; Waked et al., 2014; Khan et al., 2021). The average contributions of secondary nitrate were 27.2% and 25.7% for Seoul and Beijing, respectively. The contributions were highest in winter (12 μg/m^3, 34.7%) and spring (16 μg/m^3, 31.7%), at Seoul and Beijing, respectively. While the lowest contributions were in summer (Seoul: 2.1 μg/m^3, 11.4%; Beijing: 6.5 μg/m^3, 21.3%) for both sites. The formation of secondary nitrate is favored under a low temperature and high relative humidity by the oxidation of NO_x (Seinfeld and Pandis, 1998; Wang et al., 2006), which explains the seasonal pattern of this factor. Secondary nitrate is usually affected by several sources including traffic, coal combustion, and industrial sources, which form the nitrate precursor NO_x, resulting in the highest contribution among the nine factors. The j-PSCF map for secondary nitrate shows two clusters of potential source locations, namely, the Hebei, Shandong, and Henan provinces and the Shanghai and Jiangsu provinces. Copious emissions from the iron and steel industry and indirect emissions from upwind industries have significantly increased the NO_x emissions from Hebei province (Yang et al., 2019). In addition, Shandong and Henan provinces, which are adjacent to each other, are also known as high-NO_x producing areas (Wang et al., 2018). The Shanghai and Jiangsu provinces have high vehicle populations and many coal-fired power plants (Zhang et al., 2017).

Secondary sulfate source account for 19.5% and 22.9% of the total $PM_{2.5}$ mass concentration at Seoul and Beijing, respectively. High loadings of SO_4^{2-} and NH_4^+ and medium loadings of OC and Fe characterize this factor. The highest contributions were in the summer for both sites (Seoul: 35.8% and Beijing: 37.6%), which is due to the active formation of SO_4^{2-} through photochemical reactions under high temperature (Seinfeld and Pandis, 1998; Huang et al., 2016; Wang et al., 2016). The j-PSCF map for secondary sulfate is similar to the one for secondary nitrate, but includes additional areas encompassing the coastal area from Shanghai, China to the western part of South Korea. Coal-fired power plants are densely located in the western part of South Korea including Shin Seocheon, Dangjin, Taean, and Boryeong. As mentioned earlier, coal-fired power plants are densely populated in the Shanghai and Jiangsu provinces, where the Yangtze River is located (Zíková et al., 2016).

Mobile sources are characterized by high loadings of OC, EC, NO_3^-, and NH_4^+ and medium loadings of Al, Si, Ca, Ti, Fe, Zn, Mn, and Ba. Mobile source emissions comprise of exhaust and non-exhaust emission markers. As OC is from primary emission sources and EC is emitted mainly from diesel exhaust, they are major markers of exhaust emissions (El Haddad et al., 2009; Heo et al., 2009; Zhang et al., 2013). Non-exhaust emission markers are Al, Fe, Ca, and Ti, which are from resuspended particles (Harrison et al., 2012; Taghvaee et al., 2018). Al, Fe, Ba, and Zn are produced by the wearing of brake lining (Lough et al., 2005; Gupta et al., 2007; Jain et al., 2017). Ca and Ti originate from road dust. The contributions of mobile sources in Beijing (4.9 μg/m^3, 11.9%) were twice as high as in Seoul (2.4 μg/m^3, 9.57%) and no significant seasonal variations were observed at both sites.

Since mobile source are mostly affected by regional transport rather than long-range transport, CPF results were found to be more suitable in understanding potential source areas. Figure 3-6 shows that the high contributions of mobile source are from north part of Seoul site where eight-lane highways Olympic-daero and Gangbyeonbuk-ro are located as well as south part of Seoul site where multiple expressways are located. The high contributions of mobile source are from Beijing site (Figure 3-8) with low wind speed which implies that stagnation of air masses in 5th and 6th expressway ring road in Beijing are affecting contributions of mobile source.

Industrial sources accounted for 5.71% and 10.6% in Seoul and Beijing, respectively. While industrial source in Seoul were identified with high loadings of Zn, Mn, Fe, Pb, As, and Cr, that in Beijing had high loadings of Si, Ca, and Fe and a moderate loading of Ni and V. Thus, industrial source in Seoul site had characteristics of industry mixed with coal combustion and that in Beijing site had characteristics of industry mixed with oil combustion. Trace elements such as Fe, Mn, Pb, and Cr are emitted from the metallurgical industry. Heavy metals such as Fe, Mn, Cu, Pb, and Zn are tracers of the iron and steel industry (Wu et al., 2007; Owoade et al., 2015; Sylvestre et al., 2017; Liu et al., 2018; Zhu et al., 2018). In addition, Si, Ca, and Fe are usually emitted from cement manufacture (Lv et al., 2006; Han et al., 2015). The Sihwa and Banwol industrial complexes with industries such as machinery production, electricity generation, petroleum processing, and chemical and steel manufacturing are located near Seoul (Baek et al., 2019). The Sihwa and Banwol industrial complexes emit high quantities of Zn, Pb, and Cu (Kang et al., 2018). China's largest iron and steel industries are located in the Beijing–Tianjin–Hebei

region, which contributes large quantities of anthropogenic air pollutants (Yang et al., 2018). Also, multiple cement manufactures are located within Beijing. PSCF results (Figure 3-15 and Figure 3-16) clearly show that Seoul is affected by the Sihwa and Banwol industrial complexes and Beijing is affected by overall Beijing-Tianjin-Hebei region.

Biomass burning accounted for 11.1% and 7.68% in Seoul (2.8 μg/m^3) and Beijing (3.2 μg/m^3), respectively. Biomass burning is characterized by high loadings of K^+, with medium loadings of OC and EC (Duan et al., 2004; Song et al., 2006; Zhang et al., 2013). Biomass burning includes burning of wood and agricultural residue. In East Asia, burning of agricultural residue after barley and wheat harvests occurs from spring to summer, whereas burning after the rice harvest occurs in autumn (Jung et al., 2014). At both sites, the seasonal contribution of biomass burning was the highest in winter (Seoul: 4.1 μg/m^3, 11.5%; Beijing: 5.4 μg/m^3, 11.2%) and spring (Seoul: 3.6 μg/m^3, 11.5%; Beijing: 5.1 μg/m^3, 10.2%), owing to agricultural residue burning. The sampling sites in Seoul and Beijing are in urban areas, therefore this factor may be caused by the regional transport of air pollutants from nearby cities. These results are supported by the CPF and PSCF results. For Seoul, the CPF results show that the prevailing winds from the north and west of Seoul with 2~8 m/s wind speed showed high contributions. For Beijing, the CPF results show that the winds from south of Beijing with 5~10 m/s wind speed showed high contributions. PSCF results of biomass burning for both sites shows that the potential source areas are located in Henan, Hubei, Anhui and Shandong provinces which are agricultural provinces that burn large amounts of crop residue during the

harvest season (Yin et al., 2019). Similar PSCF results were obtained by other studies (Zíková et al., 2016).

Incinerator source is characterized by high loadings of Cl^-, NO_3^-, NH_4^+, and OC and a moderate loading of Br, and Pb. Emission of Cl^- is largely from burning of plastic made of polyvinylchloride (Yang et al., 2016). Incinerator source accounted for 8.35% and 7.43% in Seoul and Beijing, respectively. Distinctively high contributions in winter and low in summer were found in both sites this is due to photochemical reaction of Cl^- that enhance gas-phase HCl in summer (Luo et al., 2019). CPF results indicate that incinerator sources are from regional transport where municipal solid waste incinerators are located (Figure 3-6 and Figure 3-8).

The soil source includes soil particles from long-range transport and resuspended road dust from local sources. The soil source consists of crustal elements with high loadings of Al, Si, Ca, and Ti and medium loadings of Fe and Mn. Many studies have used these elements as tracers for the soil source (Heo et al., 2009; Begum et al., 2010; Zong et al., 2016; Jain et al., 2020). The annual contributions of soil to $PM_{2.5}$ were 5.12% and 7.45% in Seoul and Beijing, respectively. A high contribution of soil in spring (Seoul: 6.73% and Beijing: 7.45%) is commonly mentioned in other studies because of the occurrence of the Asian dust storms during this period. During Asian dust storms, the air masses move from Inner Mongolia through North China to the East China Sea (Zhang et al., 2003; Tan et al., 2017), affecting Beijing as well as Seoul. In Beijing, the contribution of soil peaked to 12.1% in autumn, which is even higher than that in spring, due to the dust from the Gobi Desert in eastern China (Kurosaki and Mikami, 2005). The contribution of

soil is observed in spring and autumn but not in summer because of the high relative humidity of soil and lack of extratropical cyclones (Tanaka and Chiba, 2006; Liu et al., 2014). The PSCF results for both sites show that the regions from northern China to Mongolia are potential source areas (Figure 3-12 and Figure 3-14).

Oil combustion is characterized by high loadings of Ni and V (Wu et al., 2007; Viana et al., 2009). Ni and V are typical primary emission tracers indicating that industrial oil combustion and residual oil derived from marine vessels are major sources of this factor (Guo et al., 2009; Kong et al., 2010; Pey et al., 2013). The annual contribution of oil combustion to $PM_{2.5}$ was 11.9% in Seoul and oil combustion source was not identified in Beijing. The PSCF results (Figure 3-12 and Figure 3-15) indicate that the coastal area from Shanghai, China to the western region of South Korea including the Yellow Sea as the potential source areas. The Incheon port, which is the second largest port in South Korea, is located 30 km southwest of the Seoul sampling site, and the Sihwa and Banwol industrial complexes may have caused the high contribution of the oil combustion source in Seoul. Shanghai Port in China, which was the world's largest port for eight years since 2010, contributes high emissions from ships (Mamoudou et al., 2018). The CPF result also shows that the high contributions of oil combustion are from southwest of Seoul.

Coal combustion is characterized by high loadings of As and Pb and accounted for 4.64% in Beijing. As and Pb are released during coal combustion (Tian et al., 2009; Sia et al., 2012; Cui et al., 2019; Ji et al., 2019; Dai et al., 2020). Coal combustion source was only identified in Beijing site. The highest contribution of

coal combustion was in autumn (2.5 μg/m^3, 5.77%). Northern China uses central heating systems that largely depend on coal burning from November to March (Shen and Liu, 2016). Beijing shut down its last coal-fired power plant in March 2017 to use cleaner energy (Wong et al., 2019). Therefore, large contributions of coal combustion to $PM_{2.5}$ in Beijing may be from neighboring regions. PSCF results show that regional potential source areas of coal combustion in Beijing are coal-fired power plants near the Yangtze River (Figure 3-14).

Aged sea salt source accounted for 1.51% and 1.72% in Seoul and Beijing, respectively. Distinctively high loadings of Na+, SO_4^{2-}, NO_3^- and OC characterized aged sea salt (Dai et al., 2013). Lack of Cl^- due to long retention time of particles in the air indicate this source as aged sea salt rather than fresh sea salt. As displayed in Figure 3-12 and Figure 3-14, PSCF results show that potential source areas for aged sea salt are East China Sea.

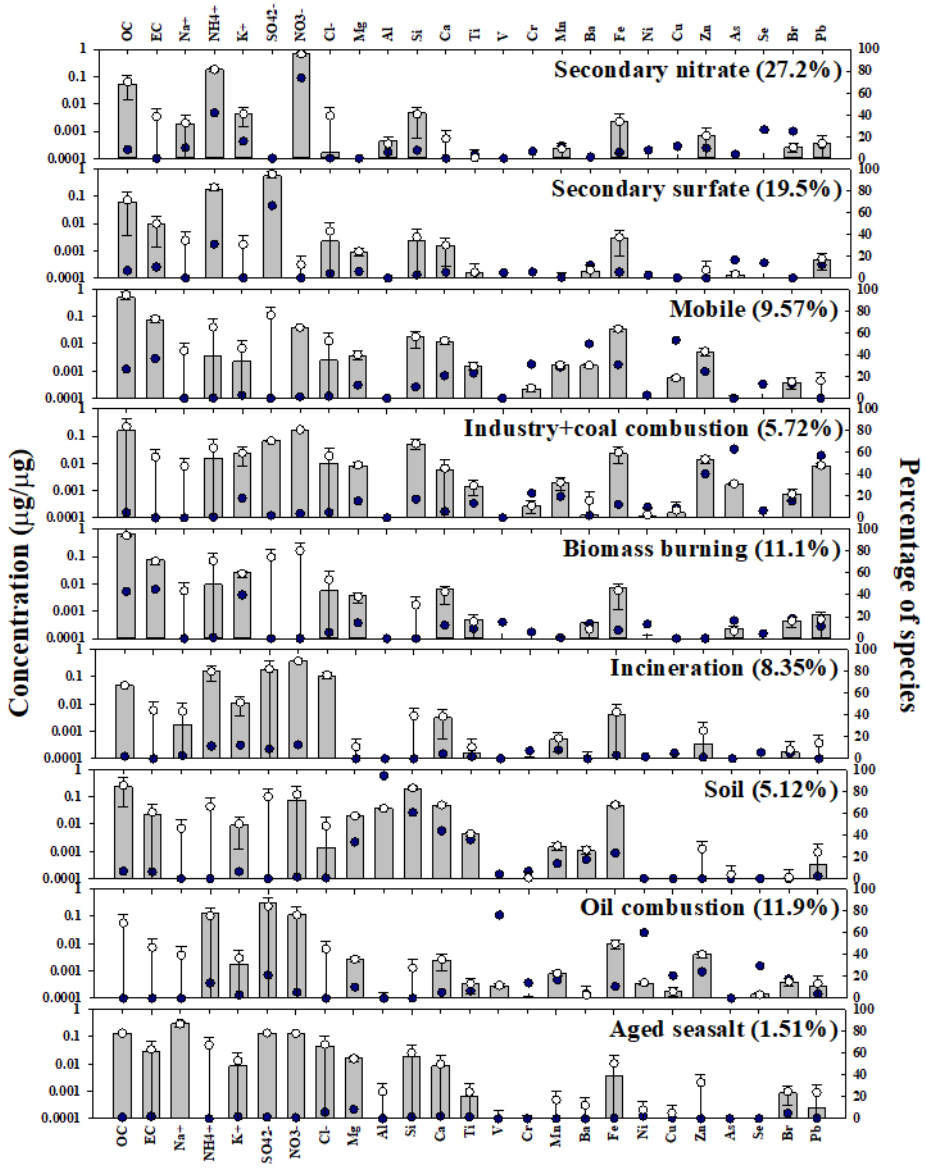

Figure 3-2 Source profiles of $PM_{2.5}$ in Seoul from January to December 2019

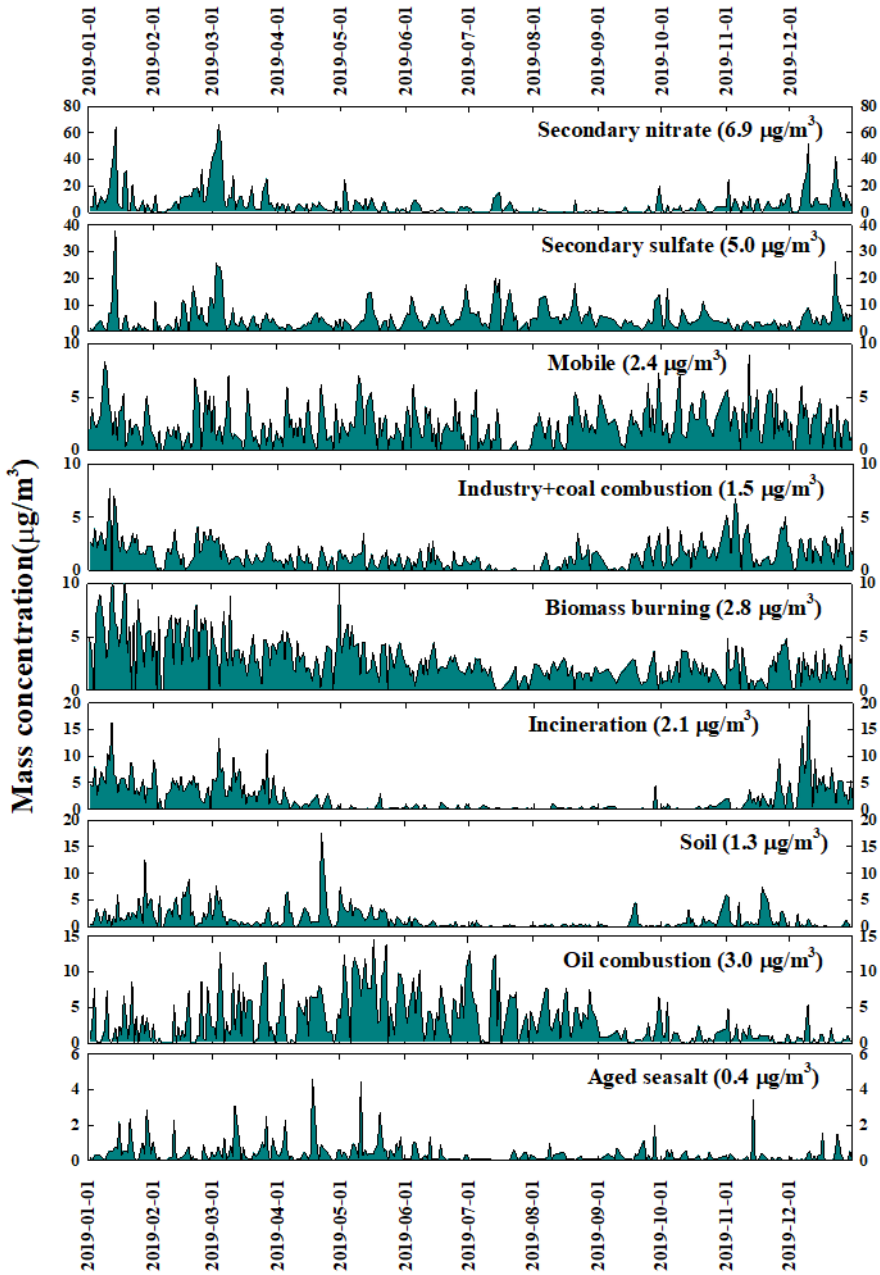

Figure 3-3 Daily PMF source contribution plot in Seoul from January to December 2019

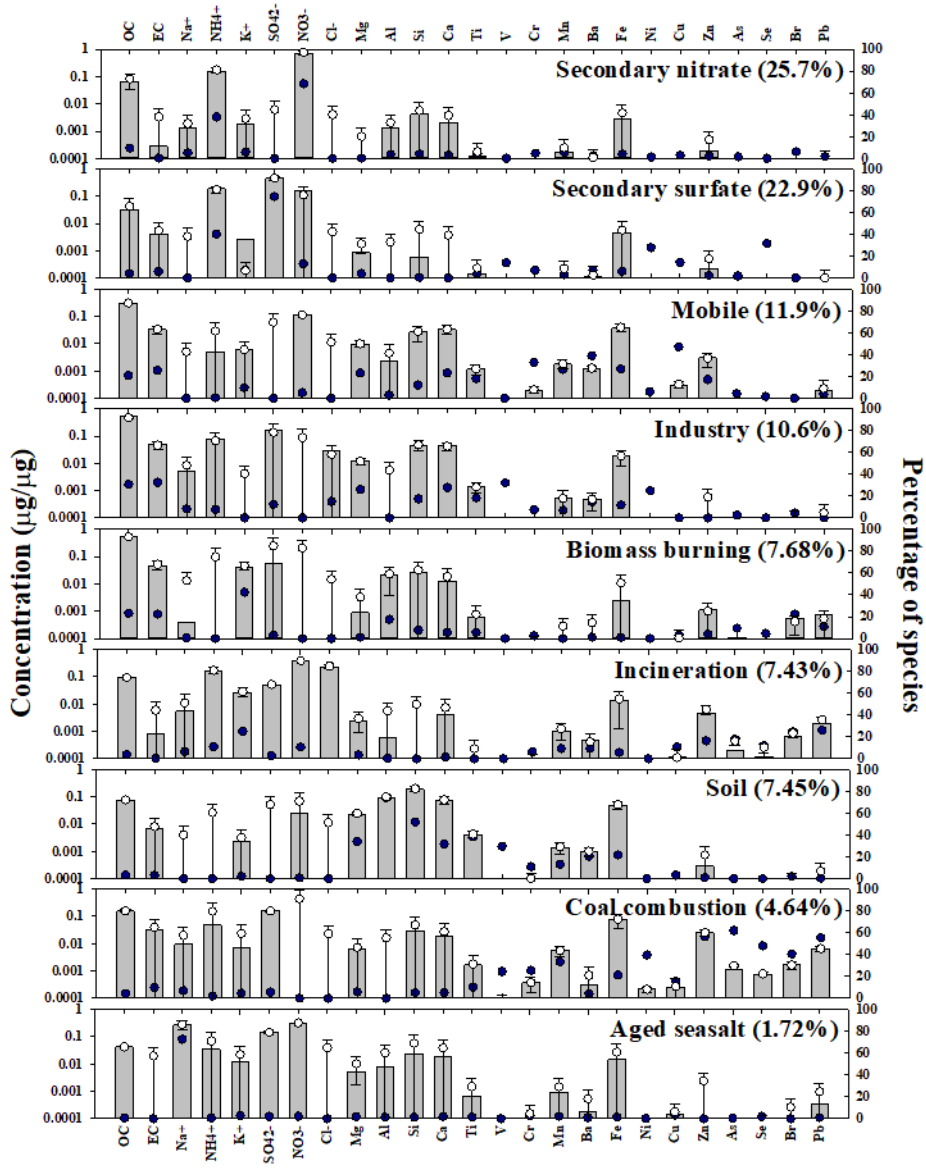

Figure 3-4 Source profiles of $PM_{2.5}$ in Beijing from January to December 2019

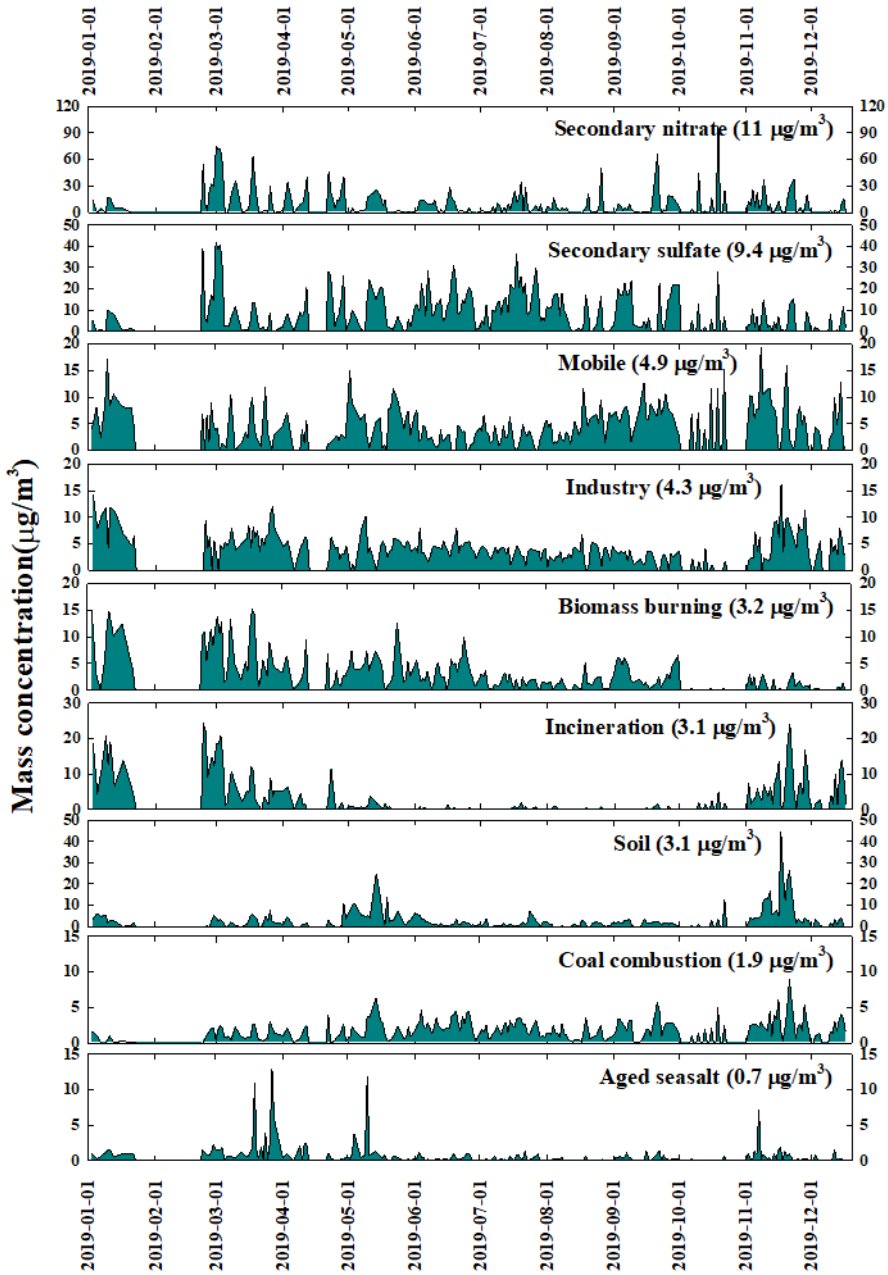

Figure 3-5 Daily PMF source contribution plot in Beijing from January to December 2019

Table 3-2 Summary of the source factors contributing to $PM_{2.5}$ based on PMF results for Seoul and Beijing

Sources	Seoul (N=294)										Beijing (N=226)									
	Annual		Spring		Summer		Autumn		Winter		Annual		Spring		Summer		Autumn		Winter	
	μg/m³	%	μg/m³	%	μg/m³	%	μg/m³	%	μg/m³	%	μg/m³	%	μg/m³	%	μg/m³	%	μg/m³	%	μg/m³	%
Secondary nitrate	6.9	27.2	9.2	29.7	2.1	11.4	4.1	22.3	12	34.7	11	25.7	16	31.7	6.5	21.3	12	26.1	9.7	20.2
Secondary sulfate	5.0	19.5	4.5	14.6	6.5	35.8	4.1	21.9	5.3	14.9	9.4	22.9	9.6	19.2	11	37.6	7.6	17.3	6.2	12.9
Mobile	2.4	9.57	2.3	7.33	2.0	10.7	3.2	17.5	2.6	7.37	4.9	11.9	4.2	8.35	3.3	10.7	7.3	16.6	6.1	12.8
Industry+coal combustion	1.5	5.72	1.2	3.87	0.7	3.75	1.9	10.1	2.2	6.26	-	-	-	-	-	-	-	-	-	-
Industry	-	-	-	-	-	-	-	-	-	-	4.3	10.6	4.9	9.79	3.6	11.6	4.1	9.21	6.2	12.9
Biomass burning	2.8	11.1	3.6	11.5	1.8	10.1	2.0	10.5	4.1	11.5	3.2	7.68	5.1	10.2	2.1	6.86	1.7	3.94	5.4	11.2
Incineration	2.1	8.35	2.2	7.15	0.2	1.30	0.9	4.87	5.1	14.3	3.1	7.43	3.7	7.34	0.2	0.51	3.4	7.69	10	21.3
Soil	1.3	5.12	2.1	6.73	0.3	1.46	1.1	5.68	1.9	5.20	3.1	7.45	3.7	7.44	1.3	4.26	5.4	12.1	2.1	4.43
Oil combustion	3.0	11.9	5.2	16.8	4.4	24.4	1.1	5.71	1.6	4.58	-	-	-	-	-	-	-	-	-	-
Coal combustion	-	-	-	-	-	-	-	-	-	-	1.9	4.64	1.5	2.98	1.9	6.32	2.5	5.77	1.3	2.73
Aged sea salt	0.4	1.51	0.7	2.22	0.2	1.10	0.3	1.41	0.4	1.15	0.7	1.72	1.5	2.99	0.2	0.81	0.6	1.26	0.8	1.63

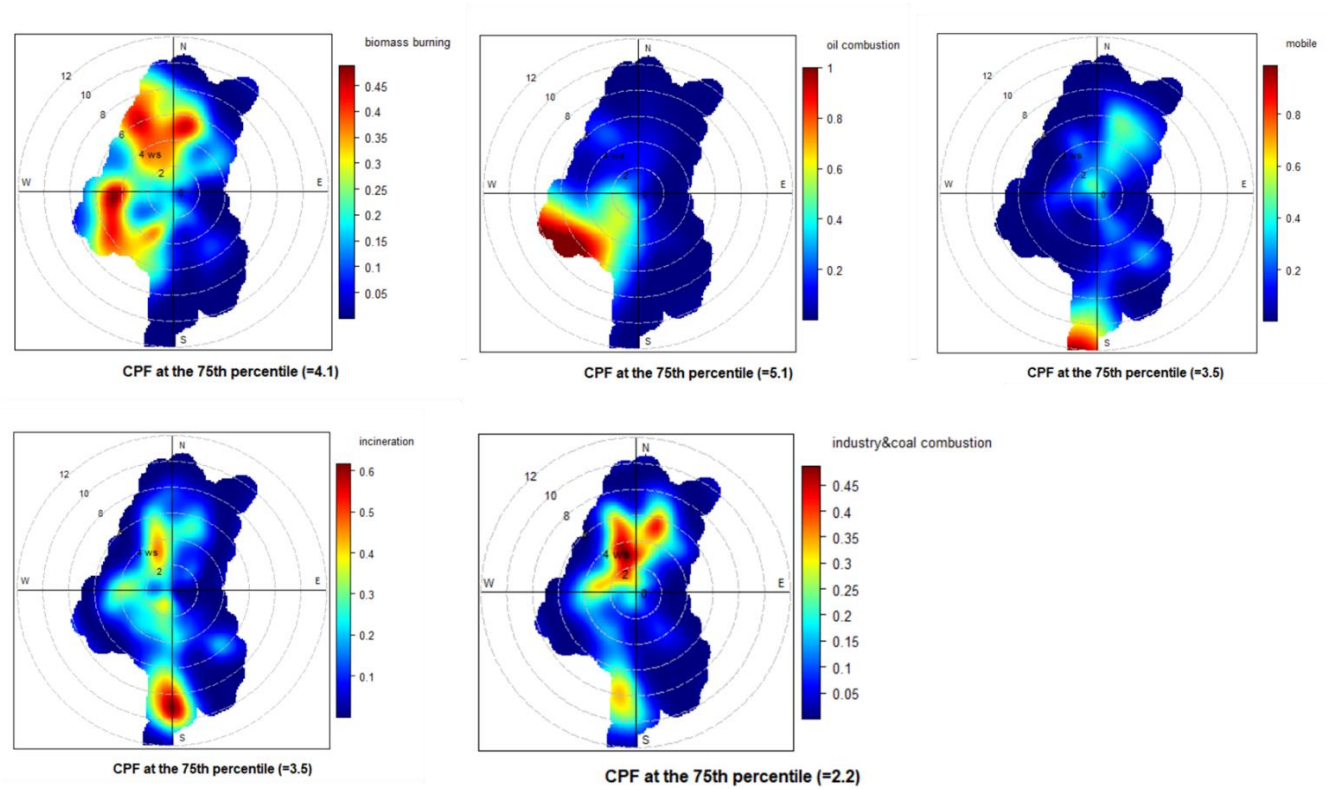

Figure 3-6 CPF results for biomass burning, oil combustion, mobile, incineration and industry/coal combustion sources in Seoul

Heating season

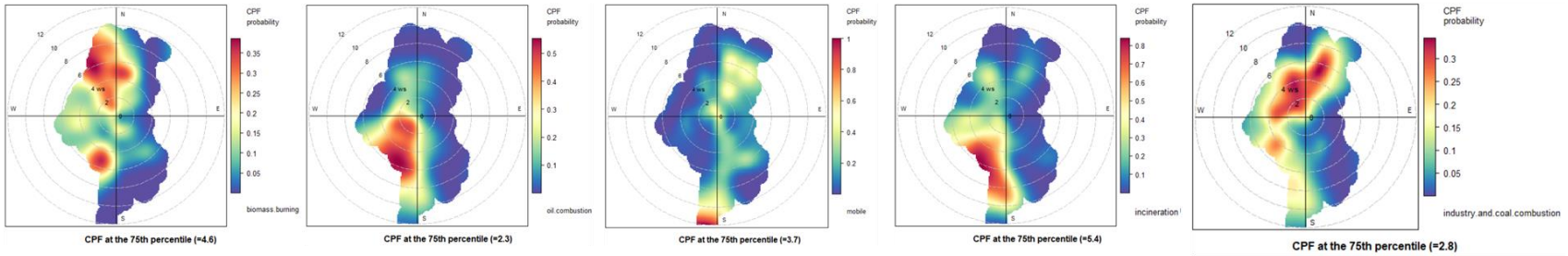

Non-heating season

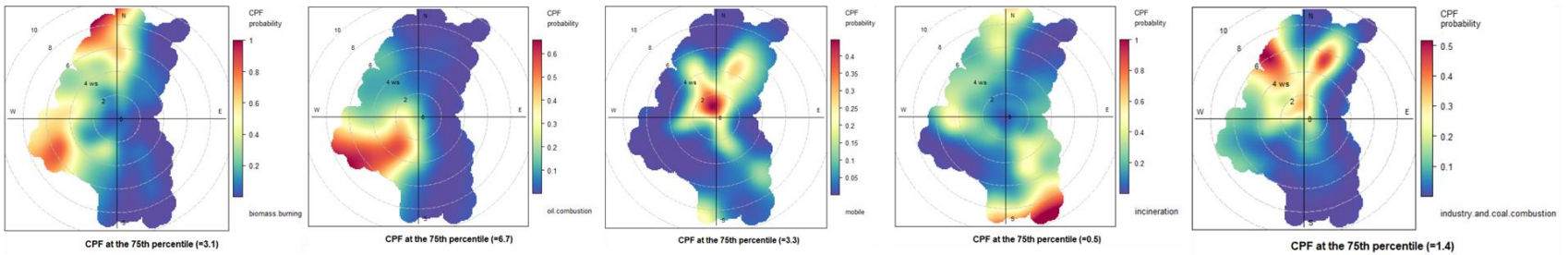

Figure 3-7 CPF results for heating and non-heating season in Seoul

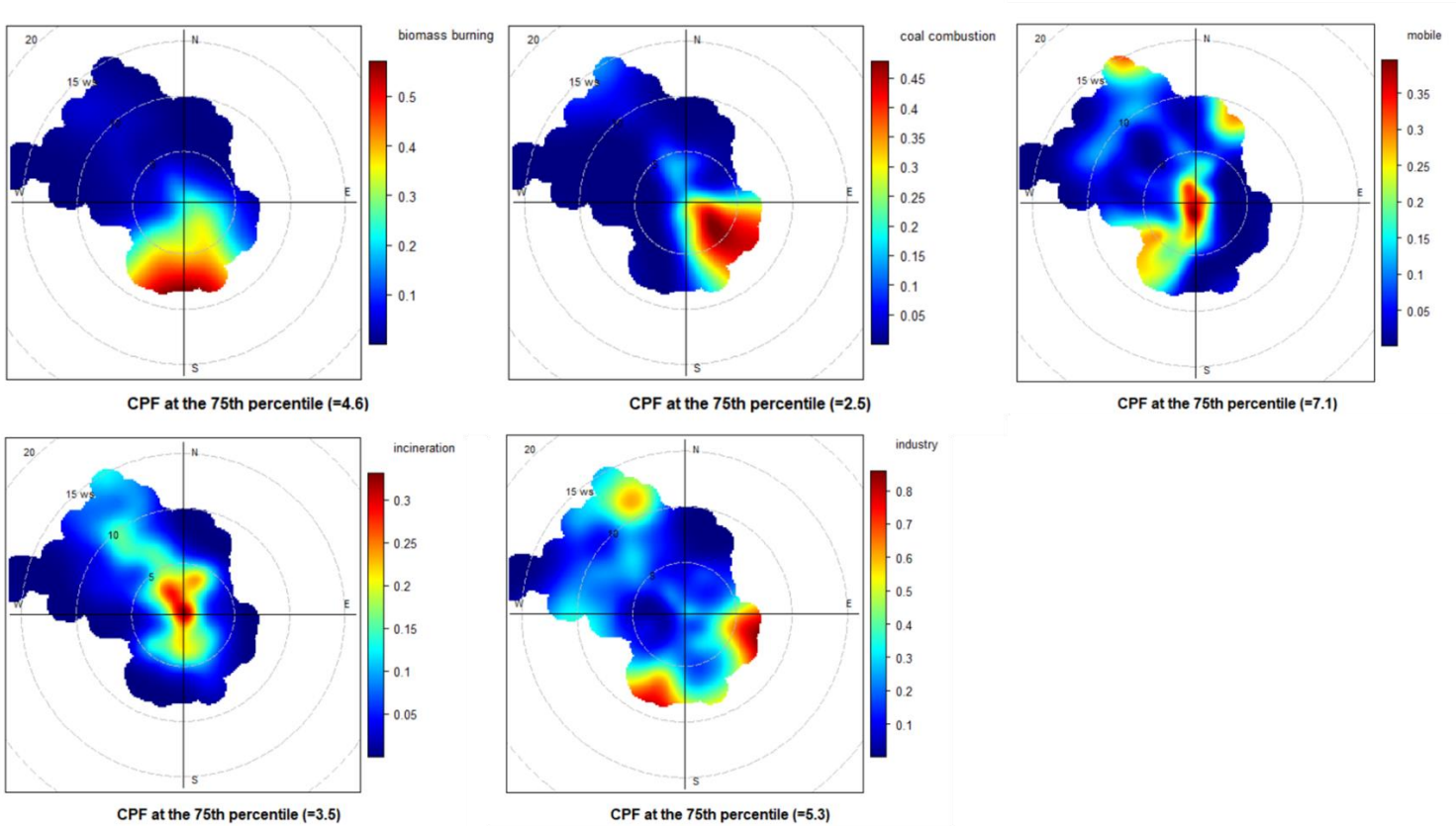

Figure 3-8 CPF results for biomass burning, coal combustion, mobile, incineration and industry sources in Beijing

Heating season

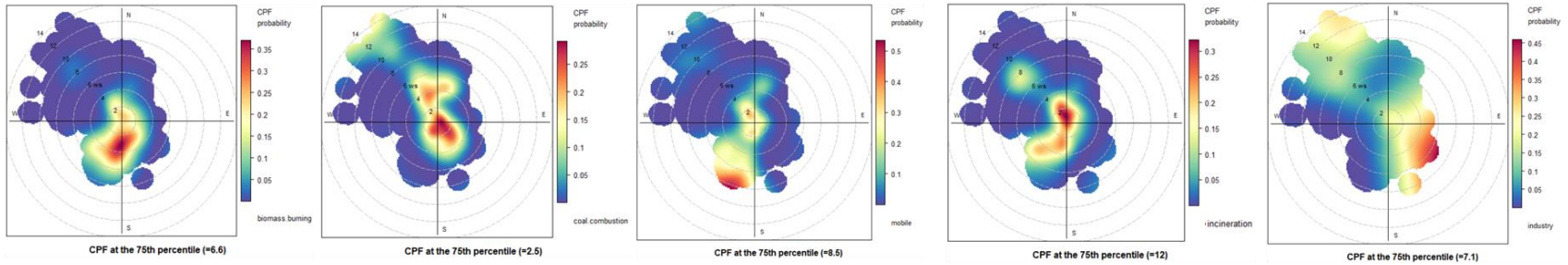

Non-heating season

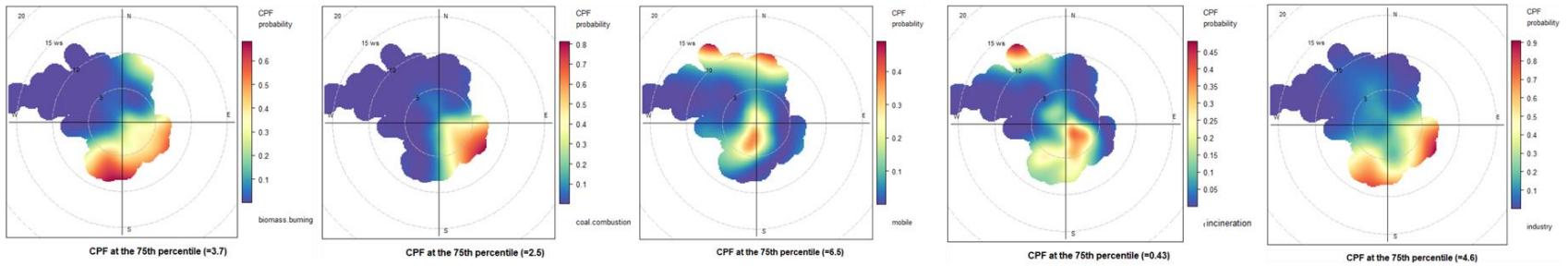

Figure 3-9 CPF results for heating and non-heating season in Beijing

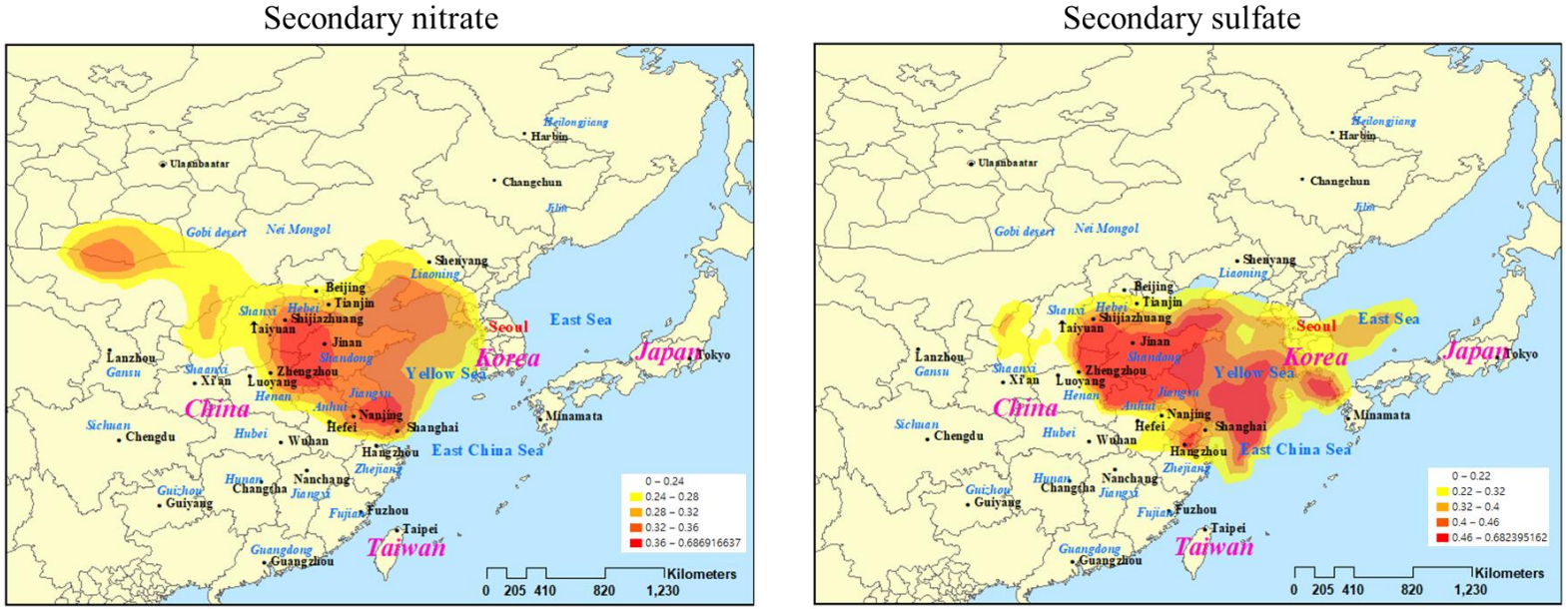

Figure 3-10 Joint-PSCF maps of potential source locations for secondary nitrate and secondary sulfate sources measured in Seoul and Beijing (upper 25%)

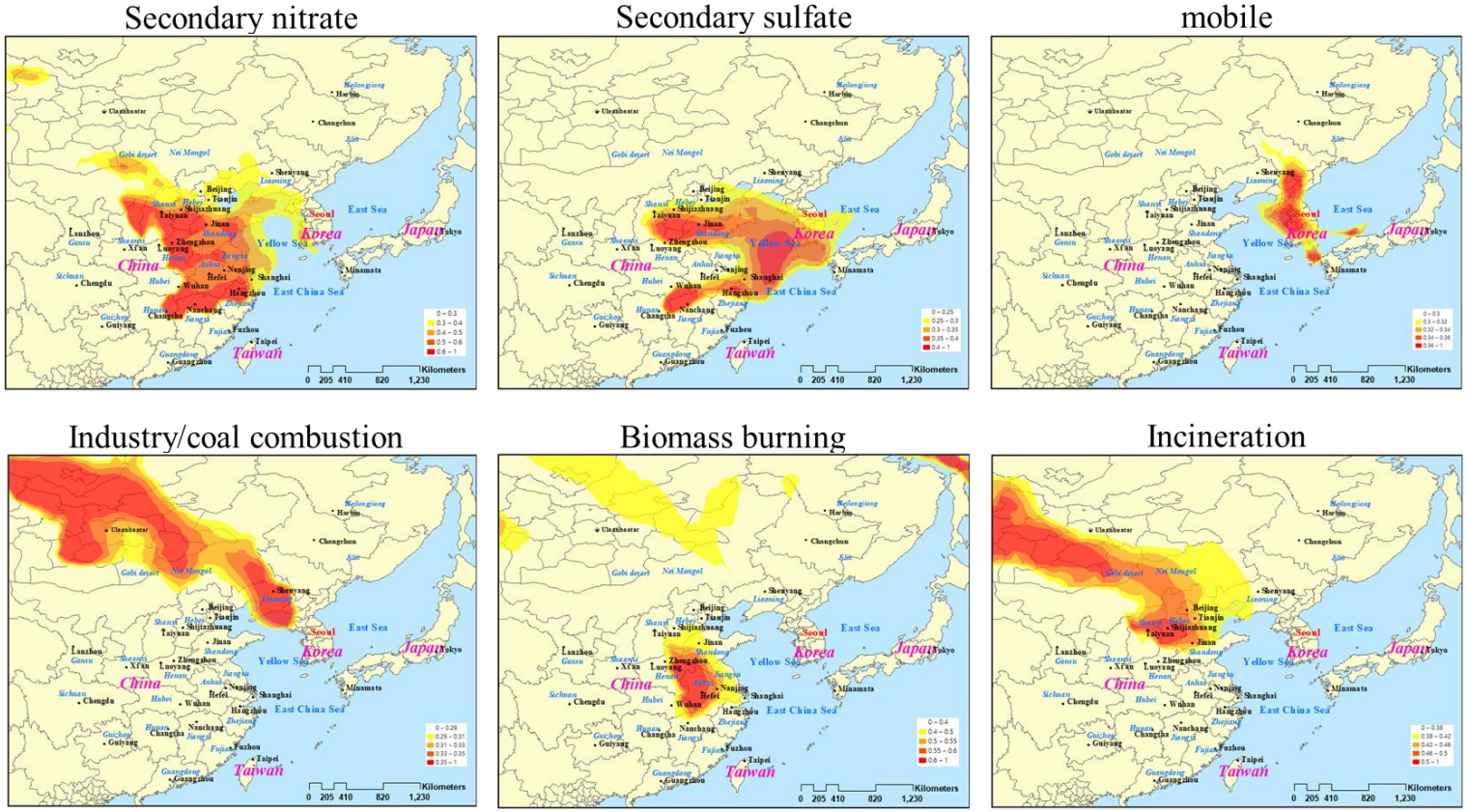

Figure 3-11 PSCF maps of potential source locations for secondary nitrate, secondary sulfate, mobile, industry/coal combustion, biomass burning, and incineration in Seoul (upper 25%)

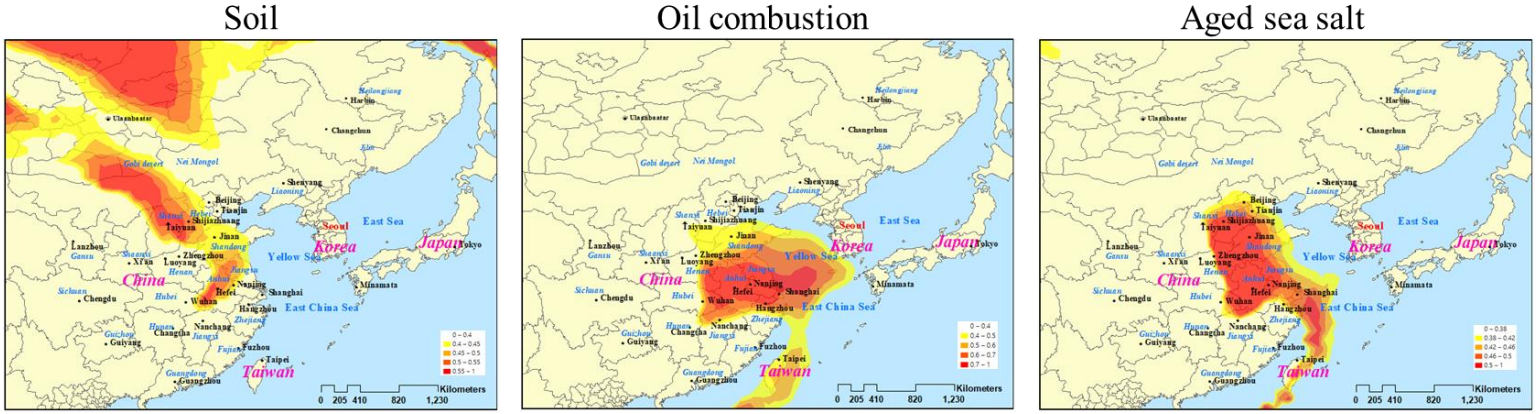

Figure 3-12 PSCF maps of potential source locations for soil, oil combustion, and aged sea salt in Seoul (upper 25%)

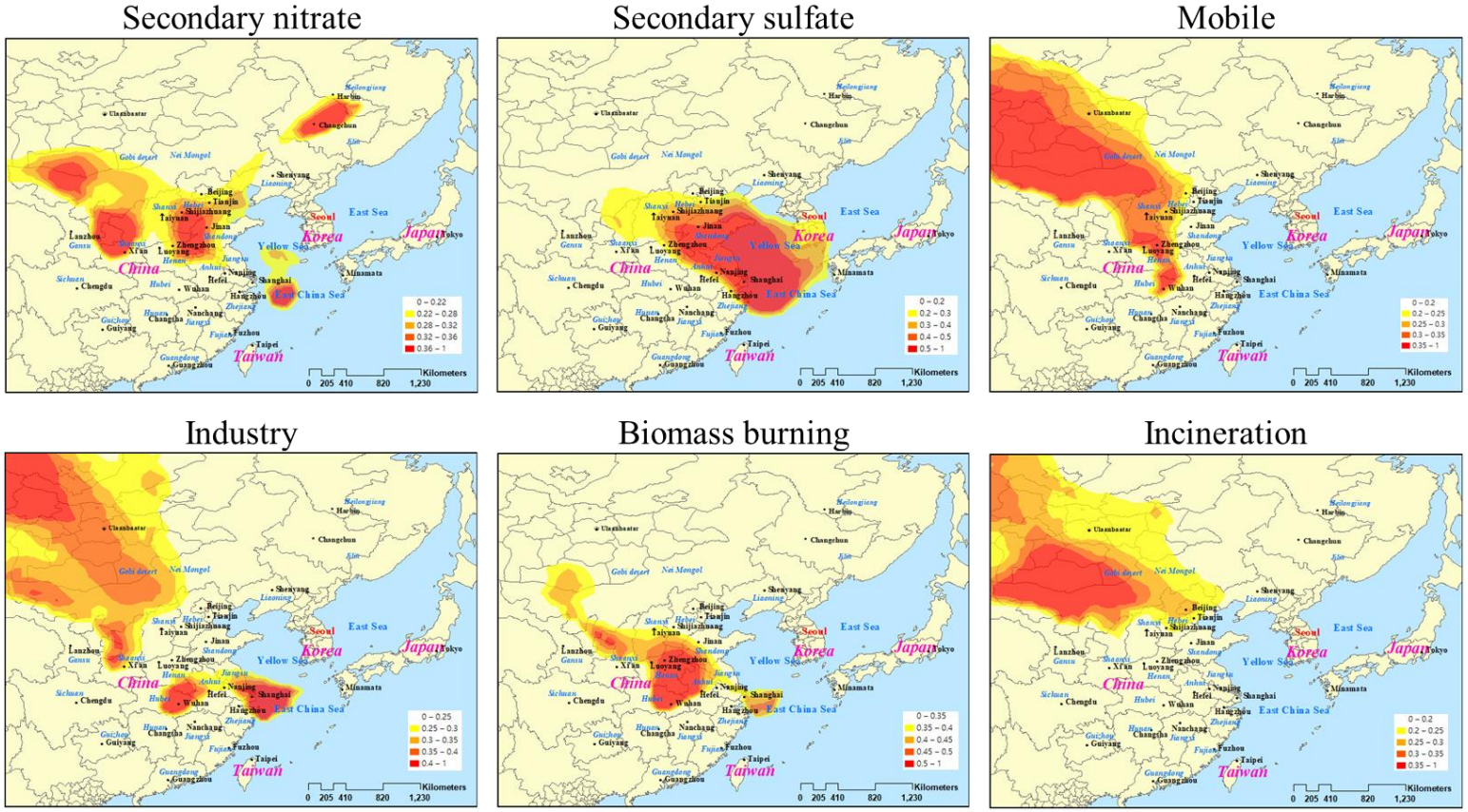

Figure 3-13 PSCF maps of potential source locations for secondary nitrate, secondary sulfate, mobile, industry, biomass burning, and incineration in Beijing (upper 25%)

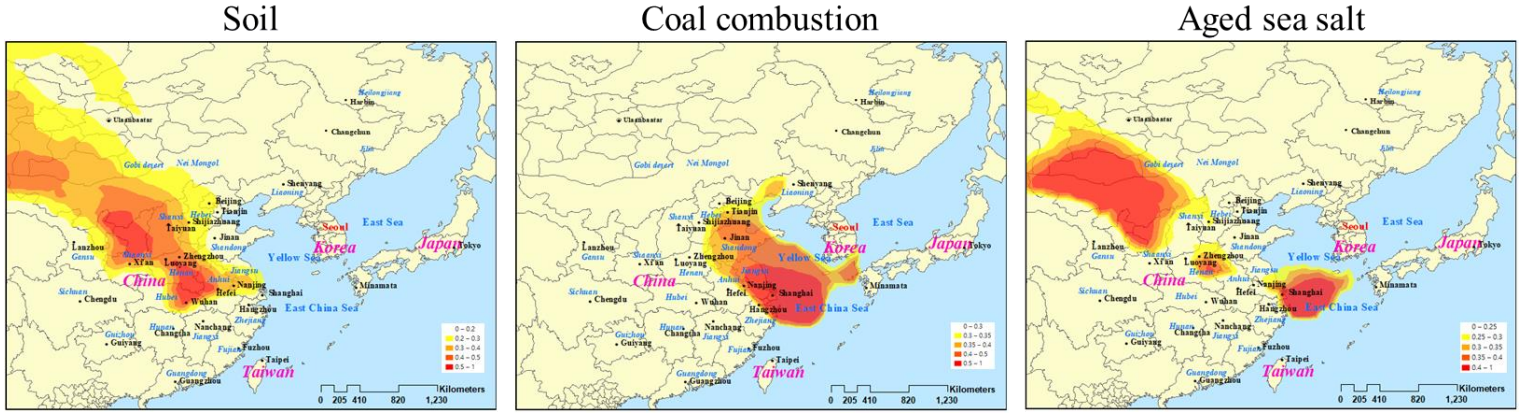

Figure 3-14 PSCF maps of potential source locations for soil, coal combustion and industry sources in Beijing (upper 25%)

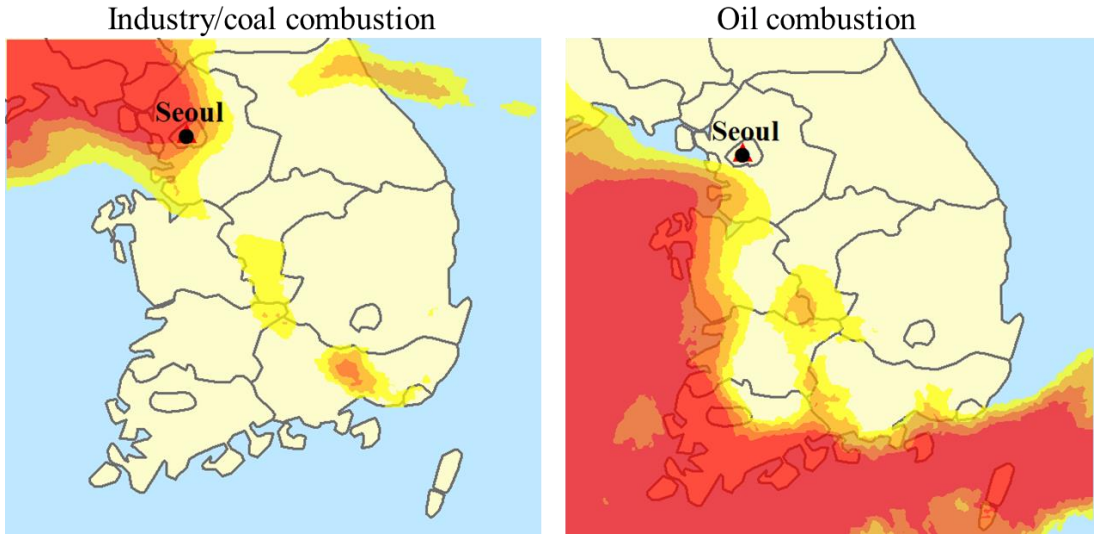

Figure 3-15 PSCF maps of potential source locations for industry/coal combustion and oil combustion sources in Seoul (upper 25%)

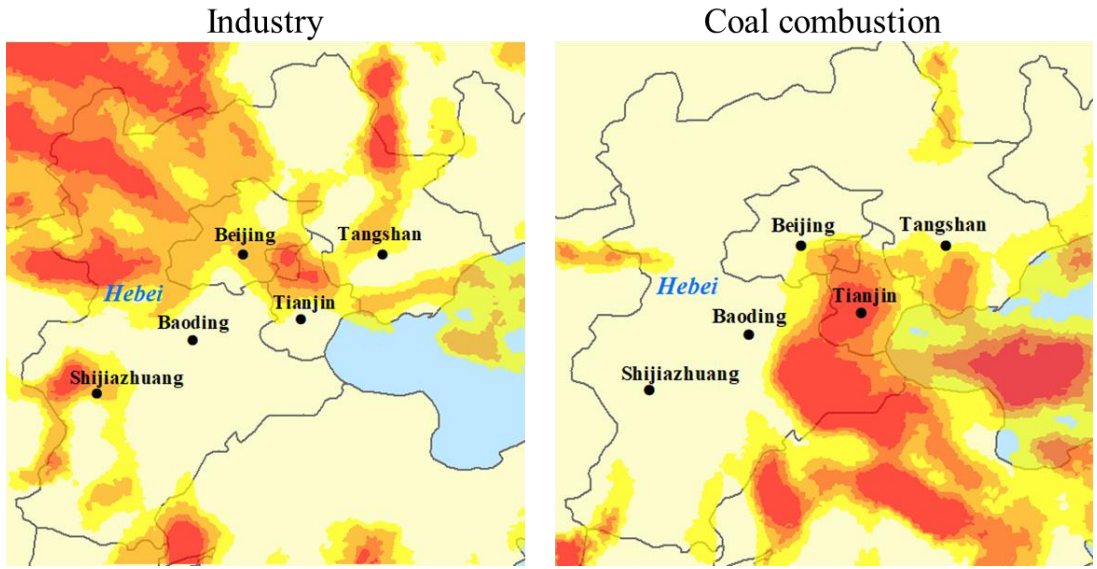

Figure 3-16 PSCF maps of potential source locations for industry and coal combustion sources in Beijing (upper 25%)

3.3 Potential source contribution function results for heating and non-heating seasons

Secondary nitrate and secondary sulfate were the highest contributing sources to $PM_{2.5}$ at both the Seoul and Beijing sites. Secondary inorganic aerosols are largely dependent on precursors from primary emissions and meteorological factors (Ma et al., 2017). Secondary nitrate forms from the NO_x emitted from mobile sources and coal-fired power plants and secondary sulfate forms by the photochemical reactions of SO_2 emitted mainly from coal combustion. As secondary inorganic aerosols are affected by coal combustion sources, we analyzed the PSCF for the heating and non-heating seasons (Figure 3-17 and Figure 3-18). Heating (November 15th to March 15th) and non-heating seasons (March 16th to November 14th) were classified based on the official central heating period implemented in Beijing, China.

During the heating season, secondary nitrate and secondary sulfate in Seoul and Beijing seem to be affected by district heating as well as coal-fired power plants in China. Although source areas are mainly located in China, the PSCF map shows that Seoul is also affected by coal-fired power plants located in west part of South Korea. As mentioned earlier, secondary nitrate is likely to form at low temperatures, whereas secondary sulfate is likely to form at high temperatures. In the heating season, the average contributions of secondary nitrate (Seoul: 13 μg/m^3 and Beijing: 14 μg/m^3) are significantly higher than those of secondary sulfate (Seoul: 5.4 μg/m^3 and Beijing: 7.0 μg/m^3). During the non-heating season in Seoul, the average contribution of secondary sulfate (4.5 μg/m^3) is higher than that of secondary nitrate

(3.4 μg/m^3) as expected. On the other hand, Beijing shows similar average contributions of secondary nitrate (9.6 μg/m^3) and secondary sulfate (9.8 μg/m^3) during non-heating season. Continuous efforts to reduce SO_2 reduction through the implementation of the Action Plan in China have significantly decreased the contribution of secondary sulfate. The Action Plan in China focused on strengthening industrial emission standards, upgrading industrial boilers, phasing out outdated industrial facilities, promoting clean fuels in residential regions, phasing out small and polluting factories, and strengthening vehicle emission standards (Zhang et al., 2019). Most of the policies focused on reducing SO_2, and therefore, additional policies to reduce NO_x and NH_3 should be implemented.

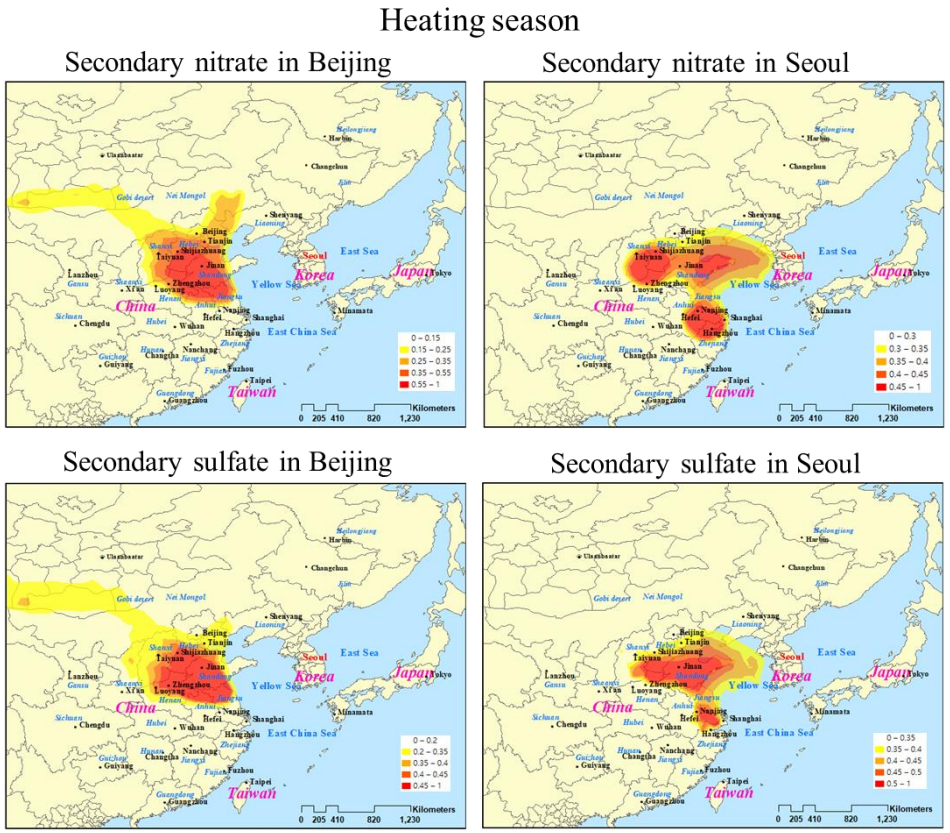

Figure 3-17 Potential source areas of secondary nitrate and secondary sulfate in Beijing and Seoul during the heating season (upper 25%)

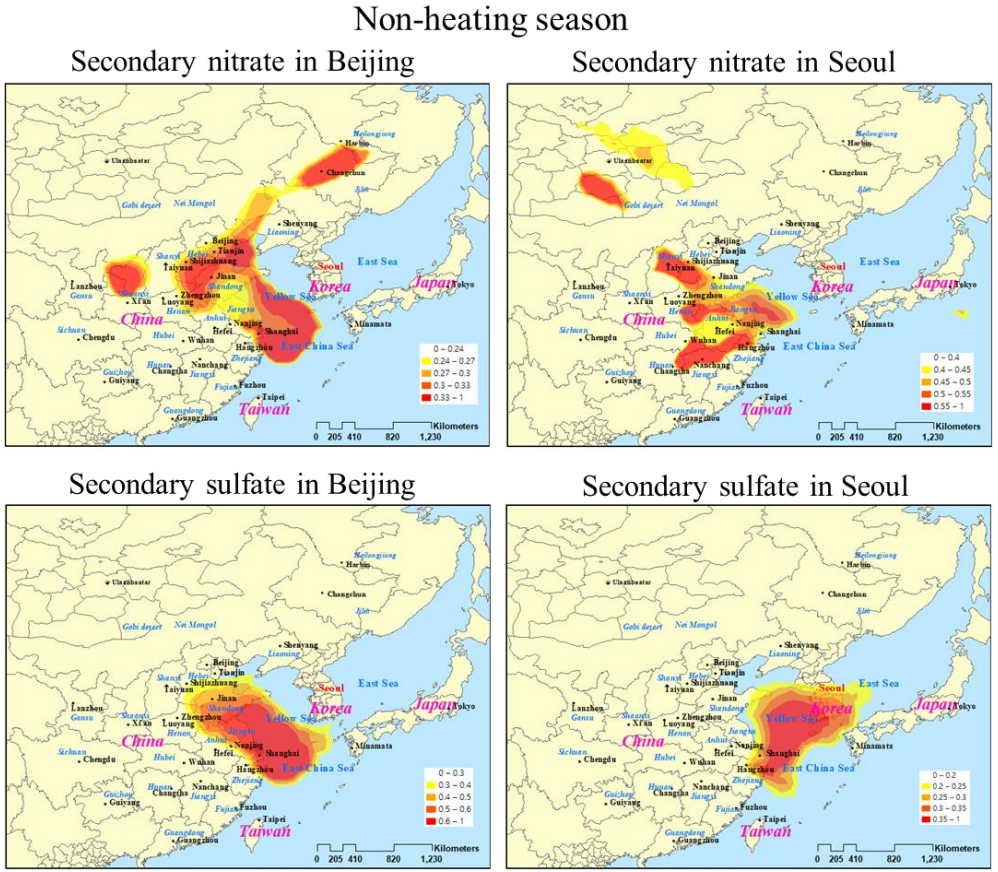

Figure 3-18 Potential source areas of secondary nitrate and secondary sulfate in Beijing and Seoul during non-heating season (upper 25%)

4. Conclusions

Daily ground-based monitoring of $PM_{2.5}$ and its chemical constituents was conducted simultaneously in the megacities of Seoul and Beijing from January to December 2019. The average annual $PM_{2.5}$ concentrations were 27.1 and 40.9 μg/m^3 in Seoul and Beijing, respectively. In both cities, ionic species including SO_4^{2-}, NO_3^-, and NH_4^+ were majority of $PM_{2.5}$ accounted for more than 50% of the total mass concentration of $PM_{2.5}$. While the concentrations of SO_4^{2-} and NH_4^+ were similar at the two sites, the concentration of NO_3^- was significantly higher in Beijing than that in Seoul. The high concentration of NO_3^- may be due to the steady emission of NH_3. PMF was employed for the source apportionment of the chemical components, and nine optimal sources were identified for both sites. In Seoul, secondary nitrate (27.2%) had the highest contribution to $PM_{2.5}$, followed by secondary sulfate (19.5%), oil combustion (11.9%), biomass burning (11.1%), mobile sources (9.57%), incineration (8.35%), industry/coal combustion (5.72%), soil (5.12%), and aged sea salt (1.51%). In Beijing, the highest contributing source was secondary nitrate (25.7%) followed by secondary sulfate (22.9%), mobile sources (11.9%), industrial sources (10.6%), biomass burning (7.68%), soil (7.45%), incineration (7.43%), coal combustion (4.64%), and aged sea salt (1.72%). High contributions of secondary inorganic aerosols align with high concentrations of ionic species. Coal combustion and secondary inorganic sources are largely affected by coal-fired power plants and individual household stoves, and thus their contributions were higher in the heating season. The PSCF results show that Seoul and Beijing were significantly affected by long-range transport of air pollutants since these cities do not have coal combustion power plants or iron and steel industries. South Korea and China have implemented

policies to reduce air pollutant emissions and improve air quality. Even though the average $PM_{2.5}$ concentration has steadily decreased in both countries, additional policies must be implemented to reduce the occurrence of HCEs in the heating season because of the stagnation of air masses due to climate change. The findings of this study may help in setting priorities in the implementation of an appropriate $PM_{2.5}$ reduction policy.

References

Air, I.Q., 2019. World Air Quality Report Region & City PM2.5 Ranking. *Index Quality Air*.

Baek, K.M., Seo, Y.K., Kim, J.Y., Baek, S.O., Baek, K.M., Seo, Y.K., Kim, J.Y. and Baek, S.O., 2019. Monitoring of particulate hazardous air pollutants and affecting factors in the largest industrial area in South Korea: The Sihwa-Banwol complex. *Environmental Engineering Research*, *25*(6), pp.908-923.

Begum, B.A., Biswas, S.K., Markwitz, A. and Hopke, P.K., 2010. Identification of sources of fine and coarse particulate matter in Dhaka, Bangladesh. *Aerosol and Air Quality Research*, *10*(4), pp.345-353.

Carslaw, D.C. and Ropkins, K., 2012. Openair—an R package for air quality data analysis. *Environmental Modelling & Software*, *27*, pp.52-61.

Cui, Y., Ji, D., Chen, H., Gao, M., Maenhaut, W., He, J. and Wang, Y., 2019. Characteristics and sources of hourly trace elements in airborne fine particles in urban Beijing, China. *Journal of Geophysical Research: Atmospheres*, *124*(21), pp.11595-11613.

Dai, W., Gao, J., Cao, G. and Ouyang, F., 2013. Chemical composition and source identification of PM2.5 in the suburb of Shenzhen, China. *Atmospheric Research*, *122*, pp.391-400.

Dai, Q., Liu, B., Bi, X., Wu, J., Liang, D., Zhang, Y., Feng, Y. and Hopke, P.K., 2020. Dispersion normalized PMF provides insights into the significant

changes in source contributions to PM2.5 after the COVID-19 outbreak. *Environmental science & technology*, *54*(16), pp.9917-9927.

Deng, J., Zhang, Y., Qiu, Y., Zhang, H., Du, W., Xu, L., Hong, Y., Chen, Y. and Chen, J., 2018. Source apportionment of PM2. 5 at the Lin'an regional background site in China with three receptor models. Atmospheric research, 202, pp.23-32.

Dockery, D.W., Pope, C.A., Xu, X., Spengler, J.D., Ware, J.H., Fay, M.E., Ferris Jr, B.G. and Speizer, F.E., 1993. An association between air pollution and mortality in six US cities. *New England journal of medicine*, *329*(24), pp.1753-1759.

Duan, F., Liu, X., Yu, T. and Cachier, H., 2004. Identification and estimate of biomass burning contribution to the urban aerosol organic carbon concentrations in Beijing. *Atmospheric Environment*, *38*(9), pp.1275-1282.

El Haddad, I., Marchand, N., Dron, J., Temime-Roussel, B., Quivet, E., Wortham, H., Jaffrezo, J.L., Baduel, C., Voisin, D., Besombes, J.L. and Gille, G., 2009. Comprehensive primary particulate organic characterization of vehicular exhaust emissions in France. *Atmospheric Environment*, *43*(39), pp.6190-6198.

Feng, Y., Chen, Y., Guo, H., Zhi, G., Xiong, S., Li, J., Sheng, G. and Fu, J., 2009. Characteristics of organic and elemental carbon in PM2. 5 samples in Shanghai, China. *Atmospheric Research*, *92*(4), pp.434-442.

Feng, S., Gao, D., Liao, F., Zhou, F. and Wang, X., 2016. The health effects of ambient PM2.5 and potential mechanisms. *Ecotoxicology and environmental safety*, *128*, pp.67-74.

Geng, G., Xiao, Q., Zheng, Y., Tong, D., Zhang, Y., Zhang, X., Zhang, Q., He, K. and Liu, Y., 2019. Impact of China's air pollution prevention and control action plan on PM 2.5 chemical composition over eastern China. *Science China Earth Sciences*, *62*(12), pp.1872-1884.

Gu, J., Bai, Z., Liu, A., Wu, L., Xie, Y., Li, W., Dong, H. and Zhang, X., 2010. Characterization of atmospheric organic carbon and element carbon of PM2.5 and PM10 at Tianjin, China. *Aerosol and Air Quality Research*, *10*(2), pp.167-176.

Guan, Q., Li, F., Yang, L., Zhao, R., Yang, Y. and Luo, H., 2018. Spatial-temporal variations and mineral dust fractions in particulate matter mass concentrations in an urban area of northwestern China. *Journal of environmental management*, *222*, pp.95-103.

Guo, H., Ding, A.J., So, K.L., Ayoko, G., Li, Y.S. and Hung, W.T., 2009. Receptor modeling of source apportionment of Hong Kong aerosols and the implication of urban and regional contribution. *Atmospheric Environment*, *43*(6), pp.1159-1169.

Gupta, A.K., Karar, K. and Srivastava, A., 2007. Chemical mass balance source apportionment of PM10 and TSP in residential and industrial sites of an urban region of Kolkata, India. *Journal of hazardous materials*, *142*(1-2), pp.279-287.

Han, Y.J., Kim, H.W., Cho, S.H., Kim, P.R. and Kim, W.J., 2015. Metallic elements in PM2.5 in different functional areas of Korea: Concentrations and source identification. *Atmospheric Research*, *153*, pp.416-428.

Harrison, R.M., Jones, A.M., Gietl, J., Yin, J. and Green, D.C., 2012. Estimation of the contributions of brake dust, tire wear, and resuspension to nonexhaust traffic particles derived from atmospheric measurements. *Environmental science & technology*, *46*(12), pp.6523-6529.

Heo, J.B., Hopke, P.K. and Yi, S.M., 2009. Source apportionment of PM 2.5 in Seoul, Korea. Atmospheric Chemistry and Physics, 9(14), pp.4957-4971.

Heo, J., McGinnis, J.E., de Foy, B. and Schauer, J.J., 2013. Identification of potential source areas for elevated PM2.5, nitrate and sulfate concentrations. *Atmospheric environment*, *71*, pp.187-197.

Heo, J., Wu, B., Abdeen, Z., Qasrawi, R., Sarnat, J.A., Sharf, G., Shpund, K. and Schauer, J.J., 2017. Source apportionments of ambient fine particulate matter in Israeli, Jordanian, and Palestinian cities. Environmental pollution, 225, pp.1-11.

Huang, X., Liu, Z., Zhang, J., Wen, T., Ji, D. and Wang, Y., 2016. Seasonal variation and secondary formation of size-segregated aerosol water-soluble inorganic ions during pollution episodes in Beijing. *Atmospheric Research*, *168*, pp.70-79.

Jain, S., Sharma, S.K., Choudhary, N., Masiwal, R., Saxena, M., Sharma, A., Mandal, T.K., Gupta, A., Gupta, N.C. and Sharma, C., 2017. Chemical characteristics and source apportionment of PM 2.5 using PCA/APCS,

UNMIX, and PMF at an urban site of Delhi, India. *Environmental Science and Pollution Research*, *24*(17), pp.14637-14656.

Jain, S., Sharma, S.K., Vijayan, N. and Mandal, T.K., 2020. Seasonal characteristics of aerosols (PM2.5 and PM10) and their source apportionment using PMF: a four year study over Delhi, India. Environmental Pollution, 262, p.114337.

Ji, P., Song, G.C., Xu, W.T. and Song, Q., 2019. Transformation characteristics of arsenic and lead during coal combustion. *Energy & Fuels*, *33*(9), pp.9280-9288.

Jung, J., Lee, S., Kim, H., Kim, D., Lee, H. and Oh, S., 2014. Quantitative determination of the biomass-burning contribution to atmospheric carbonaceous aerosols in Daejeon, Korea, during the rice-harvest period. *Atmospheric Environment*, *89*, pp.642-650.

Kang, B.W., Kim, M.J., Baek, K.M., Seo, Y.K., Lee, H.S., Kim, J.H., Han, J.S. and Baek, S.O., 2018. A study on the concentration distribution of airborne heavy metals in major industrial complexes in Korea. *Journal of Korean Society for Atmospheric Environment*, *34*(2), pp.269-280.

Khan, J.Z., Sun, L., Tian, Y., Shi, G. and Feng, Y., 2021. Chemical characterization and source apportionment of PM1 and PM2.5 in Tianjin, China: Impacts of biomass burning and primary biogenic sources. Journal of Environmental Sciences, 99, pp.196-209.

Kocbach, A., 2008. Pro-inflammatory potential of particles from residential wood smoke and traffic: Importance of physicochemical characteristics.

Kong, S., Han, B., Bai, Z., Chen, L., Shi, J. and Xu, Z., 2010. Receptor modeling of PM2.5, PM10 and TSP in different seasons and long-range transport analysis at a coastal site of Tianjin, China. *Science of the Total Environment*, *408*(20), pp.4681-4694.

Kurosaki, Y. and Mikami, M., 2005. Regional difference in the characteristic of dust event in East Asia: Relationship among dust outbreak, surface wind, and land surface condition. *Journal of the Meteorological Society of Japan. Ser. II*, *83*, pp.1-18.

Lee, S., 2018. Korea's New Comprehensive Plan on Fine Dust and Its Implications for Policy and Research. *Research in Brief*, (29), pp.1-7.

Liu, J., Chen, Y., Chao, S., Cao, H., Zhang, A. and Yang, Y., 2018. Emission control priority of PM2. 5-bound heavy metals in different seasons: A comprehensive analysis from health risk perspective. *Science of the total environment*, *644*, pp.20-30.

Liu, Q., Liu, Y., Yin, J., Zhang, M. and Zhang, T., 2014. Chemical characteristics and source apportionment of PM10 during Asian dust storm and non-dust storm days in Beijing. *Atmospheric Environment*, *91*, pp.85-94.

Lough, G.C., Schauer, J.J., Park, J.S., Shafer, M.M., DeMinter, J.T. and Weinstein, J.P., 2005. Emissions of metals associated with motor vehicle roadways. *Environmental science & technology*, *39*(3), pp.826-836.

Luo, L., Zhang, Y.Y., Xiao, H.Y., Xiao, H.W., Zheng, N.J., Zhang, Z.Y., Xie, Y.J. and Liu, C., 2019. Spatial distributions and sources of inorganic chlorine in PM2.5 across China in Winter. *Atmosphere*, *10*(9), p.505.

Lv, W., Wang, Y., Querol, X., Zhuang, X., Alastuey, A., López, A. and Viana, M., 2006. Geochemical and statistical analysis of trace metals in atmospheric particulates in Wuhan, central China. *Environmental Geology*, *51*(1), p.121.

Ma, Q., Wu, Y., Zhang, D., Wang, X., Xia, Y., Liu, X., Tian, P., Han, Z., Xia, X., Wang, Y. and Zhang, R., 2017. Roles of regional transport and heterogeneous reactions in the PM2.5 increase during winter haze episodes in Beijing. *Science of the Total Environment*, *599*, pp.246-253.

Mamoudou, I., Zhang, F., Chen, Q., Wang, P. and Chen, Y., 2018. Characteristics of PM2.5 from ship emissions and their impacts on the ambient air: A case study in Yangshan Harbor, Shanghai. *Science of the Total Environment*, *640*, pp.207-216.

Miller-Schulze, J.P., Shafer, M., Schauer, J.J., Heo, J., Solomon, P.A., Lantz, J., Artamonova, M., Chen, B., Imashev, S., Sverdlik, L. and Carmichael, G., 2015. Seasonal contribution of mineral dust and other major components to particulate matter at two remote sites in Central Asia. *Atmospheric Environment*, *119*, pp.11-20.

Owoade, K.O., Hopke, P.K., Olise, F.S., Ogundele, L.T., Fawole, O.G., Olaniyi, B.H., Jegede, O.O., Ayoola, M.A. and Bashiru, M.I., 2015. Chemical compositions and source identification of particulate matter (PM2. 5 and PM2.5–10) from a scrap iron and steel smelting industry along the Ife–Ibadan highway, Nigeria. *Atmospheric Pollution Research*, *6*(1), pp.107-119.

Park, E.H., Heo, J., Hirakura, S., Hashizume, M., Deng, F., Kim, H. and Yi, S.M., 2018. Characteristics of PM 2.5 and its chemical constituents in Beijing, Seoul, and Nagasaki. *Air Quality, Atmosphere & Health*, *11*(10), pp.1167-1178.

Park, E.H., Heo, J., Kim, H. and Yi, S.M., 2020. Long term trends of chemical constituents and source contributions of PM2. 5 in Seoul. Chemosphere, 251, p.126371.

Park, J., Park, E.H., Schauer, J.J., Yi, S.M. and Heo, J., 2018. Reactive oxygen species (ROS) activity of ambient fine particles (PM2.5) measured in Seoul, Korea. *Environment international*, *117*, pp.276-283.

Paatero, P. and Hopke, P.K., 2003. Discarding or downweighting high-noise variables in factor analytic models. *Analytica Chimica Acta*, *490*(1-2), pp.277-289.

Pey, J., Pérez, N., Cortés, J., Alastuey, A. and Querol, X., 2013. Chemical fingerprint and impact of shipping emissions over a western Mediterranean metropolis: Primary and aged contributions. *Science of the total environment*, *463*, pp.497-507.

Pinkerton, K.E., Green, F.H., Saiki, C., Vallyathan, V., Plopper, C.G., Gopal, V., Hung, D., Bahne, E.B., Lin, S.S., Ménache, M.G. and Schenker, M.B., 2000. Distribution of particulate matter and tissue remodeling in the human lung. *Environmental Health Perspectives*, *108*(11), pp.1063-1069.

Seinfeld, J.H., Pandis, S.N. and Noone, K., 1998. Atmospheric chemistry and physics: from air pollution to climate change. *Physics Today*, *51*(10), p.88.

Sia, S.G. and Abdullah, W.H., 2012. Enrichment of arsenic, lead, and antimony in Balingian coal from Sarawak, Malaysia: Modes of occurrence, origin, and partitioning behaviour during coal combustion. *International journal of coal geology*, *101*, pp.1-15.

Shen, X. and Liu, B., 2016. Changes in the timing, length and heating degree days of the heating season in central heating zone of China. *Scientific reports*, *6*(1), pp.1-10.

Song, Y., Zhang, Y., Xie, S., Zeng, L., Zheng, M., Salmon, L.G., Shao, M. and Slanina, S., 2006. Source apportionment of PM2. 5 in Beijing by positive matrix factorization. *Atmospheric Environment*, *40*(8), pp.1526-1537.

Su, L., Yuan, Z., Fung, J.C. and Lau, A.K., 2015. A comparison of HYSPLIT backward trajectories generated from two GDAS datasets. *Science of the Total Environment*, *506*, pp.527-537.

Sylvestre, A., Mizzi, A., Mathiot, S., Masson, F., Jaffrezo, J.L., Dron, J., Mesbah, B., Wortham, H. and Marchand, N., 2017. Comprehensive chemical characterization of industrial PM2.5 from steel industry activities. *Atmospheric Environment*, *152*, pp.180-190.

Taghvaee, S., Sowlat, M.H., Mousavi, A., Hassanvand, M.S., Yunesian, M., Naddafi, K. and Sioutas, C., 2018. Source apportionment of ambient PM2. 5 in

two locations in central Tehran using the Positive Matrix Factorization (PMF) model. *Science of the total environment*, *628*, pp.672-686.

Tan, S.C., Li, J., Che, H., Chen, B. and Wang, H., 2017. Transport of East Asian dust storms to the marginal seas of China and the southern North Pacific in spring 2010. *Atmospheric Environment*, *148*, pp.316-328.

Tanaka, T.Y. and Chiba, M., 2006. A numerical study of the contributions of dust source regions to the global dust budget. *Global and Planetary Change*, *52*(1-4), pp.88-104.

Tian, H.Z. and Qu, Y.P., 2009. Inventories of atmospheric arsenic emissions from coal combustion in China, 2005. *Huan jing ke xue= Huanjing kexue*, *30*(4), pp.956-962.

Viana, M., Amato, F., Alastuey, A., Querol, X., Moreno, T., Garcia Dos Santos, S., Herce, M.D. and Fernández-Patier, R., 2009. Chemical tracers of particulate emissions from commercial shipping. *Environmental science & technology*, *43*(19), pp.7472-7477.

Viana, M., Kuhlbusch, T.A., Querol, X., Alastuey, A., Harrison, R.M., Hopke, P.K., Winiwarter, W., Vallius, M., Szidat, S., Prévôt, A.S. and Hueglin, C., 2008. Source apportionment of particulate matter in Europe: a review of methods and results. *Journal of aerosol science*, *39*(10), pp.827-849.

Waked, A., Favez, O., Alleman, L.Y., Piot, C., Petit, J.E., Delaunay, T., Verlinden, E., Golly, B., Besombes, J.L., Jaffrezo, J.L. and Leoz-Garziandia, E., 2014. Source apportionment of PM 10 in a north-western Europe regional urban background site (Lens, France) using positive matrix

factorization and including primary biogenic emissions. *Atmospheric Chemistry and Physics*, *14*(7), pp.3325-3346.

Wang, J., Qiu, Y., He, S., Liu, N., Xiao, C. and Liu, L., 2018. Investigating the driving forces of NOx generation from energy consumption in China. *Journal of Cleaner Production*, *184*, pp.836-846.

Wang, D., Zhou, B., Fu, Q., Zhao, Q., Zhang, Q., Chen, J., Yang, X., Duan, Y. and Li, J., 2016. Intense secondary aerosol formation due to strong atmospheric photochemical reactions in summer: observations at a rural site in eastern Yangtze River Delta of China. *Science of the Total Environment*, *571*, pp.1454-1466.

Wang, Y., Zhuang, G., Tang, A., Zhang, W., Sun, Y., Wang, Z. and An, Z., 2007. The evolution of chemical components of aerosols at five monitoring sites of China during dust storms. *Atmospheric Environment*, *41*(5), pp.1091-1106.

Wang, Y., Zhuang, G., Zhang, X., Huang, K., Xu, C., Tang, A., Chen, J. and An, Z., 2006. The ion chemistry, seasonal cycle, and sources of PM2.5 and TSP aerosol in Shanghai. *Atmospheric Environment*, *40*(16), pp.2935-2952.

Wong, P., Lin, M. and Jackson, J., 2019. China 2019 best-performing cities: The nation's most successful economies, Milken Institute.

Wu, Y.S., Fang, G.C., Lee, W.J., Lee, J.F., Chang, C.C. and Lee, C.Z., 2007. A review of atmospheric fine particulate matter and its associated trace metal pollutants in Asian countries during the period 1995–2005. *Journal of hazardous materials*, *143*(1-2), pp.511-515.

Wuebbles, D.J., Lei, H. and Lin, J., 2007. Intercontinental transport of aerosols and photochemical oxidants from Asia and its consequences. *Environmental pollution*, *150*(1), pp.65-84.

Yang, H.H., Luo, S.W., Lee, K.T., Wu, J.Y., Chang, C.W. and Chu, P.F., 2016. Fine particulate speciation profile and emission factor of municipal solid waste incinerator established by dilution sampling method. *Journal of the Air & Waste Management Association*, *66*(8), pp.807-814.

Yang, H., Tao, W., Liu, Y., Qiu, M., Liu, J., Jiang, K., Yi, K., Xiao, Y. and Tao, S., 2019. The contribution of the Beijing, Tianjin and Hebei region's iron and steel industry to local air pollution in winter. *Environmental pollution*, *245*, pp.1095-1106.

Yang, Y., Liu, Y., Li, Y. and Li, J., 2018. Measure of urban-rural transformation in Beijing-Tianjin-Hebei region in the new millennium: Population-land-industry perspective. *Land Use Policy*, *79*, pp.595-608.

Yin, L., Du, P., Zhang, M., Liu, M., Xu, T. and Song, Y., 2019. Estimation of emissions from biomass burning in China (2003–2017) based on MODIS fire radiative energy data. *Biogeosciences*, *16*(7), pp.1629-1640.

Zhang, H., Wang, S., Hao, J., Wang, X., Wang, S., Chai, F. and Li, M., 2016. Air pollution and control action in Beijing. *Journal of Cleaner Production*, *112*, pp.1519-1527.

Zhang, Q., Zheng, Y., Tong, D., Shao, M., Wang, S., Zhang, Y., Xu, X., Wang, J., He, H., Liu, W. and Ding, Y., 2019. Drivers of improved PM2. 5 air

quality in China from 2013 to 2017. *Proceedings of the National Academy of Sciences*, *116*(49), pp.24463-24469.

Zhang, R., Jing, J., Tao, J., Hsu, S.C., Wang, G., Cao, J., Lee, C.S.L., Zhu, L., Chen, Z., Zhao, Y. and Shen, Z., 2013. Chemical characterization and source apportionment of PM 2.5 in Beijing: seasonal perspective. *Atmospheric Chemistry and Physics*, *13*(14), pp.7053-7074.

Zhang, S., Wu, Y., Zhao, B., Wu, X., Shu, J. and Hao, J., 2017. City-specific vehicle emission control strategies to achieve stringent emission reduction targets in China's Yangtze River Delta region. *Journal of Environmental Sciences*, *51*, pp.75-87.

Zhang, X.Y., Gong, S.L., Shen, Z.X., Mei, F.M., Xi, X.X., Liu, L.C., Zhou, Z.J., Wang, D., Wang, Y.Q. and Cheng, Y., 2003. Characterization of soil dust aerosol in China and its transport and distribution during 2001 ACE-Asia: 1. Network observations. *Journal of Geophysical Research: Atmospheres*, *108*(D9).

Zhang, Y., Xia, J., Fang, H., Zuo, H. and Jiang, Y., 2019. Roadmap towards clean heating in 2035: Case study of inner Mongolia, China. *Energy*, *189*, p.116152.

Zheng, M., Salmon, L.G., Schauer, J.J., Zeng, L., Kiang, C.S., Zhang, Y. and Cass, G.R., 2005. Seasonal trends in PM2.5 source contributions in Beijing, China. *Atmospheric Environment*, *39*(22), pp.3967-3976.

Zhu, C., Tian, H., Hao, Y., Gao, J., Hao, J., Wang, Y., Hua, S., Wang, K. and Liu, H., 2018. A high-resolution emission inventory of anthropogenic trace

elements in Beijing-Tianjin-Hebei (BTH) region of China. *Atmospheric environment*, *191*, pp.452-462.

Zíková, N., Wang, Y., Yang, F., Li, X., Tian, M. and Hopke, P.K., 2016. On the source contribution to Beijing PM2.5 concentrations. *Atmospheric Environment*, *134*, pp.84-95.

Zong, Z., Wang, X., Tian, C., Chen, Y., Qu, L., Ji, L., Zhi, G., Li, J. and Zhang, G., 2016. Source apportionment of PM 2.5 at a regional background site in North China using PMF linked with radiocarbon analysis: insight into the contribution of biomass burning. *Atmospheric Chemistry and Physics*, *16*(17), pp.11249-11265.

Zong, Z., Wang, X., Tian, C., Chen, Y., Fu, S., Qu, L., Ji, L., Li, J. and Zhang, G., 2018. PMF and PSCF based source apportionment of PM2.5 at a regional background site in North China. *Atmospheric Research*, *203*, pp.207-215.

Chapter 4.

Characteristics of $PM_{2.5}$ organic extracts from Seoul and Beijing on human lung epithelial cells

ABSTRACT

This study focused on investigating the characteristics of organic compounds and sources of the $PM_{2.5}$ organic extracts collected in Seoul, South Korea and Beijing, China and evaluated the production of $PM_{2.5}$ organic extract induced IL-8 on human lung epithelial cells. The expression levels of IL-8 in Beijing were significantly higher than that of Seoul and organic compounds within $PM_{2.5}$ were found to be more important in inducing neutrophilic inflammation than $PM_{2.5}$ mass concentrations itself. For Seoul, PAHs and biomass burning source showed strong correlations with IL-8 expression levels. However, organic compounds such as aliphatic diacaids, alkylcyclohexanes and alkanoic acids showed positive correlations with expression levels of IL-8 at Beijing. Moreover, SOC-1 (biogenic SOC) and SOC-2 (anthropogenic SOC) showed strong correlations with IL-8 expression levels. The results indicated that organic compounds and sources which play important role in inflammation at Seoul and Beijing are different.

Keywords: $PM_{2.5}$, organic compounds, lung epithelial cells, IL-8, inflammation

1. Introduction

East Asian countries has been suffering from frequent occurrence of severe air pollution. With significant adverse impacts on human health such as pulmonary and cardiovascular diseases (Pope and Dockery, 2006; Polichetti et al., 2009; Lee et al., 2014; Lu et al., 2015), $PM_{2.5}$ is one of the major air pollutants that has been regulated worldwide. Unlike PM_{10}, $PM_{2.5}$ can penetrate into the end of the respiratory tract without filtration (Pinkerton et al., 2000) and cause local inflammation which may even lead to systemic inflammation (Kocbach, 2008; Xing et al., 2016). Among $PM_{2.5}$ constituents, carbonaceous components which takes up about 20 to 40% of $PM_{2.5}$ are one of the major components which is highly toxic to humans (Ramdahl, 1983; He et al., 2001; Kanakidou et al., 2005; Putaud et al., 2010). Though only take small part of carbonaceous components, organic compounds such as polycyclic aromatic hydrocarbons (PAHs), n-alkanes were found to be carcinogenic substances (Mastrangelo et al., 1996; Baird et al., 2005; Taghvaee et al., 2018).

Active emissions from anthropogenic sources in addition to meteorological conditions increase $PM_{2.5}$ concentrations (Sun et al., 2006; Ji et al., 2014). OC can be formed from primary emitting sources as well as gas to particle conversion processes. Biomass burning, coal combustion, gasoline and diesel exhaust from vehicles, cooking, and vegetative detritus were found to be major sources of organic aerosols in previous studies (Jaeckels et al., 2007; Zhang et al., 2009; Arhami et al., 2018). As South Korea is located in downwind of China, faith of high $PM_{2.5}$ concentration events are unavoidable (Kim et al., 2009; Park et al., 2016). However, $PM_{2.5}$ is a mixture of complex chemicals elucidated from various sources under

different meteorological conditions, thus fraction of its constituents varies greatly depending on the location. Seoul and Beijing are urbanized megacities with high population density. As capital cities, regional and long range transported air pollutants from various sources will affect large group of population in these sites. Thus, it is important to perform a comprehensive study on the characteristics of organic compounds and contributing sources in both two sites and their effects on human lung epithelial cells.

Prior study (chapter 2) found that $PM_{2.5}$ organic extracts collected from Seoul induced high expression levels of active extracellular signal-regulated kinase (ERK) and interleukin-8 (IL-8). The small number of samples and source apportionment based only on non-polar compounds have inhibited to identify secondary sources and to find the statistical significance. In order to overcome the limitations, this chapter increased the number of samples collected in 2019 and analysis on polar compounds were added to perform detailed source apportionment using PMF. Therefore, this study investigated the characteristics of organic compounds and sources of the $PM_{2.5}$ organic extracts collected in Seoul, South Korea and Beijing, China and evaluated the production of $PM_{2.5}$ organic extract induced IL-8 on human lung epithelial cells.

2. Materials and methods

2.1 Sampling sites and collection procedure

$PM_{2.5}$ samples from two sampling sites were used to compare between Seoul and Beijing. The locations of the sampling sites are same as the sampling sites mentioned in chapter 3. In each site, samples were collected for twenty-four hour by using a high-volume air sampler (TE-HVPLUS, TISCH, USA) and a low-volume air sampler with filter pack (URG-2000-30FG, URG, USA) and cyclone (URG-2000-30EH, URG, USA). Low-volume air samplers were loaded with Teflon filters (PTFE membrane, Pall Corporation, USA) and high-volume air samplers were loaded with pre-baked (450℃ for 24 h) quartz filters.

2.2 $PM_{2.5}$ chemical analyses

Collected samples were kept below -20℃ before use. Teflon filters were stored in desiccator at least 24 h before and after sampling to be accurately weighted in a semi-micro balance (accuracy of 0.01 mg) (CP225D, Sartorius). 17 samples and 18 samples were selected from Seoul and Beijing, respectively. These samples encompass summer and winter.

Quartz filters from high volume air samplers were used to analyze OC, EC, organic compounds and cell exposure. The filters were punched (1.5 cm x 1.0 cm) to analyze OC and EC using a carbon aerosol analyzer (Sunset Laboratory Inc., USA) and thermal/optical transmittance (TOT) method was used for the data quantification. The filters were also punched by a stainless cutter in size of 4 cm x 8 cm and were

used for extraction. As mentioned in chapter 2, solvent mixture of dichloromethane:methanol (3:1, v/v) was used for sample extractions with ultrasonic bath. A Turbovap II (Zymark Co., USA) with N_2 gas was used to concentrate the extracted samples into 10 mL. Then the samples were filtered with 0.45 μm Acrodisc Syringe Filters (Pall Corporation, USA) and concentrated in to 1 mL with a Turbovap II and Reacti-Therm (Thermo Fisher Scientific, USA) under a gentle stream of N_2 gas. The extracted samples were used for analysis of organic compound and *in vitro* experiments. Gas chromatography-mass spectrometry (7080B/5977B, Agilent Technologies, Inc., USA) was used for quantification of 57 species of non-polar and 52 species of polar compounds with 6 calibration standards. From 1 mL concentrated extraction, 50 μL was silylated for the analysis of polar compounds. Conditions of silylation was reaction at 75℃ for 90 minutes after adding N, O-bis-(trimethylsilyl) trifluoroacetamide (BSTFA) with 1% trimethylchlorosilane (TMCS) (99%, Sigma Aldrich, USA) and pyridine (HPLC grade, Sigma Aldrich, USA).

2.3 Cell culture and exposure

Normal human bronchial epithelial cells (BEAS-2B from ATCC, Manassas, VA, USA) were maintained in defined keratinocyte-SFM (Gibco by Thermo Fisher Scientific, Waltham, MA, USA) at 37°C under 5% CO_2. The same exposure dose (1%) and time (24 h) were used as previous experiment in chapter 2. The levels of IL-8 in cell culture media were measured by enzyme-linked immunosorbent assay (ELISA) using the Human IL-8 (DuoSet ELISA kit, R&D Systems, Minneapolis, MN).

2.4 Source apportionment of organic compounds in $PM_{2.5}$ using PMF

PMF model is widely used for ambient $PM_{2.5}$ source apportionment. In this study, EPA's PMF 5.0 was employed for the source apportionment of $PM_{2.5}$ of OC in Seoul and Beijing. Unlike CMB, PMF is more advanced model that does require source profiles. A total of 41 and 43 parameters were used for Seoul and Beijing, respectively. Though 109 species of organic compounds have been analyzed these organic compounds were specifically selected as molecular marker which are usually used as source tracer (Schauer and Sioutas, 2012). In addition, among selected molecular markers, species with the low signal to noise ratio were excluded (Paatero and Hopke, 2003). Inputs included mass concentrations and associated uncertainties. Once sources have been identified, the source contributions were only calculated for samples which were selected for lung epithelial cell exposure analysis.

2.5 Trajectory cluster analysis

72 h backward trajectories for Seoul and Beijing site were calculated by using HYSPLIT 4 model of the National Oceanic and Atmospheric Administration, USA. Meteorological data with a resolution of 1° from GDAS for 2019 was used to calculate endpoint dataset for every hour. Four clustering pathways were identified.

3. Results and Discussion

3.1 $PM_{2.5}$ and chemical constituents

A summary of $PM_{2.5}$ mass concentrations, its chemical constituents and expression levels IL-8 of Seoul and Beijing are displayed in Table 4-1 and Figure 4-1. The average $PM_{2.5}$ mass concentrations in Seoul and Beijing were 27.0 μg/m^3 and 37.5 μg/m^3, respectively. Also, the average OC concentrations in Seoul and Beijing were 5.0 μg/m^3 and 6.8 μg/m^3, respectively. Both of the average $PM_{2.5}$ mass concentrations and OC concentrations in Beijing were higher than that of Seoul, but the difference was not statistically significant. However, the average concentration of organic compounds in Beijing (526.0 ng/m^3) was significantly higher than that of Seoul (340.7 ng/m^3). Moreover, the expression levels of IL-8 was significantly higher in Beijing (130.6 pg/mL) than that of Seoul (84.2 pg/mL). The results align with the chapter 2 results that organic compounds within $PM_{2.5}$ are more important in inducing neutrophilic inflammation than $PM_{2.5}$ mass concentrations itself.

While Beijing had higher average concentrations of most of the organic compounds, n-alkanes, dicarboxylic acids, benzenecarboxylic acids, alkanoic acids, and fatty acids were especially higher than that of Seoul (Table 4-1 and Figure 4-2). Major sources of n-alkanes include biogenic sources such as vegetative detritus, plant wax emission and anthropogenic sources such as biomass burning, road-dust, and fossil fuel combustion (Bi et al., 2003; Feng et al., 2006). Dicarboxylic acids, benzenecarboxylic acids, alkanoic acids, and fatty acids are usually used as markers for secondary organic carbon (SOC) (Jaeckels et al., 2007; Wu et al., 2018). Though Seoul had lower average concentrations of organic compounds, hopanes and sugars/glycerides showed higher concentrations than that of Beijing. Hopanes are

widely known as markers for vehicle emission (Fraser et al., 1998; Yan et al., 2009; Yin et al., 2015) and levoglucosan (sugar) is a widely used marker of biomass burning (Simoneit et al., 1999; Schauer et al., 2001).

Correlations between the expression levels of IL-8 and organic compounds for Seoul and Beijing are presented in Table 4-2 and Table 4-3, respectively. Organic compounds which had statistically significant ($p<0.05$) positive correlations with IL-8 were only included in Table 4-2 and Table 4-3. As shown in chapter 2, PAHs and n-alkanes showed high correlations ($r>0.5$) with the expression levels of IL-8. Though, in this study, the samples not only included HCEs but also non-HCEs and the samples did not represent four seasons, the number of PAH and n-alkanes species which showed high correlations were different from chapter 2. However, for Seoul samples, PAHs such as indeno[1,2,3-cd]pyrene, dibenzo[a,h]anthracene, picene, benzo[ghi]perylene, coronene, dibenz[a,e]pyrene showed high correlations with the expression levels of IL-8 which align with the results in chapter 2. In addition, polar compounds such as benzenecarboxylic acids, fatty acids and sterols showed high correlations with the expression levels of IL-8. For Beijing samples, alkylcyclohexanes, aliphatic diacaids and alkanoic acids showed high correlations with the expression levels of IL-8. Only two species of PAHs and n-alkanes showed high correlations with IL-8 which indicate that organic compounds which play important role in inflammation at Seoul and Beijing are different. Moreover, not only primary emissions but also secondary source may induce the inflammation.

Table 4-1 Summary of $PM_{2.5}$, chemical constituents and expression levels of IL-8 in Seoul and Beijing

	unit	Seoul (N=17)		Beijing (N=18)	
		Average	Stdev.	Average	Stdev.
IL-8	pg/mL	84.2	18.7	130.6	54.1
$PM_{2.5}$	$\mu g/m^3$	27.0	11.2	37.5	34.3
EC	$\mu g/m^3$	0.6	0.4	0.7	0.3
OC	$\mu g/m^3$	5.0	2.3	6.8	3.9
Σ Organic compounds	ng/m^3	340.7	82.8	526.0	133.0
Σ PAHs	ng/m^3	19.1	11.1	18.4	20.0
Σ n-alkanes	ng/m^3	159.2	44.5	275.6	67.3
Σ Hopanes and steranes	ng/m^3	10.3	5.6	8.4	2.3
Σ Alkylcyclohexanes and isoprenoids	ng/m^3	16.5	9.7	15.2	9.8
Σ Aliphatic Diacaids	ng/m^3	29.9	21.2	47.2	30.4
Σ Benzenecarboxylic Acids	ng/m^3	5.6	3.1	12.1	7.2
Σ Alkanoic Acids	ng/m^3	27.6	8.6	51.6	11.5
Σ fatty acids	ng/m^3	32.2	9.4	59.0	17.2
Σ Sugars/Glycerides	ng/m^3	28.2	18.7	21.7	24.9
Σ sterols	ng/m^3	1.1	0.5	1.8	2.0
Σ methoxyPheols	ng/m^3	6.5	1.9	8.7	3.2
Σ Resin Acids	ng/m^3	4.5	3.0	6.2	4.1

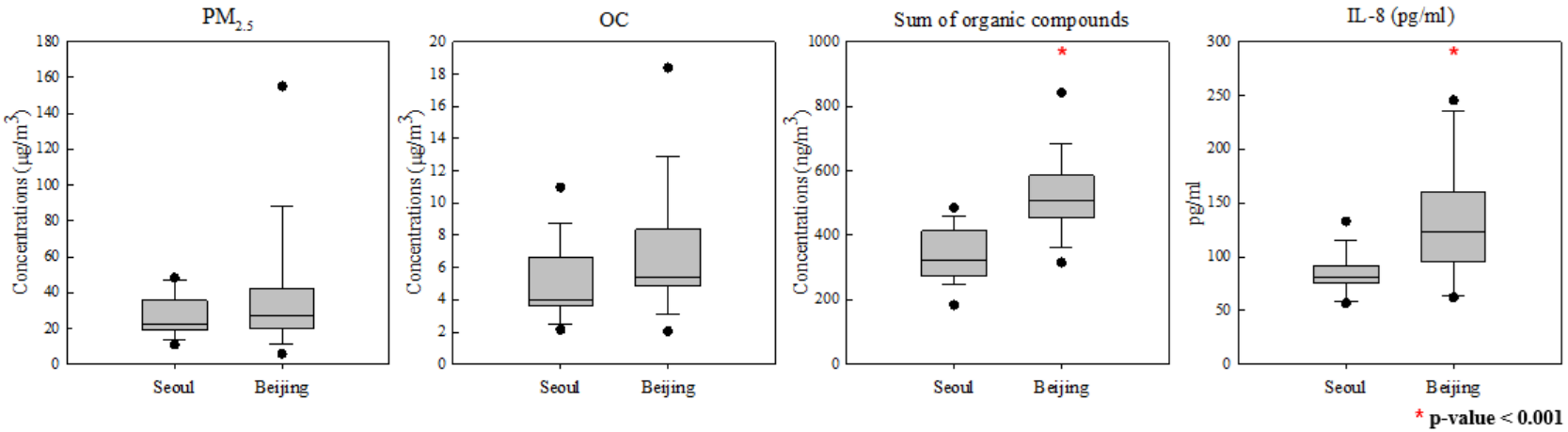

Figure 4-1 Box plots of $PM_{2.5}$, OC, organic compounds and IL-8 for Seoul and Beijing

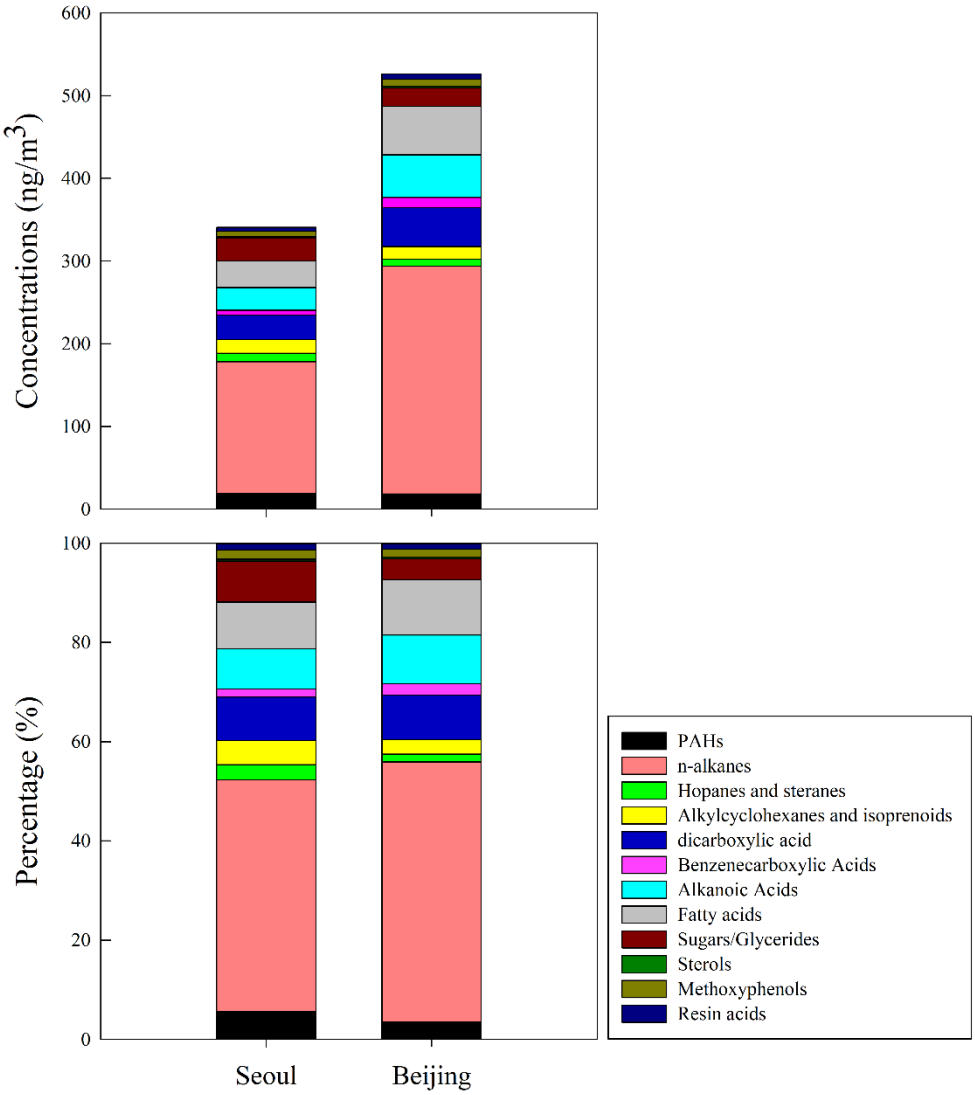

Figure 4-2 Stacked concentrations and percent composition of organic compounds in Seoul and Beijing

Table 4-2 Correlation between IL-8 and organic compounds for Seoul

	r	p-value
PAHs		
Indeno[1,2,3-cd]pyrene	0.77	<0.001
Dibenzo[a,h]anthracene	0.55	<0.001
Picene	0.55	0.028
Benzo[ghi]perylene	0.68	0.004
Coronene	0.76	0.001
Dibenz[a,e]pyrene	0.58	0.018
ΣPAHs	0.67	0.005
n-alkanes		
n-C27	0.62	0.010
Benzenecarboxylic Acids		
Phthalic Acid (1,2)	0.71	0.047
Fatty acids		
Palmitoleic Acid (C16:1)	0.59	0.015
Triacontanoic acid	0.83	0.001
Sterols		
ΣSterols	0.50	0.050

Table 4-3 Correlation between IL-8 and organic compounds for Beijing

	r	p-value
PAHs		
Dibenzo[a,e]pyrene	0.58	0.016
n-alkanes		
n-C22	0.63	0.005
Alkylcyclohexanes and isoprenoids		
2-Methylnonadecane	0.66	0.003
3-Methylnonadecane	0.71	0.001
ΣAlkylcyclohexanes and isoprenoids	0.78	<0.001
Aliphatic Diacaids		
Glutaric (C5)	0.49	0.039
Suberic (C8)	0.50	0.036
Azelaic (C9)	0.47	0.047
Sebacic (C10)	0.51	0.030
ΣAliphatic Diacaids	0.49	0.040
Alkanoic Acids		
C16:0	0.61	0.007
C18:0	0.50	0.034
ΣAlkanoic Acids	0.49	0.038

3.2 PMF results

While CMB are used for identifying primary sources with few numbers of samples, PMF are widely used for source apportionment of primary as well as secondary sources. In order to trace primary and secondary sources to ambient OC, PMF was employed with 41 and 43 molecular markers for Seoul and Beijing samples, respectively. 52 samples and 73 samples were used for Seoul and Beijing, respectively. PMF has been performed number of times with four, five, and six factors for each site. Five factors at Seoul and six factors at Beijing were selected as optimal solution.

For Seoul, primary biogenic, mobile, biomass burning, SOC-1/cooking, and SOC-2 were identified as contributing sources to ambient OC (Figure 4-3). Primary biogenic source was characterized by high loadings of n-alkanes (n-C25~n-C33), phthalic acid, and levoglucosan and accounted for 23.7% to OC at Seoul which was second highest contributing source. High contribution of primary biogenic source may be due to the Gwanak mountain nearby which is one of the highest mountains in Seoul. Mobile source was identified with high loading of hopanes (17A(H)-21B(H)-30-norhopane, 17A(H)-21B(H)-hopane), steranes (AAA-20S-C27-Cholestane, ABB-20R-C27-Cholestane), PAHs (coronene, perylene, indeno[1,2,3-cd]pyrene, benzo[ghi]perylene, benzo[a]pyrene, benzo[e]pyrene) and n-alkanes (n-C27~n-C33) (Shrivastava et al., 2007; Schauer and Sioutas, 2012). As EC and hopanes are used as markers for diesel vehicles (Schauer et al., 1999) and PAHs and steranes are well known markers for gasoline vehicles (Schauer et al., 2002; Heo et al., 2013), mobile factor in Seoul comprises of both diesel and gasoline

vehicles. Mobile factor contributed about 13.1% to OC and had steady contributions throughout the year. Biomass burning source was characterized by high loadings of levoglucosan and PAHs (Simoneit et al., 1999; Schauer et al., 2001; Sarigiannis et al., 2015; Zhang et al., 2016). Burning of agricultural residue after wheat and rice harvest may have caused the high contributions in spring, autumn, and winter but not in summer. The contributions of biomass burning accounted for 16.8% to OC at Seoul. SOC-1/cooking source accounted for 31.8% and showed highest contributions to OC. This factor was characterized by high loadings of palmitoleic acid, methylphthalic acid, phthalic acid, succinic acid and pinonic acid. While pinonic acid is a marker for biogenic SOA, methylphthalic acid, phthalic acid and succinic acid are markers for anthropogenic SOA as they are produced from photochemical oxidation of PAHs (Sheesley et al., 2004; Baltensperger et al., 2005). Thus SOC-1 is a mixed source of biogenic and anthropogenic SOC. Palmitoleic acid and PAHs (benzo[k]fluoranthene, benzo[a]pyrene, and benzo[e]pyrene) are usually used as tracer for cooking (Rogge et al., 1991; Schauer et al., 1999). SOC-2 was identified by high loadings to aliphatic diacaids such as succinic acid, glutaric acid, pimelic acid, suberic acid, azelaic acid, and sebacic acid and moderate loading of pinonic acid. This factor accounted for 14.5% to OC. Aliphatic dicarboxylic acids are known indicators of anthropogenic SOC which are formed through photo-oxidation process of pollutants (Shrivastava et al., 2007; Choi et al., 2012) from primary sources such as vehicles, meat cooking and wood combustion (Simoneit, 1986; Park et al., 2006). Thus, SOC-2 was dominated by anthropogenic sources.

For Beijing, SOC-1, SOC-2, mobile-1/SOC, biomass burning, mobile-2, and coal related combustion were identified as contributing sources to ambient OC (Figure 4-4). The contributions of SOC-1 source to OC was 15.7% and had higher contributions in summer and fall. High loadings of pinonic acid, n-alkanes (n-C27~n-C33), and methylphthalic acid were used to identify the factor. As mentioned earlier, pinonic acid is formed through oxidation of biogenic precursors and n-alkanes are from plant waxes which are non-volatile and carried out by long-range transport (Feng et al., 2006). Thus, SOC-1 was interpreted as biogenic SOC. SOC-2 only had high loadings of aliphatic diacaids which can be characterized as anthropogenic SOC. The contributions of SOC-2 to OC was 8.5% and had high contributions in winter. Mobile-1/SOC source was characterized by high loadings of hopanes (17A(H)-21B(H)-30-norhopane and 17A(H)-21B(H)-hopane), EC, and medium loadings of isophthalic acid, phthalic acid, methyphthalic acid, succinic and glutaric acid. High contributions of hopanes and EC could distinguish diesel from gasoline vehicles (Schauer et al., 1999). In addition, succinic and glutaric acid are more likely to be found in diesel vehicle exhaust compare to gasoline vehicle exhaust (Dabek-Zlotorzynska et al., 2005). This factor showed distinct characteristics of diesel related mobile source and was highest contributing source (39.3%). As mentioned earlier, biomass burning source had high loadings of levoglucosan and mannosan. Similar to seasonal trend of Seoul, high contributions were shown in spring, autumn and winter. Though the percent contribution of biomass burning at Beijing (17.7%) was similar to that of Seoul (16.8%), the concentrations were twice as high at Beijing (1.46 $\mu g/m^3$) than that of Seoul (0.71 $\mu g/m^3$). Previous studies

have reported that the contribution of biomass burning to $PM_{2.5}$ OC at Beijing ranged from 18 to 38% (Zhang et al., 2008) which is similar to the result of this study. Mobile-2 source had high loadings of steranes (AAA-20S-C27-cholestane and ABB-20R-C27-cholestane), hopane (17A(H)-22, 29, 30-trisnorhopane), n-alkanes (n-C28~n-C33) and PAHs (coronene and perylene). Numerous studies have reported that significant enrichment of AAA-20S-C27-cholestane, ABB-20R-C27-cholestane, 17A(H)-22, 29, 30-trisnorhopane, coronene and perylene were shown in gasoline vehicle exhaust (Schauer et al., 1996; Schauer et al., 2002; Cai et al., 2017). Coal related combustion source had high loadings of PAHs (Phenanthrene, fluoranthene, pyrene, benzo[a]anthracene, chrysene, benzo[b]fluoranthene, benzo[k]fluoranthene, benzo[a]pyrene, benzo[e]pyrene, perylene, indeno[1,2,3-cd]pyrene, picene, and benzo[ghi]perylene. These organic compounds are used as markers for coal combustion in China (Zhang et al., 2008).

The source contributions and percent contributions of the samples which were sent for exposure analysis were presented in Figure 4-5 and Figure 4-6. At Seoul (N=17), the source with highest contribution to $PM_{2.5}$ OC was SOC-1/cooking (38.2%), followed by biomass burning (27.4%), primary biogenic (15.4%), mobile (9.7%) and SOC-2 (9.3%). The highest contributing source at Beijing (N=18) was SOC-1 (28.3%), followed by mobile-1/SOC (25.2%), mobile-2 (17.8%), biomass burning (13.0%), SOC-2 (9.2%), and coal related combustion (6.4%).

Levels of IL-8, source contributions and percent contributions to $PM_{2.5}$ OC at Seoul and Beijing were displayed in Figure 4-7. At Seoul, source which showed positive correlations with IL-8 expression levels was biomass burning (r=0.5, p-

value=0.047). High correlations with IL-8 corroborates with the result from chapter 2 that vegetative detritus had high correlations with IL-8 production. Moreover, biomass burning source at Seoul had high loadings of PAHs which also align with the result from chapter 2 which PAHs are important chemical composition that cause adverse health effects. On the other hand, sources which showed positive correlations with IL-8 expression levels at Beijing were SOC-1 (r=0.5, p-value=0.025) and SOC-2 (r=0.51, p-value=0.030).

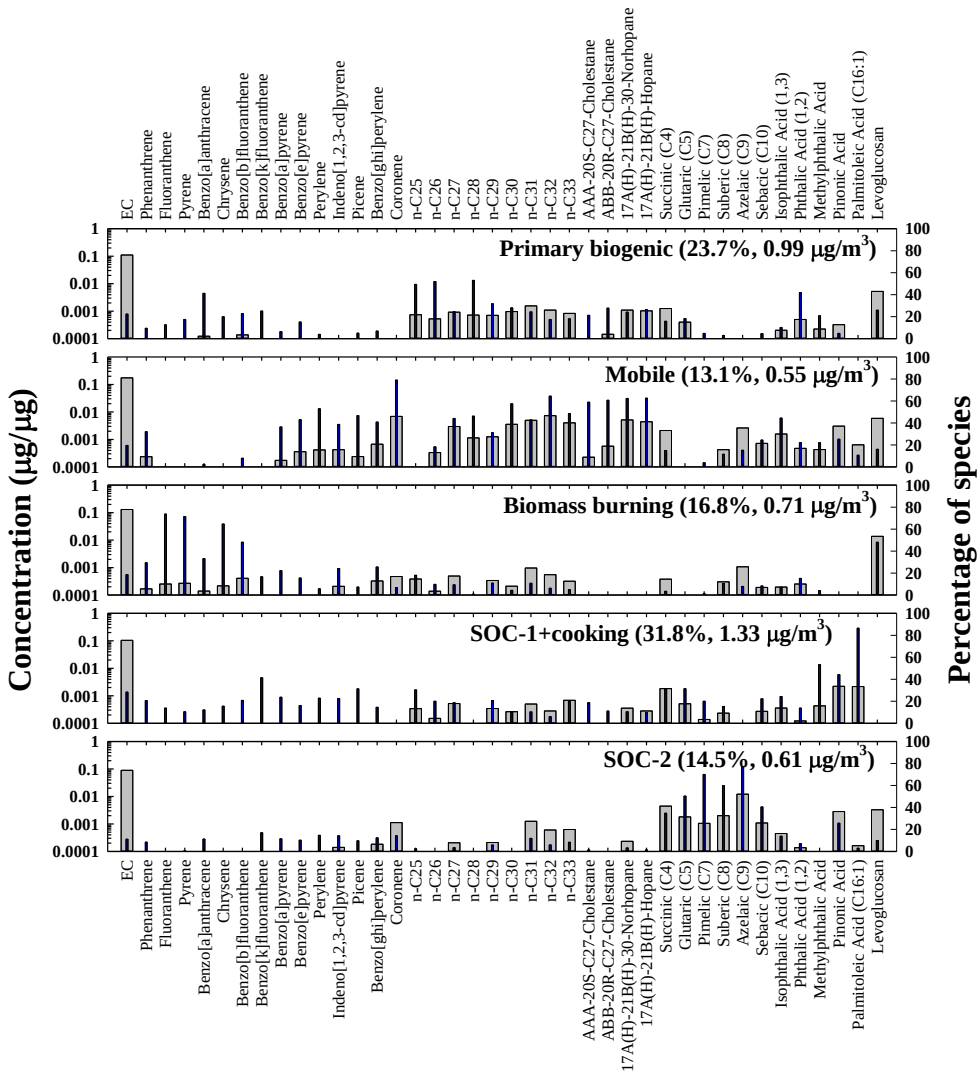

Figure 4-3 Source profiles of $PM_{2.5}$ OC in Seoul (N=52)

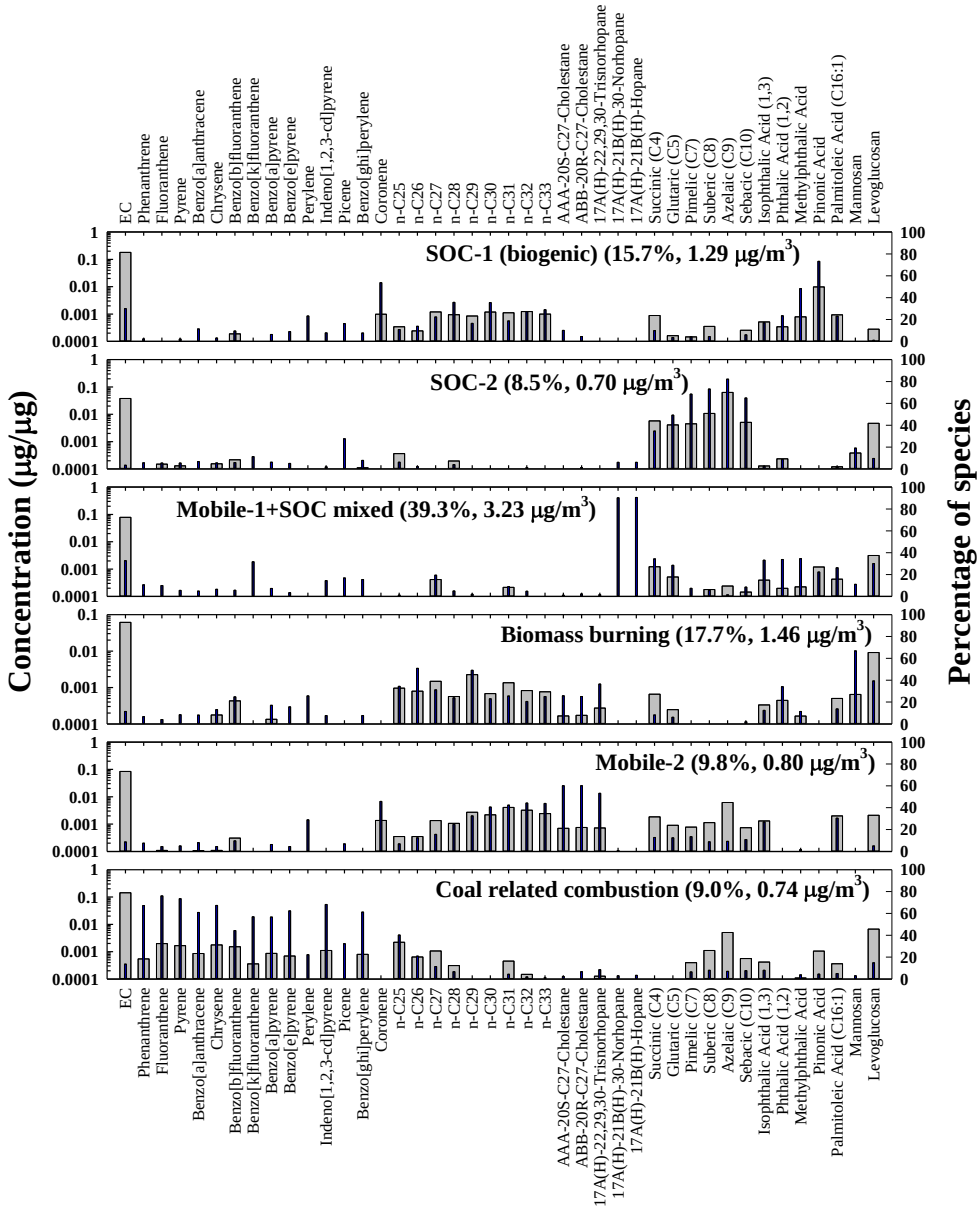

Figure 4-4 Source profiles of $PM_{2.5}$ OC in Beijing (N=73)

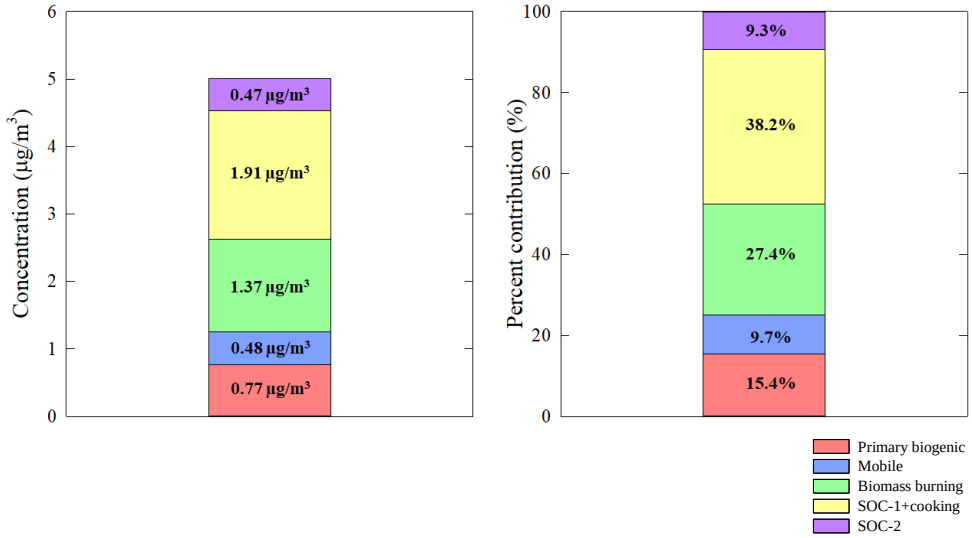

Figure 4-5 Stacked source concentrations and percent contributions of samples with exposure analysis in Seoul (N=17)

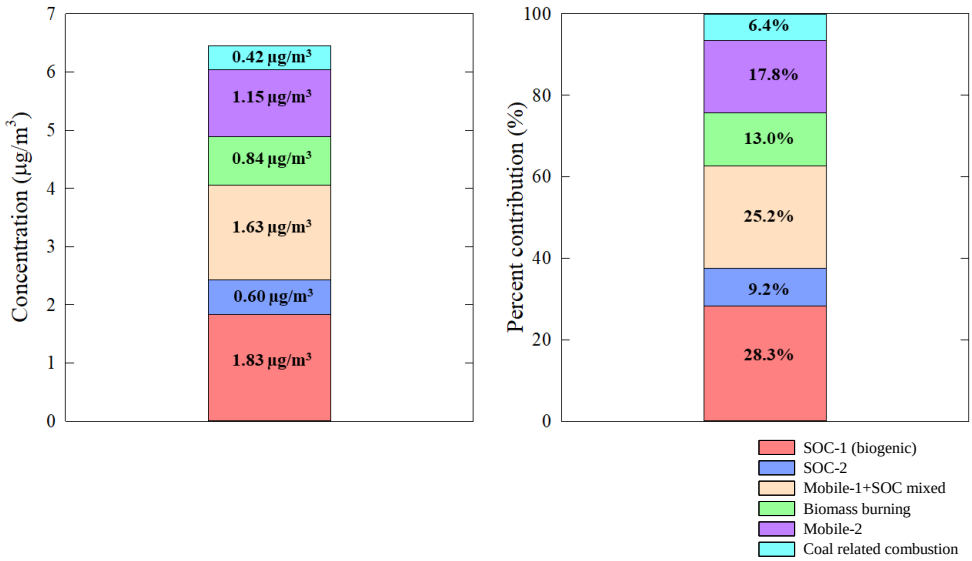

Figure 4-6 Stacked source concentrations and percent contributions of samples with exposure analysis in Beijing (N=18)

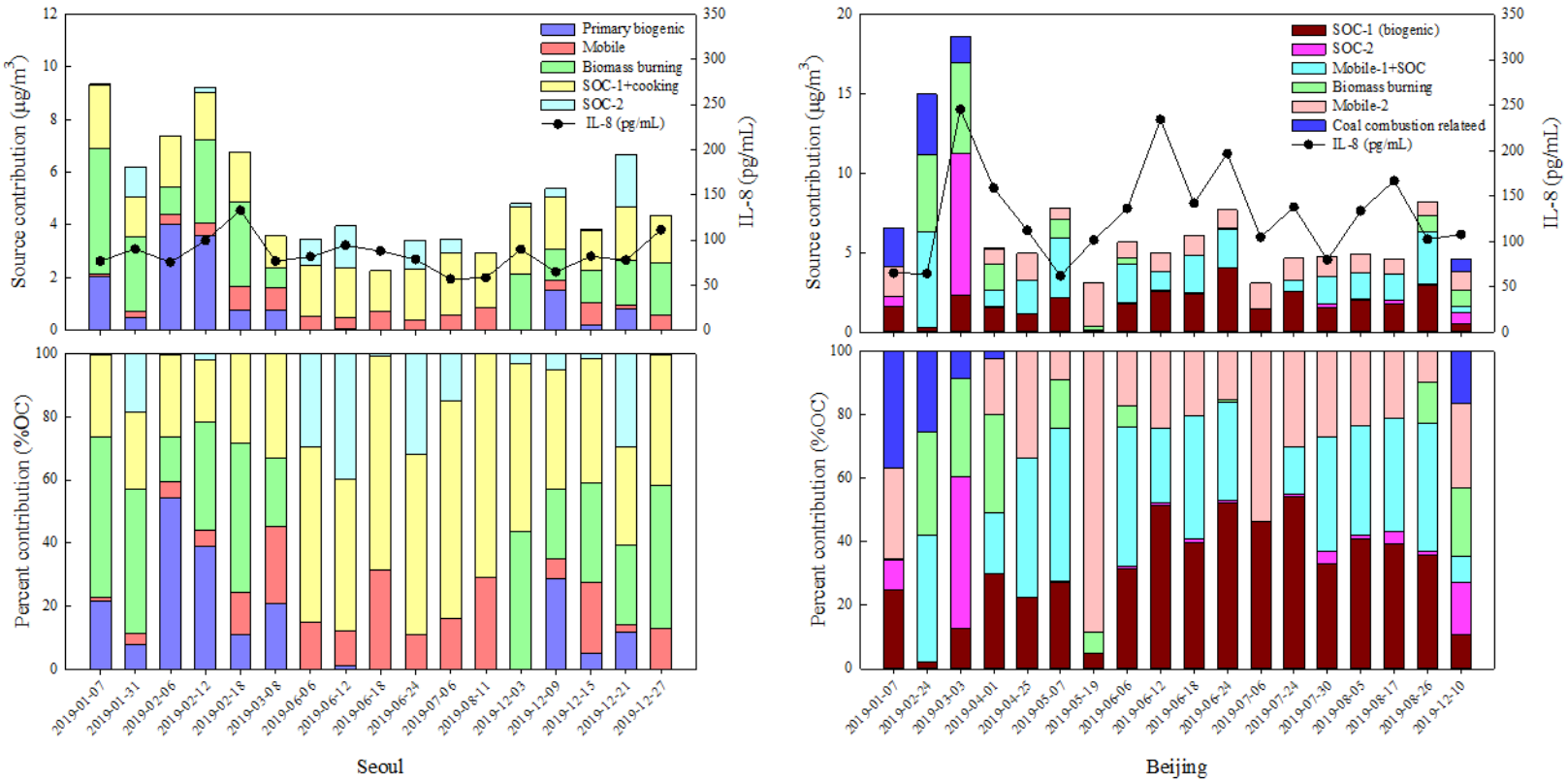

Figure 4-7 Levels of IL-8, source contributions and percent contributions to $PM_{2.5}$ OC at Seoul (N=17) and Beijing (N=18)

3.3 Cluster analysis and expression levels of IL-8 at Seoul and Beijing

The results of clustering pathways arriving at Seoul and Beijing were presented in Figure 4-8 and Figure 4-9, respectively. Four clustering pathways were identified for Seoul. Cluster 1 (27%) and 3 (13%) came in northwestern direction from northern China and Russia, respectively and passed through northern China and North Korea. Cluster 2 accounted for 50% of trajectories and was from east China. Cluster 4 came from east of South Korea where Japan is located and accounted for 10%. Out of 17 samples which were selected at Seoul site, most of the samples came through cluster 1 (N=6) and 2 (N=8). The average IL-8 expression level was highest for cluster 1 (97.6 pg/mL) and lowest for cluster 4 (57.4 pg/mL). In addition, two dates (winter) with highest IL-8 expression levels came from cluster 1 and two dates (summer) with lowest IL-8 expression levels came from cluster 4. The greatest difference in contributions between two dates with highest IL-8 expression levels and two dates with lowest IL-8 expression levels were shown in primary biogenic and biomass burning sources.

At Beijing, three clustering pathways were identified. Cluster 1 accounted for 37% of trajectories which came in from southeast of Beijing along the coastal area. Cluster 2 (39%) started from Mongolia passed through northern China and cluster 3 (23%) came in from Russia and passed through Mongolia. Among 18 samples, most of the samples came through cluster 1 (N=7) and 2 (N=7). Dates with highest expression levels of IL-8 were from cluster 1 (170.1 pg/mL) and lowest were from cluster 3 (84.0 pg/mL). The greatest difference in contributions between two

dates with highest IL-8 expression levels and two dates with lowest IL-8 expression levels were SOC-1 and SOC-2 sources.

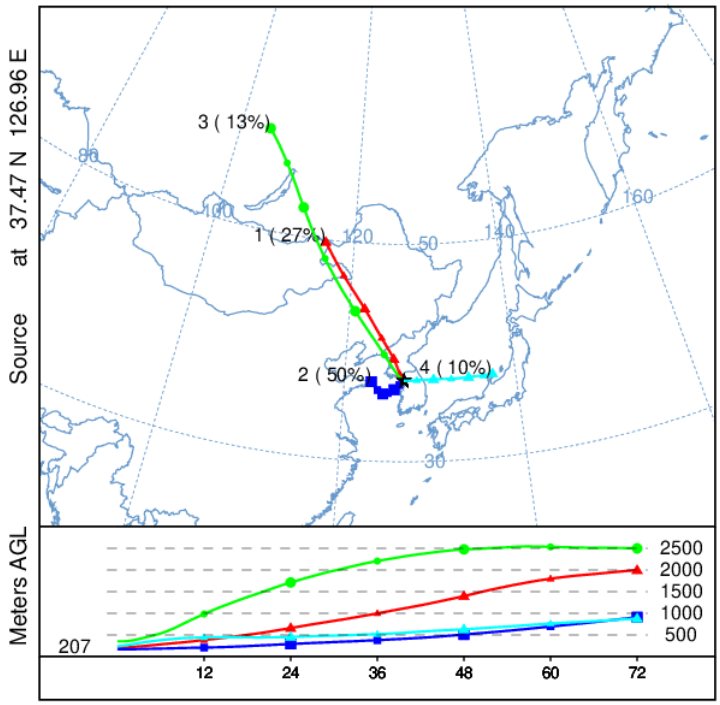

Figure 4-8 Mean 72 h backward trajectory clusters arriving at Seoul in 2019

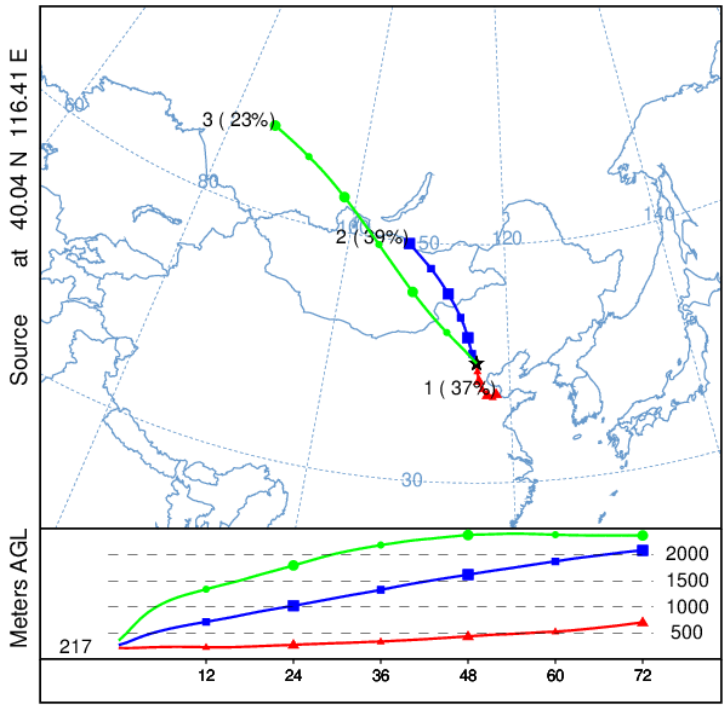

Figure 4-9 Mean 72 h backward trajectory clusters arriving at Beijing in 2019

4. Conclusions

In this study, 17 samples and 18 samples which were collected from Seoul and Beijing, respectively were selected for lung epithelial cell exposure to determine expression levels of IL-8. Samples were collected in 2019 and encompass winter and summer. The average $PM_{2.5}$ mass concentrations and OC concentrations in Beijing were higher than that of Seoul, but the difference was not statistically significant. However, the average concentration of organic compounds and the expression levels of IL-8 in Beijing were significantly higher than that of Seoul. The results indicate that organic compounds within $PM_{2.5}$ are more important in inducing neutrophilic inflammation than $PM_{2.5}$ mass concentrations itself.

For Seoul samples, PAHs such as indeno[1,2,3-cd]pyrene, dibenzo[a,h]anthracene, picene, benzo[ghi]perylene, coronene, dibenz[a,e]pyrene showed high correlations with the expression levels of IL-8 which align with the results in chapter 2. However, alkylcyclohexanes, aliphatic diacaids and alkanoic acids in Beijing samples showed strong association with the expression levels of IL-8. The results indicate that organic compounds which play important role in inflammation at Seoul and Beijing are different.

PMF was performed separately for Seoul and Beijing with 52 samples and 73 samples, respectively, and these data included samples which were selected for exposure analysis. For Seoul samples (N=17), the source with highest contributions to $PM_{2.5}$ OC was SOC-1/cooking (38.2%), followed by biomass burning (27.4%), primary biogenic (15.4%), mobile (9.7%) and SOC-2 (9.3%). Source which showed positive correlations with IL-8 expression levels was biomass burning (r=0.5, p-

value=0.047). The highest contributing source at Beijing (N=18) was SOC-1 (28.3%), followed by mobile-1/SOC (25.2%), mobile-2 (17.8%), biomass burning (13.0%), SOC-2 (9.2%), and coal related combustion (6.4%). Unlike Seoul, sources which showed positive correlations with IL-8 expression levels at Beijing were (r=0.5, p-value=0.025) and SOC-2 (r=0.51, p-value=0.030). Lastly, 72 h backward trajectory clusters were identified to be arriving at Seoul and Beijing in 2019. For Seoul, most of the samples came through cluster 1 (N=6) which came in from northwestern direction through Northern China and cluster 2 (N=8) which came in from western direction from Northern China. The average IL-8 expression level was highest for cluster 1 (97.6 pg/mL) and lowest for cluster 4 (57.4 pg/mL). Moreover, the greatest difference in contributions between two dates with highest IL-8 expression levels and two dates with lowest IL-8 expression levels were shown in primary biogenic and biomass burning sources. However, three clustering pathways were identified for Beijing and most of the samples came through cluster 1 (N=7) which came in from southeast of Beijing along the coastal area and cluster 2 (N=7) from Mongolia. Dates with highest expression levels of IL-8 were from cluster 1 (170.1 pg/mL) and lowest were from cluster 3 (84.0 pg/mL). Furthermore, the greatest difference in contributions between two dates with highest IL-8 expression levels and two dates with lowest IL-8 expression levels were SOC-1 and SOC-2 sources.

References

Arhami, M., Shahne, M.Z., Hosseini, V., Haghighat, N.R., Lai, A.M. and Schauer, J.J., 2018. Seasonal trends in the composition and sources of PM2.5 and carbonaceous aerosol in Tehran, Iran. *Environmental pollution*, *239*, pp.69-81.

Baird, W.M., Hooven, L.A. and Mahadevan, B., 2005. Carcinogenic polycyclic aromatic hydrocarbon-DNA adducts and mechanism of action. *Environmental and molecular mutagenesis*, *45*(2-3), pp.106-114.

Baltensperger, U., Kalberer, M., Dommen, J., Paulsen, D., Alfarra, M.R., Coe, H., Fisseha, R., Gascho, A., Gysel, M., Nyeki, S. and Sax, M., 2005. Secondary organic aerosols from anthropogenic and biogenic precursors. *Faraday Discussions*, *130*, pp.265-278.

Bi, X., Sheng, G., Chen, Y., Zhang, Z. and Fu, J., 2003. Distribution of particulate- and vapor-phase n-alkanes and polycyclic aromatic hydrocarbons in urban atmosphere of Guangzhou, China. *Atmospheric Environment*, *37*(2), pp.289-298.

Cai, T., Zhang, Y., Fang, D., Shang, J., Zhang, Y. and Zhang, Y., 2017. Chinese vehicle emissions characteristic testing with small sample size: Results and comparison. *Atmospheric Pollution Research*, *8*(1), pp.154-163.

Choi, J.K., Heo, J.B., Ban, S.J., Yi, S.M. and Zoh, K.D., 2012. Chemical characteristics of PM2.5 aerosol in Incheon, Korea. *Atmospheric environment*, *60*, pp.583-592.

Dabek-Zlotorzynska, E., Aranda-Rodriguez, R. and Graham, L., 2005. Capillary electrophoresis determinative and GC-MS confirmatory method for water-soluble organic acids in airborne particulate matter and vehicle emission. *Journal of separation science*, *28*(13), pp.1520-1528.

Feng, J., Chan, C.K., Fang, M., Hu, M., He, L. and Tang, X., 2006. Characteristics of organic matter in PM2.5 in Shanghai. *Chemosphere*, *64*(8), pp.1393-1400.

Feng, J., Hu, M., Chan, C.K., Lau, P.S., Fang, M., He, L. and Tang, X., 2006. A comparative study of the organic matter in PM2.5 from three Chinese megacities in three different climatic zones. *Atmospheric Environment*, *40*(21), pp.3983-3994.

Fraser, M.P., Cass, G.R. and Simoneit, B.R., 1998. Gas-phase and particle-phase organic compounds emitted from motor vehicle traffic in a Los Angeles roadway tunnel. *Environmental science & technology*, *32*(14), pp.2051-2060.

Gao, B., Yu, J.Z., Li, S.X., Ding, X., He, Q.F. and Wang, X.M., 2011. Roadside and rooftop measurements of polycyclic aromatic hydrocarbons in PM2.5 in urban Guangzhou: evaluation of vehicular and regional combustion source contributions. *Atmospheric Environment*, *45*(39), pp.7184-7191.

He, K., Yang, F., Ma, Y., Zhang, Q., Yao, X., Chan, C.K., Cadle, S., Chan, T. and Mulawa, P., 2001. The characteristics of PM2.5 in Beijing, China. *Atmospheric Environment*, *35*(29), pp.4959-4970.

Heo, J., Dulger, M., Olson, M.R., McGinnis, J.E., Shelton, B.R., Matsunaga, A., Sioutas, C. and Schauer, J.J., 2013. Source apportionments of PM2.5 organic carbon using molecular marker Positive Matrix Factorization and comparison of results from different receptor models. *Atmospheric Environment*, *73*, pp.51-61.

Jaeckels, J.M., Bae, M.S. and Schauer, J.J., 2007. Positive matrix factorization (PMF) analysis of molecular marker measurements to quantify the sources of

organic aerosols. *Environmental science & technology*, *41*(16), pp.5763-5769.

Ji, D., Li, L., Wang, Y., Zhang, J., Cheng, M., Sun, Y., Liu, Z., Wang, L., Tang, G., Hu, B. and Chao, N., 2014. The heaviest particulate air-pollution episodes occurred in northern China in January, 2013: Insights gained from observation. *Atmospheric Environment*, *92*, pp.546-556.

Kanakidou, M., Seinfeld, J.H., Pandis, S.N., Barnes, I., Dentener, F.J., Facchini, M.C., Dingenen, R.V., Ervens, B., Nenes, A.N.C.J.S.E., Nielsen, C.J. and Swietlicki, E., 2005. Organic aerosol and global climate modelling: a review. *Atmospheric Chemistry and Physics*, *5*(4), pp.1053-1123.

Kim, Y.J., Woo, J.H., Ma, Y.I., Kim, S., Nam, J.S., Sung, H., Choi, K.C., Seo, J., Kim, J.S., Kang, C.H. and Lee, G., 2009. Chemical characteristics of long-range transport aerosol at background sites in Korea. *Atmospheric Environment*, *43*(34), pp.5556-5566.

Kocbach, A., 2008. Pro-inflammatory potential of particles from residential wood smoke and traffic: Importance of physicochemical characteristics.

Lee, B.J., Kim, B. and Lee, K., 2014. Air pollution exposure and cardiovascular disease. *Toxicological research*, *30*(2), pp.71-75.

Lu, F., Xu, D., Cheng, Y., Dong, S., Guo, C., Jiang, X. and Zheng, X., 2015. Systematic review and meta-analysis of the adverse health effects of ambient PM2.5 and PM10 pollution in the Chinese population. *Environmental research*, *136*, pp.196-204.

Mastrangelo, G., Fadda, E. and Marzia, V., 1996. Polycyclic aromatic hydrocarbons and cancer in man. *Environmental health perspectives*, *104*(11), pp.1166-1170.

Paatero, P. and Hopke, P.K., 2003. Discarding or downweighting high-noise variables in factor analytic models. *Analytica Chimica Acta*, *490*(1-2), pp.277-289.

Park, S.S., Bae, M.S., Schauer, J.J., Kim, Y.J., Cho, S.Y. and Kim, S.J., 2006. Molecular composition of PM2.5 organic aerosol measured at an urban site of Korea during the ACE-Asia campaign. *Atmospheric Environment*, *40*(22), pp.4182-4198.

Park, S.S., Cho, S.Y., Jung, C.H. and Lee, K.H., 2016. Characteristics of water-soluble inorganic species in PM10 and PM2.5 at two coastal sites during spring in Korea. *Atmospheric Pollution Research*, *7*(2), pp.370-383.

Pinkerton, K.E., Green, F.H., Saiki, C., Vallyathan, V., Plopper, C.G., Gopal, V., Hung, D., Bahne, E.B., Lin, S.S., Ménache, M.G. and Schenker, M.B., 2000. Distribution of particulate matter and tissue remodeling in the human lung. *Environmental Health Perspectives*, *108*(11), pp.1063-1069.

Polichetti, G., Cocco, S., Spinali, A., Trimarco, V. and Nunziata, A., 2009. Effects of particulate matter (PM10, PM2.5 and PM1) on the cardiovascular system. *Toxicology*, *261*(1-2), pp.1-8.

Pope III, C.A. and Dockery, D.W., 2006. Health effects of fine particulate air pollution: lines that connect. *Journal of the air & waste management association*, *56*(6), pp.709-742.

Putaud, J.P., Van Dingenen, R., Alastuey, A., Bauer, H., Birmili, W., Cyrys, J., Flentje, H., Fuzzi, S., Gehrig, R., Hansson, H.C. and Harrison, R.M., 2010. A European aerosol phenomenology–3: Physical and chemical characteristics of particulate matter from 60 rural, urban, and kerbside sites across Europe. *Atmospheric Environment*, *44*(10), pp.1308-1320.

Ramdahl, T., 1983. Retene—a molecular marker of wood combustion in ambient air. *Nature*, *306*(5943), pp.580-582.

Rogge, W.F., Hildemann, L.M., Mazurek, M.A., Cass, G.R. and Simoneit, B.R., 1991. Sources of fine organic aerosol. 1. Charbroilers and meat cooking operations. *Environmental Science & Technology*, *25*(6), pp.1112-1125.

Sarigiannis, D.A., Karakitsios, S.P., Zikopoulos, D., Nikolaki, S. and Kermenidou, M., 2015. Lung cancer risk from PAHs emitted from biomass combustion. *Environmental Research*, *137*, pp.147-156.

Schauer, J.J., Kleeman, M.J., Cass, G.R. and Simoneit, B.R., 1999. Measurement of emissions from air pollution sources. 1. C1 through C29 organic compounds from meat charbroiling. *Environmental science & technology*, *33*(10), pp.1566-1577.

Schauer, J.J., Kleeman, M.J., Cass, G.R. and Simoneit, B.R., 1999. Measurement of emissions from air pollution sources. 2. C1 through C30 organic compounds from medium duty diesel trucks. *Environmental science & technology*, *33*(10), pp.1578-1587.

Schauer, J.J., Kleeman, M.J., Cass, G.R. and Simoneit, B.R., 2001. Measurement of emissions from air pollution sources. 3. C1− C29 organic compounds from fireplace combustion of wood. *Environmental science & technology*, *35*(9), pp.1716-1728.

Schauer, J.J., Kleeman, M.J., Cass, G.R. and Simoneit, B.R., 2002. Measurement of emissions from air pollution sources. 5. C1− C32 organic compounds from gasoline-powered motor vehicles. *Environmental science & technology*, *36*(6), pp.1169-1180.

Schauer, J.J., Rogge, W.F., Hildemann, L.M., Mazurek, M.A., Cass, G.R. and Simoneit, B.R., 1996. Source apportionment of airborne particulate matter using organic compounds as tracers. *Atmospheric Environment*, *30*(22), pp.3837-3855.

Schauer, J.J. and Sioutas, C., 2012. *Source Apportionment of Carbonaceous Aerosols Using Integrated Multi-variant and Source Tracer Techniques and a Unique Molecular Marker Data Set*. California Environmental Protection Agency, Air Resources Board, Research Division.

Sheesley, R.J., Schauer, J.J., Hemming, J.D., Barman, M.A., Geis, S.W. and Tortorelli, J.J., 2004. Toxicity of ambient atmospheric particulate matter from the Lake Michigan (USA) airshed to aquatic organisms. *Environmental Toxicology and Chemistry: An International Journal*, *23*(1), pp.133-140.

Shrivastava, M.K., Subramanian, R., Rogge, W.F. and Robinson, A.L., 2007. Sources of organic aerosol: Positive matrix factorization of molecular marker data and comparison of results from different source apportionment models. *Atmospheric Environment*, *41*(40), pp.9353-9369.

Simoneit, B.R., 1986. Characterization of organic constituents in aerosols in relation to their rigin and transport: a review. *International Journal of Environmental Analytical Chemistry*, *23*(3), pp.207-237.

Simoneit, B.R., Schauer, J.J., Nolte, C.G., Oros, D.R., Elias, V.O., Fraser, M.P., Rogge, W.F. and Cass, G.R., 1999. Levoglucosan, a tracer for cellulose in biomass burning and atmospheric particles. *Atmospheric Environment*, *33*(2), pp.173-182.

Sun, Y., Zhuang, G., Tang, A., Wang, Y. and An, Z., 2006. Chemical characteristics of PM2. 5 and PM10 in haze− fog episodes in Beijing. *Environmental science & technology*, *40*(10), pp.3148-3155.

Taghvaee, S., Sowlat, M.H., Hassanvand, M.S., Yunesian, M., Naddafi, K. and Sioutas, C., 2018. Source-specific lung cancer risk assessment of ambient PM2.5-bound polycyclic aromatic hydrocarbons (PAHs) in central Tehran. *Environment international*, *120*, pp.321-332.

Wu, X., Vu, T.V., Shi, Z., Harrison, R.M., Liu, D. and Cen, K., 2018. Characterization and source apportionment of carbonaceous PM2.5 particles in China-A review. *Atmospheric Environment*, *189*, pp.187-212.

Xing, Y.F., Xu, Y.H., Shi, M.H. and Lian, Y.X., 2016. The impact of PM2.5 on the human respiratory system. *Journal of thoracic disease*, *8*(1), p.E69.

Yan, B., Zheng, M., Hu, Y., Ding, X., Sullivan, A.P., Weber, R.J., Baek, J., Edgerton, E.S. and Russell, A.G., 2009. Roadside, urban, and rural comparison of primary and secondary organic molecular markers in ambient PM2. 5. *Environmental science & technology*, *43*(12), pp.4287-4293.

Yin, H.L., Qiu, C.Y., Ye, Z.X., Li, S.P. and Liang, J.F., 2015. Seasonal variation and source apportionment of organic tracers in PM 10 in Chengdu, China. *Environmental geochemistry and health*, *37*(1), pp.195-205.

Zhang, T., Claeys, M., Cachier, H., Dong, S., Wang, W., Maenhaut, W. and Liu, X., 2008. Identification and estimation of the biomass burning contribution to Beijing aerosol using levoglucosan as a molecular marker. *Atmospheric Environment*, *42*(29), pp.7013-7021.

Zhang, Y., Lin, Y., Cai, J., Liu, Y., Hong, L., Qin, M., Zhao, Y., Ma, J., Wang, X., Zhu, T. and Qiu, X., 2016. Atmospheric PAHs in North China: spatial distribution and sources. *Science of the Total Environment*, *565*, pp.994-1000.

Zhang, Y., Schauer, J.J., Zhang, Y., Zeng, L., Wei, Y., Liu, Y. and Shao, M., 2008. Characteristics of particulate carbon emissions from real-world Chinese coal combustion. *Environmental science & technology*, *42*(14), pp.5068-5073.

Zhang, Y., Sheesley, R.J., Schauer, J.J., Lewandowski, M., Jaoui, M., Offenberg, J.H., Kleindienst, T.E. and Edney, E.O., 2009. Source apportionment of primary and secondary organic aerosols using positive matrix

factorization (PMF) of molecular markers. *Atmospheric Environment*, *43*(34), pp.5567-5574.

Chapter 5.

Conclusions

1. Summary

1.1 The impact of organic extracts of seasonal $PM_{2.5}$ on primary human lung epithelial cells and their chemical characterization

This study assessed the impact of $PM_{2.5}$ organic extracts collected during the high concentration events in Seoul, South Korea on primary human lung epithelial cells. Twelve selected $PM_{2.5}$ samples from May 2016 to January 2017 were used to evaluate the effects of organic compounds of $PM_{2.5}$ on inflammation, cellular aging, and macroautophagy in human lung epithelial cells isolated from healthy donors. Organic extracts of $PM_{2.5}$ collected in Seoul, South Korea, during HCEs induced inflammation, cellular aging, and macroautophagy activation in primary lung epithelial cells. The average mass concentrations, OC and EC had no significant correlations with $PM_{2.5}$ effects. Both PAHs and n-alkanes were the most relevant components of $PM_{2.5}$ for inflammation, aging and macroautophagy activation. Vegetative detritus and residential bituminous coal combustion sources were strongly correlated with neutrophilic inflammation, aging, and macroautophagy activation. The findings support the idea that the chemical constituents of $PM_{2.5}$ are more important than the level of $PM_{2.5}$ mass concentrations and even low concentration of $PM_{2.5}$ may have adverse impacts on the public health.

1.2 Source apportionment of $PM_{2.5}$ in Seoul, South Korea and Beijing, China

Simultaneous ground-based monitoring and chemical analyses of $PM_{2.5}$ in Seoul, South Korea and Beijing, China were conducted for a period of one year. PMF model was utilized for the source apportionment of ambient $PM_{2.5}$ in the two sites and nine optimal sources were identified. In Seoul, secondary nitrate (27.2%) had the highest contribution to $PM_{2.5}$, followed by secondary sulfate (19.5%), oil combustion (11.9%), biomass burning (11.1%), mobile sources (9.57%), incineration (8.35%), industry/coal combustion (5.72%), soil (5.12%), and aged sea salt (1.51%). In Beijing, the highest contributing source was secondary nitrate (25.7%) followed by secondary sulfate (22.9%), mobile sources (11.9%), industrial sources (10.6%), biomass burning (7.68%), soil (7.45%), incineration (7.43%), coal combustion (4.64%), and aged sea salt (1.72%). High contributions of secondary inorganic aerosols aligned with high concentrations of ionic species. The PSCF maps show that Seoul and Beijing were significantly affected by long-range transport of air pollutants since these cities do not have coal combustion power plants or iron and steel industries. NOx and NH_3 must be included in pollution reduction policy in South Korea and China.

1.3 Characteristics of $PM_{2.5}$ organic extracts from Seoul and Beijing on human lung epithelial cells

This study investigated the characteristics of organic compounds and sources of the $PM_{2.5}$ organic extracts collected in Seoul, South Korea and Beijing, China and evaluated the production of $PM_{2.5}$ organic extract induced IL-8 on human lung epithelial cells. The average $PM_{2.5}$ mass concentrations and OC concentrations in Beijing were higher than that of Seoul, but the difference was not statistically significant. However, the average concentration of organic compounds and the expression levels of IL-8 in Beijing were significantly higher than that of Seoul. The results indicate that organic compounds within $PM_{2.5}$ are more important in inducing neutrophilic inflammation than $PM_{2.5}$ mass concentrations itself.

For Seoul samples, PAHs mainly showed high correlations with the expression levels of IL-8. However, alkylcyclohexanes, aliphatic diacaids and alkanoic acids in Beijing samples showed strong association with the expression levels of IL-8. The results indicate that organic compounds which play important role in inflammation at Seoul and Beijing are different. For Seoul samples (N=17), source which showed positive correlations with IL-8 expression levels was biomass burning (r=0.5, p-value=0.047). However, sources which showed positive correlations with IL-8 expression levels at Beijing (N=18) were (r=0.5, p-value=0.025) and SOC-2 (r=0.51, p-value=0.030). 72 h backward trajectory clusters were identified to be arriving at Seoul (four clusters) and Beijing (three clusters) in 2019. For Seoul, the average IL-8 expression level was highest for cluster 1 (97.6 pg/mL) which came in from northwestern direction through northern China and for

Beijing, the average IL-8 expression level was highest for cluster 1 (170.1 pg/mL) which starts from southeast of Beijing along the coastal area.

2. Conclusions

In this study, the $PM_{2.5}$ organic extracts which were collected from Seoul, South Korea specifically induced neutrophilic chemokine, IL-8 via ERK activation. IL-8 is a chemokine that recruit neutrophils which are known to be involved in the pathogenesis of inflammatory lung diseases such as asthma, COPD, adult respiratory distress syndrome (ARDS) (Pease and Sabroe, 2002). Many studies have reported that IL-8 and neutrophils have been detected in COPD patients. Moreover, cigarette smoking which is one of the major factors that develops COPD was reported to enhance IL-8 production (Lee et al., 2018). The specific mechanisms of $PM_{2.5}$ in lung epithelial cells are still unclear, but the inflammation via induced chemokine (IL-8) and recruitment of neutrophils is quite similar to the effects of cigarette smoking. Though the average mass concentrations and OC and EC were highest in spring than that of other seasons, the expression levels of active ERK and IL-8 were significantly higher when the cells were exposed to $PM_{2.5}$ organic extracts from fall and winter. High production of IL-8 by fall and winter $PM_{2.5}$ organic extracts were due to the high concentrations of organic compounds in cold season. Organic compounds such as PAHs and n-alkanes and primary sources such as vegetative detritus and residential coal combustion were found to be crucially important in determining the adverse health effects of $PM_{2.5}$.

As China is among the largest countries in the world, the deterioration in its air quality has been affecting downwind countries including South Korea through the long-range transport of pollutants. Since specific chemical constituents of $PM_{2.5}$

and sources play important role in causing health effects, understanding of characteristics of $PM_{2.5}$ in South Korea and China was needed. In this study, simultaneous daily ground-based continuous monitoring of $PM_{2.5}$ in Seoul and Beijing was conducted for one year in 2019. Main finding was that continuous efforts towards SO_2 reduction through the implementation of the Action Plan in China have significantly decreased the contribution of secondary sulfate. Reduction of SO_2 have led to increased contribution of secondary nitrate source both in Beijing and Seoul, therefore, additional policies to reduce NOx and NH_3 should be implemented.

The last study investigated the characteristics of organic compounds and sources of the $PM_{2.5}$ organic extracts collected in Seoul, South Korea and Beijing, China and evaluated the production of $PM_{2.5}$ organic extract induced IL-8 on human lung epithelial cells. While the average $PM_{2.5}$ mass concentrations and OC concentrations in Beijing were higher than that of Seoul, the difference was not statistically significant. On the other hand, the average concentration of organic compounds and the expression levels of IL-8 in Beijing were significantly higher than that of Seoul. For Seoul, PAHs and biomass burning source showed strong correlations with IL-8 expression levels which corroborate with the results of first study. However, organic compounds and sources which induce neutrophilic inflammation at Beijing were different from Seoul. For Beijing, organic compounds such as aliphatic diacaids, alkylcyclohexanes and alkanoic acids showed positive correlations with expression levels of IL-8. Moreover, SOC-1 (biogenic SOC) and SOC-2 (anthropogenic SOC) showed strong correlations with IL-8 expression levels.

The results indicate that organic compounds and sources which play important role in inflammation at Seoul and Beijing are different.

APPENDIX

Table 1 QA/QC for GC/MS

	GC/MS	Ionic species
Calibration curves	6 points of non-polar and polar standards	7 points of anion and cation standards
Method detection limit (MDL)	7 duplicates were used 3.707 x σ at one side (99% confidence)	7 duplicates were used 3.143 x σ at one side (98% confidence)
Recovery	1) Spiked filters recovery 2) Internal & surrogate standard recovery (Measured/True)*100 (%)	-

Table 2 GC/MS MDLs for Seoul data

Compounds	MDL (ng/m^3)	Compounds	MDL (ng/m^3)
PAHs		**n-alkanes**	
Acenapthene	0.475	Heneicosane (n-C21)	0.173
Fluorene	0.030	Docosane (n-C22)	0.025
Phenanthrene	0.035	Tricosane (n-C23)	0.153
Anthracene	0.061	Tetracosane (n-C24)	0.192
9-Methylanthracene	0.091	Pentacosane (n-C25)	0.186
Fluoranthene	0.048	Hexacosane (n-C26)	0.174
Pyrene	0.022	Heptacosane (n-C27)	0.187
Retene	0.053	Octacosane (n-C28)	0.337
Benzo[ghi]flouranthene	0.051	Nonacosane (n-C29)	0.341
Cyclopenta[cd]pyrene	0.052	Triacontane (n-C30)	0.274
Benzo[a]anthracene	0.057	Hentriacontane (n-C31)	0.116
Chrysene	0.049	Dotriacontane (n-C32)	0.201
Benzo[b]fluoranthene	0.025	Tritriacontane (n-C33)	0.240
Benzo[k]fluoranthene	0.043	Tetratriacontane (n-C34)	0.231
Benzo[a]pyrene	0.027	Pentatriacontane (n-C35)	0.201
Benzo[e]pyrene	0.043	Hexatriacontane (n-C36)	0.215
Perylene	0.048	Heptatriacontane (n-C37)	0.151
Indeno[1,2,3-cd]pyrene	0.081		
Dibenzo[a,h]anthracene	0.076	**Alkylcyclohexanes/Isoprenoids**	
Picene	0.157	Dibenzofuran	0.060
Benzo[ghi]perylene	0.166	9-Methyl-fluorene	0.088
Coronene	0.087	2-Methylnonadecane	0.091
Dibenz[a,e]pyrene	0.056	3-Methylnonadecane	0.156
		Pentadecylcyclohexane	0.096
Hopanes/Steranes		Methyl-fluoranthene	0.028
AAA-20S-C27-Cholestane	0.017	Hexadecylcyclohexane	0.078
ABB-20R-C27-Cholestane	0.024	Heptadecylcyclohexane	0.280
ABB-20R-C28-Methylcholestane	0.014	Octadecylcyclohexane	0.250
17A(H)-22,29,30-Trisnorhopane	0.031	Nonadecylcyclohexane	0.050
ABB-20R-C29-Ethylcholestane	0.012	Methyl-chrysene	0.045
17A(H)-21B(H)-30-Norhopane	0.011		
17A(H)-21B(H)-Hopane	0.014		

Table 2 GC/MS MDLs for Seoul data (Continued)

Compounds	MDL (ng/m^3)	Compounds	MDL (ng/m^3)
Dicarboxylic acids		**Sugars/Glycerides**	
Malonic (C3)	0.643	Mannosan	0.082
Maleic (C3=)	0.144	Levoglucosan	0.570
Succinic (C4)	0.478	Monopalmitin (16:0)	0.231
Fumaric (C4=)	0.191	Monoolein (18:1)	N.D.
Glutaric (C5)	0.346	Monostearin (18:0)	0.273
Adipic (C6)	0.649		
Pimelic (C7)	0.325	**Sterols**	
Suberic (C8)	0.583	Coprostanol	0.003
Azelaic (C9)	0.807	Cholesterol	0.003
Sebacic (C10)	0.288	Cholestanol	0.001
		Stigmasterol	0.004
Benzenecarboxylic Acids		β-Sitosterol	0.006
Terephthalic Acid (1,4)	0.094	Stigmastanol	0.003
Isophthalic Acid (1,3)	0.245		
Phthalic Acid (1,2)	0.534	**MethoxyPhenols**	
Methylphthalic Acid	0.131	Vanillin	0.178
		Acetovanillone	0.176
Alkanoic Acids		Syringaldehyde	0.228
C10:0	0.366	3,5-Dimethoxy-4-hydroxyacetophenone	0.105
C12:0	0.194	4-Hydroxy-3-methoxycinnamaldehyde	0.042
C14:0	0.375	3,5-Dimethoxy-4-hydroxycinnamaldehyde	N.D.
C16:0	0.137		
C18:0	0.716	**Resin Acids**	
C20:0	0.295	Iso-Pimaric Acid	0.086
C22:0	0.209	Pimaric Acid	0.035
C24:0	0.079	Abietic Acid	0.112
		Dehydroabietic Acid	0.057
Fatty Acids		Campesterol	0.215
Pinonic Acid	0.676		
Palmitoleic Acid (C16:1)	0.219		
Linoleic Acid (18:2)	0.017		
Oleic Acid (C18:1)	0.041		
Linolenic Acid	N.D.		
Octacosanoic Acid	N.D.		
Triacontanoic acid	N.D.		

Table 3 GC/MS MDLs for Beijing data

Compounds	MDL (ng/m^3)	Compounds	MDL (ng/m^3)
PAHs		**n-alkanes**	
Acenapthene	0.481	Heneicosane (n-C21)	0.172
Fluorene	0.030	Docosane (n-C22)	0.477
Phenanthrene	0.033	Tricosane (n-C23)	0.150
Anthracene	0.051	Tetracosane (n-C24)	0.189
9-Methylanthracene	0.088	Pentacosane (n-C25)	0.184
Fluoranthene	0.046	Hexacosane (n-C26)	0.170
Pyrene	0.022	Heptacosane (n-C27)	0.185
Retene	0.053	Octacosane (n-C28)	0.303
Benzo[ghi]flouranthene	0.049	Nonacosane (n-C29)	0.309
Cyclopenta[cd]pyrene	0.047	Triacontane (n-C30)	0.249
Benzo[a]anthracene	0.052	Hentriacontane (n-C31)	0.114
Chrysene	0.050	Dotriacontane (n-C32)	0.201
Benzo[b]fluoranthene	0.019	Tritriacontane (n-C33)	0.235
Benzo[k]fluoranthene	0.051	Tetratriacontane (n-C34)	0.226
Benzo[a]pyrene	0.021	Pentatriacontane (n-C35)	0.210
Benzo[e]pyrene	0.045	Hexatriacontane (n-C36)	0.219
Perylene	0.039	Heptatriacontane (n-C37)	0.156
Indeno[1,2,3-cd]pyrene	0.126		
Dibenzo[a,h]anthracene	0.096	**Alkylcyclohexanes/Isoprenoids**	
Picene	0.159	Dibenzofuran	0.061
Benzo[ghi]perylene	0.280	9-Methyl-fluorene	0.089
Coronene	0.089	2-Methylnonadecane	0.092
Dibenz[a,e]pyrene	0.052	3-Methylnonadecane	0.158
		Pentadecylcyclohexane	0.092
Hopanes/Steranes		Methyl-fluoranthene	0.030
AAA-20S-C27-Cholestane	0.016	Hexadecylcyclohexane	0.076
ABB-20R-C27-Cholestane	0.024	Heptadecylcyclohexane	0.274
ABB-20R-C28-Methylcholestane	0.014	Octadecylcyclohexane	0.245
17A(H)-22,29,30-Trisnorhopane	0.030	Nonadecylcyclohexane	0.049
ABB-20R-C29-Ethylcholestane	0.012	Methyl-chrysene	0.046
17A(H)-21B(H)-30-Norhopane	0.011		
17A(H)-21B(H)-Hopane	0.014		

Table 3 GC/MS MDLs for Beijing data (Continued)

Compounds	MDL (ng/m^3)	Compounds	MDL (ng/m^3)
Dicarboxylic acids		**Sugars/Glycerides**	
Malonic (C3)	0.643	Mannosan	0.106
Maleic (C3=)	0.123	Levoglucosan	0.697
Succinic (C4)	0.416	Monopalmitin (16:0)	0.264
Fumaric (C4=)	0.173	Monoolein (18:1)	N.D.
Glutaric (C5)	0.302	Monostearin (18:0)	0.295
Adipic (C6)	0.555		
Pimelic (C7)	0.283	**Sterols**	
Suberic (C8)	0.472	Coprostanol	0.003
Azelaic (C9)	0.670	Cholesterol	0.003
Sebacic (C10)	0.252	Cholestanol	0.002
		Stigmasterol	0.004
Benzenecarboxylic Acids		β-Sitosterol	0.007
Terephthalic Acid (1,4)	0.148	Stigmastanol	0.003
Isophthalic Acid (1,3)	0.384		
Phthalic Acid (1,2)	0.534	**MethoxyPhenols**	
Methylphthalic Acid	0.207	Vanillin	0.379
		Acetovanillone	0.382
Alkanoic Acids		Syringaldehyde	0.398
C10:0	0.590	3,5-Dimethoxy-4-hydroxyacetophenone	0.179
C12:0	0.267	4-Hydroxy-3-methoxycinnamaldehyde	0.078
C14:0	0.479	3,5-Dimethoxy-4-hydroxycinnamaldehyde	N.D.
C16:0	0.137		
C18:0	0.716	**Resin Acids**	
C20:0	0.364	Iso-Pimaric Acid	0.137
C22:0	0.250	Pimaric Acid	0.055
C24:0	0.091	Abietic Acid	0.178
		Dehydroabietic Acid	0.092
Fatty Acids		Campesterol	0.364
Pinonic Acid	0.676		
Palmitoleic Acid (C16:1)	0.339		
Linoleic Acid (18:2)	0.027		
Oleic Acid (C18:1)	0.054		
Linolenic Acid	N.D.		
Octacosanoic Acid	N.D.		
Triacontanoic acid	N.D.		

Exposure analysis

Cells were exposed to various dose of $PM_{2.5}$ organic extracts (0.1, 0.5, 1, 2%) for 24 h. $PM_{2.5}$ organic extracts with 1% or less did not affect cell viability but greater than 1% affected cell viability, thus all the samples were used in 1% for this study. For 1 mL media, 10 µL of organic extracts were added and 450 µL of 1% organic extracts were treated to lung epithelial cells for 24 h.

국문 초록

한국 서울과 중국 베이징의 대기 중 $PM_{2.5}$의 오염원 기여도 및 독성 평가

서울대학교 보건대학원
환경보건학과 환경보건학 전공
박 지 은

중국과 한국을 포함하는 동아시아 지역은 급격한 발전으로 인하여 대기오염 문제가 심각한 환경문제로 거론되고 있다. 그 중에서도 직경이 2.5 μm 이하인 초미세먼지($PM_{2.5}$)는 미세한 입자의 특성으로 인해 흡입 시 걸러지지 않고 폐포 깊숙히 침투하여 심혈관계 및 호흡기계 질환 등을 야기하여 사망률과 유병률에 높은 상관성을 나타낸다고 보고된 바 있다. 특히 기관지는 $PM_{2.5}$의 인체 노출 시 가장 먼저 반응하는 호흡기계 세포로써 산화 스트레스와 염증을 야기하여 만성 폐쇄성 폐질환과 같은 호흡기 질환이나 폐암, 더 나아가 심혈관계 질환을 유발하는 것으로 알려져 있다.

$PM_{2.5}$에 의한 건강영향은 다수의 역학 및 독성 연구를 통해 활발히 진행 되어 왔지만, $PM_{2.5}$의 독성영향은 지역의 특성이나 화학구성성분 그리고 오염원에 의해 달라질 수 있기 때문에 해당

지역에서의 $PM_{2.5}$ 의 특성 파악이 중요하다. 특히 우리나라의 경우 중국의 풍하 지역에 위치하고 있어 중국에서 발생한 $PM_{2.5}$ 의 장거리 이동에 의한 영향을 받을 수 밖에 없다. 따라서, 중국과 한국에서 채취된 $PM_{2.5}$ 의 화학적 특성 및 오염원을 파악하고, 호흡기 질환을 유발하는 염증 발현에 중요한 화학 성분 및 오염원을 규명하는 것이 해당지역의 올바른 저감대책을 세우는 데 꼭 필요하다고 할 수 있다.

본 연구에서는 한국과 중국의 수도인 서울과 베이징에서 1 년동안 1 일 간격으로 동시에 $PM_{2.5}$를 채취하고 그 화학 구성성분들을 분석하여 종합적으로 비교하였다. 수용모델을 이용한 두 도시의 오염원 기여도 산정 결과 및 오염원 별 발생원 추정 결과는 동아시아 지역의 장거리 이동에 대한 자료를 구축하고 정책 방안을 제시하는데 활용될 수 있을 것으로 생각된다. 또한, 두 도시의 $PM_{2.5}$ 시료를 사람의 기관지 상피 세포에 처치하여 염증 발현에 중요한 역할을 하는 화학 구성성분 및 오염원을 파악함으로써 향후 대기오염 연관성에 대한 기초자료로 활용될 수 있을 것으로 예상된다.

서울시에서 채취한 계절별 $PM_{2.5}$ 의 유기 성분을 배양 기관지 상피세포와 직접 채취한 일차 기관지 상피세포에 처치하고 염증, 노화, 그리고 자가포식에 미치는 영향을 평가하였다. 2016 년 5 월부터 2017 년 1 월까지의 기간 중 $PM_{2.5}$ 질량농도가 35 $\mu g/m^3$ 이상인 고농도 사례를 계절별로 3 개씩 총 12 개의 샘플을 선별하였다. 고용량 공기시료

채취기에 석영섬유여과지를 장착하여 채취하였고 해당 날짜의 필터들에 대하여 유기성분을 추출하였다. 추출액은 무극성 물질 60 여 종을 분석하는데 사용하였고, 일부는 서울대병원 호흡기내과에 보내져 기관지 상피세포 노출을 진행하였다. 정상인 환자에서 유래된 일차기관지 상피세포에 처치한 결과, 다환 방향족 탄화수소와 알칸류가 호중구성 염증발현과 가장 높은 상관성을 보였다. 또한, 식생 자연 발생 오염원과 주거석탄연소 오염원이 호중구성 염증발현, 노화 그리고 자가포식과 연관성이 있는 것으로 나타났다.

모델링을 통해 서울과 베이징의 $PM_{2.5}$ 의 영향을 미치는 오염원 구분 및 기여도를 정량적으로 파악하고 오염원 별 발생원을 추정하였다. 서울에서 2019 년 1 월부터 12 월까지 채취된 샘플 중 294 개와 베이징에서 2019 년 2 월부터 12 월까지 채취된 샘플 중 226 개에 대하여 총 26 개의 화학 구성 성분들을 정량하여 PMF 에 적용하였다. 두 도시에서 공통적으로 구분된 오염원은 이차 질산염, 이차 황산염, 자동차 오염원, 식생 연소 오염원, 소각시설 오염원, 토양 오염원, 그리고 노후 해염입자 오염원이었다. 추가적으로 서울에서는 산업/석탄 연소 오염원과 기름 연소 오염원이 구분되었고, 베이징에서는 산업 오염원과 석탄 연소 오염원이 구분되었다. 두 도시에서 이온 성분의 질량이 $PM_{2.5}$ 의 50% 이상을 차지하였고, 이차 질산염과 이차 황산염의 기여도가 가장 높은 것으로 나타났다. 이차 질산염과 이차 황산염에

대한 PSCF 결과에 따르면 난방기간과 비난방기간동안 두 도시 모두 장거리 이동의 영향을 받는 것으로 나타났다.

서울과 베이징에서 채취한 $PM_{2.5}$ 의 유기성분을 배양 기관지 상피세포에 처치하여 사이토카인의 발현량을 확인하고 도시 별 오염원 및 유기성분에 따른 차이를 비교하였다. 서울과 베이징에서 난방기간과 비난방기간의 시료들을 적절하게 섞어 선정하였다. 고용량 공기시료채취기에 석영섬유여과지를 장착하여 채취하였고 해당 날짜의 필터들에 대하여 유기성분을 추출하였다. 추출액은 무극성 물질 59 여 종과 극성 물질 52 여 종을 분석하는데 사용하였고, 일부는 서울대병원 호흡기내과에 보내져 기관지 상피세포 노출을 진행하였다. $PM_{2.5}$ 질량농도와 유기탄소 농도가 서울보다 베이징에서 높았지만 그 차이가 유의미하지는 않은 것으로 나타났다. 하지만 유기성분 농도와 IL-8 의 발현량이 서울보다 베이징에서 유의미하게 높은 것으로 보아, $PM_{2.5}$ 의 질량농도 보다는 유기성분이 호중구성 염증발현에 영향을 미치는 것으로 보인다. 서울 시료에 대한 분석 결과, 첫번째 연구에서 나온 결과와 같이 다환 방향족 탄화수소와 식생연소 오염원이 호중구성 염증발현과 높은 상관성을 나타냈다. 반면에 베이징 시료에 대한 분석 결과, 디카르복시산 등의 극성이 높은 유기성분 및 자연적 배출원의 이차 유기탄소 오염원과 인위적 배출원의 이차 유기탄소 오염원이 호중구성 염증발현과 높은 상관성을 보였다. 역궤적 분석을 통해 서울로 들어오는

총 4 개의 군집과 베이징으로 들어오는 총 3 개의 군집을 분류하였다. 서울로 들어오는 군집 중 외부에서 유입되는 군집 1 이 가장 높은 IL-8 발현량을 나타내었고, 다른 군집에 비해 식생연소 오염원의 기여도가 크게 나타났다. 베이징으로 들어오는 군집 중에서는 베이징의 동남쪽에서부터 해안가를 따라 들어오는 군집 1 이 가장 높은 IL-8 발현량을 나타내었고, 다른 군집에 비해 이차 유기탄소 오염원(자연적/인위적)들의 기여도가 비교적 크게 나타났다. 따라서, 서울은 장거리 이동을 통해 외부에서 유입되는 연소 관련 오염원의 영향이 큰 것으로 보이며, 베이징은 비교적 국지적 이동을 통해 중국내에서 이차적으로 생성되는 오염원의 영향이 큰 것으로 추정된다.

주요어: 초미세먼지, 수용모델, 장거리이동, 폐 상피세포, 사이토카인

학 번: 2018-39295